

**The regulation of hypoxia-responsive gene expression by
hydroxyl radicals and intracellular calcium**

Dissertation

zur Erlangung des Doktorgrades

der Mathematisch-Naturwissenschaftlichen Fakultäten

der Georg-August-Universität zu Göttingen

Vorgelegt von

Liu Qing

aus Shandong, China

Göttingen 2003

D7

Referent: Prof. Dr. D. Doenecke

Korreferent: Prof. Dr. R. Hardeland

Tag der mündlichen Prüfung:

Index

List of figures	V
List of Tables	VI
Abbreviations	VII
Summary	1
1. Introduction	3
1.1 Oxygen sensing	3
1.1.1 The heme oxygen sensor hypothesis	3
1.1.2 Role of mitochondria in O ₂ -sensing	5
1.1.3 The new oxygen sensor: a family of novel protein hydroxylases	5
1.2 Hypoxia-inducible transcription factors (HIFs)	7
1.2.1 HIF-1 structure and the HIF family	7
1.2.2 Regulation of HIF-1	10
HIF-1 α mRNA regulation	10
HIF-1 α stabilization	11
HIF-1 α transcriptional activity	11
Nuclear localization of HIF-1 α	13
HIF-1 DNA binding and transcriptional complex	13
1.3 Reactive oxygen species (ROS) as messengers	14
1.4 Aim of the work	15
2. MATERIALS	16
2.1 Animals	16
2.2 Bacterial strains, vectors and plasmid constructs	16
2.2.1 Bacterial strains	16
2.2.2 Vectors	16
2.2.3 pECFP and pDsRed mammalian expression constructs	18
2.2.4 pGL3-basic constructs	21
2.2.5 pGL3-Promoter constructs	21
2.2.6 Other constructs used in the experiments	22
2.3 Oligonucleotides	27
2.3.1 Oligonucleotides for sequencing of the plasmides	27
2.3.2 Oligonucleotides for PCR reaction	28
2.4 Enzymes	28

2.5	Antibodies	31
2.6	Detection, Purification and synthesis systems (“Kits“)	31
2.7	Stock solutions	31
2.8	Chemicals	33
2.9	Other materials	34
2.10	Instruments	35
3.	Methods	37
3.1	Molecular biological methods	37
3.1.1	Polymerase chain reaction (PCR)	37
3.1.2	DNA electrophoresis and purification from agarose gel	38
3.1.3	Cloning of the PCR product	39
3.1.4	Isolation of plasmid DNA (minipreparation)	41
3.1.5	Isolation of plasmid DNA with silicate columns (maxipreparation)	42
3.1.6	Sequencing of plasmids	43
3.2	Cell biological methods	45
3.2.1	Isolation of primary rat hepatocytes	45
	<i>Liver perfusion</i>	45
	<i>Preparation of the hepatocyte suspension</i>	45
3.2.2	Primary rat hepatocyte culture	47
3.2.3	Culture of HepG2 cells	48
3.2.4	Transfection of hepatocytes and HepG2 cells	48
3.2.5	Luciferase detection	50
3.2.6	Detection of OH• generation in living cells by two photon confocal laser microscopy (2P-CLSM)	50
3.2.7	Immunofluorescence	51
3.2.8	RNA isolation from cultured cells	51
3.2.9	Preparation of digoxigenin-labeled RNA probes	53
	<i>Linearization of plasmids</i>	53
	<i>In vitro transcription</i>	53
	<i>Estimation of the labeling efficiency</i>	54
3.2.10	Northern blot analysis	55
	<i>Denaturation of RNA sample</i>	55
	<i>Electrophoresis of RNA samples</i>	56
	<i>RNA transfer to nylon membrane</i>	57
	<i>Hybridization of the RNA with digoxigenin-labeled RNA probes</i>	57

<i>Detection and quantification of the RNA expression</i>	57
3.2.11 Western blot analysis	58
<i>Total protein isolation from the cultured cells</i>	58
<i>SDS-Polyacrylamide Gel Electrophoresis of protein (SDS-PAGE)</i>	58
<i>Electroblotting of immobilized proteins</i>	59
<i>Immunological detection of immobilized proteins</i>	61
3.2.12 Expression and purification of GST-TADN fusion protein	61
<i>Expression of GST-TADN</i>	61
<i>Purification the fusion protein by Glutathione Sepharose 4B</i>	61
3.2.13 HIF-1 α peptide hydroxylation assay	62
3.2.14 VHL pull-down assay	63
³⁵ S-VHL <i>in vitro</i> translation	63
<i>GST pull-down assay</i>	64
3.3 Statistical analysis	65
3.4 Security measures	65
4. RESULTS	66
4.1 Localization of the OH\bullet-generating Fenton reaction at the endoplasmic reticulum	66
4.2 Localization of HIF-1α at the endoplasmic reticulum under normoxia	69
4.3 Modulation of HIF-1 functions by the OH\bullet scavenger Dihydrorhodamine (DHR)	69
4.3.1 Induction of HIF-1 dependent genes by DHR	70
4.3.2 Induction of HIF-1 α protein levels by DHR	70
4.3.3 Induction of HIF-1 α nuclear translocation by DHR	73
4.3.4 Induction of HIF-1 α transactivity by DHR	75
4.3.5 Modulation of HIF-1 α stability by DHR	75
4.4 Modulation of HIF-1 by endoplasmic reticulum stress	77
4.4.1 Modulation of LUC activity in EPO-HRE-Luc transfected cells by endoplasmic reticulum stress	78
4.4.2 Modulation of HIF-1 α protein levels by endoplasmic reticulum stress	78
4.5 The role of calcium in HIF-1-dependent responses	80
4.5.1 Modulation of HIF-1 α protein levels by intracellular calcium	80
4.5.2 The calcium ionophore induces HIF-1 α expression at the transcriptional level	82
4.5.3 The intracellular calcium chelator leads to HIF-1 α protein stabilization	83
4.5.4 The calcium chelator but not the calcium ionophore induces	

Index	IV
HIF-1 α TADN transactivity	86
4.5.5 Both calcium ionophore and intracellular calcium chelator induce HIF-1-dependent gene expression	86
5. Discussion	90
5.1 ROS as messengers in O₂-signaling	90
5.1.1 Localization of intracellular ROS generation	90
5.1.2 Production of reactive oxygen species under normoxia and hypoxia	91
5.1.3 Regulation of HIF-1 α by ROS	92
5.2 The involvement of the ER in hypoxic responses	94
5.3 The role of calcium ions in HIF-1α regulation	95
5.3.1 Implication of calcium ion in HIF-1 α accumulation	96
5.3.2 Involvement of calcium in HIF-1-dependent gene expression	97
References	100
Acknowledgements	111

List of figures

Figure 1.	Schematic representation of HIF-1 α , HIF-2 α , HIF-3 α , HIF-1 β , and IPAS	9
Figure 2.	Regulation of HIF-1 α by hydroxylases	12
Figure 3.	Oxygen sensing for the modulation of gene activation (hypothesis)	15
Figure 4.	Structure of the pBluescript vector (pBS-KSII)	17
Figure 5.	Structure of the plasmid pCRII-TOPO	17
Figure 6.	Structure of the construct pECFP-Golgi	19
Figure 7.	Structure of the construct pECFP-Mito	20
Figure 8.	Structure of the construct pECFP-ER	20
Figure 9.	Structure of the construct pDsRed2-Peroxi	21
Figure 10.	Structure of the pGL3-basic vector	22
Figure 11.	The fragments of human PAI-1 promoter	22
Figure 12.	Structure of the pGL3-Promoter vector	23
Figure 13.	Sequences of HRE and HREm from EPO gene	23
Figure 14.	Structure of the pGFP-HIF-1 α construct	24
Figure 15.	Structure of the pGFP-HIF-1 α construct	24
Figure 16.	Structure of the pGEX-5X construct	25
Figure 17.	Structure of pcDNA6/Myc-His	26
Figure 18.	Structure of pG ₅ E1B-luc and pcDNA6-Gal4-HIF1 α TAD constructs	27
Figure 19.	Detection of OH• generation at the endoplasmic reticulum	67
Figure 20.	Hypoxia-mediated inhibition of OH• generation at the endoplasmic reticulum	68
Figure 21.	Hypoxia-mediated HIF-1 α translocation from the endoplasmic reticulum to the nucleus	69
Figure 22.	Induction of PAI-1 and HO-1 gene expression by DHR under normoxia	71
Figure 23.	The induction of PAI-1 promoter activity by DHR	72
Figure 24.	Induction of EPO-HRE Luc gene expression by DHR	72
Figure 25.	Induction of HIF-1 α protein expression by DHR under normoxia	73
Figure 26.	Induction of HIF-1 α nuclear translocation by dihydrorhodamine (DHR) under normoxia	74
Figure 27.	Induction of HIF-1 α transactivation by DHR	76
Figure 28.	Inhibition of HIF-1 α prolyl hydroxylase activity by DHR	77
Figure 29.	The modulation of EPO-HRE activity by ER stress	78
Figure 30.	Modulation of HIF-1 α protein expression by ER stress	79
Figure 31.	Modulation of HIF-1 α protein expression by intracellular calcium	81

Figure 32.	Time-course of the HIF-1 α protein expression after treatment with A23187 or BAPTA-AM	81
Figure 33.	Inhibition of A23187 induced HIF-1 α protein expression by actinomycin D and cycloheximide	82
Figure 34.	Modulation of HIF-1 α mRNA expression by the calcium ionophore A23187	83
Figure 35.	Modulation of BAPTA-AM induced HIF-1 α protein expression by actinomycin D and cycloheximide	84
Figure 36.	Modulation of HIF-1 α mRNA expression by the intracellular calcium chelator BAPTA-AM	85
Figure 37.	Inhibition of HIF prolyl hydroxylase activity by the calcium chelator BAPTA-AM	85
Figure 38.	Induction of HIF-1 α TADN transactivation by BAPTA-AM	87
Figure 39.	Induction of PAI-1 gene expression by the calcium ionophore A23187 and the calcium chelator BAPTA-AM	88
Figure 40.	The modulation of EPO-HRE LUC activity by intracellular calcium	89
Figure 41.	Model of the HIF-1 α regulation	98

List of tables

Table 1.	HIF-1 target genes	8
Table 2.	Antibodies used in the experiments	31

Abbreviations

AA	Amino acid
AHR	Arylhydrocarbon receptor
Akt	Corresponds to PKB (homolog of v-Akt)
AP	Alkaline phosphatase
APS	Ammonium persulfate
ARNT	Arylhydrocarbon receptor-nuclear translocator protein
BMAL-1	Brain and muscle ARNT-like protein-1
BSA	Bovine serum albumin
bHLH	Basic helix-loop-helix
bp	Base pair
C-TAD	C-terminal transactivation domain
cAMP	Cyclic adenosine-3',5'-monophosphate
CBP	CREB-binding protein
cDNA	Complementary deoxyribonucleic acid
Ci	Curie
CMV	Cytomegalie virus
CRE	cAMP responsive element
CREB	CRE-binding protein
CSPD	Dinatrium 3-(4-methoxyspiro{1,2-dioxetane-3,2-(5'-chloro)-Tricyclo[3.3.1.1 ^{3,7}]decan}-4-yl)-phenylphosphate
ddNTP	Cytochrome P450-2D
DEPC	Diethylpyrocarbonate
DHR	Dihydrorhodamine
DIG	Digoxigenin
DMSO	Dimethylsulfoxide
DMTU	Dimethylthiourea
ds	Double strand
DSF	Desferrioxamine
DTT	Dithiothreitol
ECL	Enhanced chemiluminescence
EDTA	Ethylendinitrilo-N,N,N',N',-tetra-acetate
EGTA	Ethylenglycol-bis-(2-aminoethylether)-N,N',-tetra-acetate
EPAS	Endothelial PAS domain protein
EPO	Erythropoietin

ER	Endoplasmic reticulum
FCS	Fetal calf serum
FIH	Factor-inhibiting HIF-1
GK	Glucokinase
GST	Glutathione S-transferase
HC	Hepatocyte
Hepes	2-(4-hydroxyethyl)-piperazinyl-1-ethansulfonate
HepG2	Hepatoma cell line HepG2
HIF-1	Hypoxia-inducible factor-1
HLF	HIF-1-like factor
HNF	Hepatic nuclear factor
HO	Heme oxygenase
HPLC	High Performance Liquid Chromatography
HRE	Hypoxia responsive element
HRF	HIF related factor
HRP	Horseradish peroxidase
HVR	Hypoxic ventilatory response
IPAS	Inhibitory PAS protein
IPTG	Isopropyl β -D-thiogalactoside
IP3	Inositol triphosphate
kb	Kilo base
kDa	Kilo Dalton
LB	Luria Bertani
LMW	Low molecular weight
LUC	Luciferase
MAP	Mitogen-activated protein
MOP	Member of PAS superfamily
MOPS	3-(N-Morpholino)-propanesulfonic acid
MW	Molecular weight
NaAc	Sodium acetate
N-TAD	N-terminal transactivation domain
NaOH	Sodium hydroxide
NLS	Nuclear localization signal
OD	Optical density
ODDD	Oxygen-dependent degradation domain

PAI-1	Plasminogen activator inhibitor-1
PAS	Per-AHR-Sim
PCK	Phosphoenolpyruvate carboxykinase
PCR	Polymerase Chain Reaction
PDI	Protein disulfide isomerase
Per	Periodic (Drosophila protein)
PHD	Prolyl hydroxylase domain protein
PI3K	Phosphatidylinositol-3-kinase
PI(4,5)P ₂	Phosphatidyl-inositol-4,5-bisphosphate
PK	Pyruvatekinase
PKB	Proteinkinase B
PLGF	Placental growth factor
PMSF	Phenylmethyl sulfonylfluoride
PTEN	Phosphatase tensin homolog
Ref-1	Redox factor-1
RH	Rhodamine
RNase	Ribonuclease
ROS	Reactive oxygen species
rpm	Revolutions per minute
RT	Room temperature
SDS	Sodium dodecylsulfate
SEM	Standard error of the mean
Sim	Single minded protein
ss	Single strand
SSC	Sodium chloride sodium citrate
TAD	Transactivation domain
TAE	Tris acetate EDTA buffer
TEMED	N',N',N',N'-Tetramethyldiamine
TNF	Tumor necrosis factor
Tris	Tris-(hydroxymethyl)-aminomethan
UV	Ultraviolet
VEGF	Vascular endothelial growth factor
VHL	von Hippel-Lindau
X-phosphate	5-Brom-4-chlor-3-indolyl phosphate

Summary

The heterogeneous oxygen distribution in tissues requires an oxygen-sensing system to detect a decrease in oxygen concentration and a subsequent signaling pathway to allow the execution of adaptive responses. It has been proposed that hydroxyl radicals (OH•) generated in a perinuclear iron-dependent Fenton reaction are involved as messengers in the oxygen signaling pathway. Thus, it was the first aim of this study to localize the cellular compartment in which the Fenton reaction takes place and to prove whether scavenging of the OH• can modulate hypoxia-inducible factor-1 (HIF-1) activity and expression of its target genes plasminogen activator inhibitor-1 (PAI-1) and heme oxygenase-1 (HO-1).

The Fenton reaction was localized by using the non-fluorescent dihydrorhodamine (DHR) that is irreversibly oxidized to fluorescent rhodamine (RH) while scavenging OH• together with gene constructs allowing fluorescent labeling of mitochondria, endoplasmic reticulum (ER), golgi apparatus, peroxisomes, or lysosomes. Two photon confocal laser scanning microscopy and three-dimensional reconstruction of the cells revealed that the OH• generation was localized at the ER and this ER-based Fenton reaction was strictly pO₂-dependent. Furthermore, the oxygen-sensitive transcription factor HIF-1 α was also detected at the ER when the cells were kept under normoxia whereas under hypoxia HIF-1 α was only present in the nucleus. Scavenging OH• by DHR attenuated HIF-prolyl hydroxylase activity and interaction with the von Hippel-Lindau tumor suppressor protein (VHL) thus leading to enhanced HIF-1 α protein expression, nuclear translocation, transactivity and increased expression of HIF-1 target genes including plasminogen activator inhibitor-1 (PAI-1) and heme oxygenase-1 (HO-1). Moreover, OH• scavenging appeared to enhance redox factor-1 (Ref-1) binding and thus recruitment of the transcriptional coactivator p300/CBP to the HIF-1 α C-terminal transactivation domain (C-TAD) since mutation of the Ref-1 binding site cysteine 800 abolished DHR induced transactivation.

The colocalization of the OH•-generating Fenton reaction and HIF-1 α under normoxia in the ER indicated that proper ER function was required for oxygen signaling in cells. Tunicamycin, an inhibitor of protein glycosylation, brefeldin A, an inhibitor of protein transport out of ER, and thapsigargin, an inhibitor of Ca²⁺-ATPase on the ER membrane, were used to induce ER stress conditions. Their effects on oxygen signaling were checked by HIF-1-dependent reporter gene analysis and presence of the HIF-1 α protein. It was found that both tunicamycin and brefeldin A abolished hypoxia-induced HIF-1 α activation in HepG2 cells. However, thapsigargin did not repress the hypoxia induced EPO-HRE luciferase activity in the reporter gene analysis. Indeed, the treatment of thapsigargin accumulated HIF-1 α protein under

normoxia in HepG2 cells. As an inhibitor of the Ca^{2+} -ATPase, thapsigargin can cause an elevation of the cytosolic Ca^{2+} concentration implicating that intracellular calcium is also involved in oxygen signaling.

Thus, the second aim was to investigate whether different reagents which cause increases or decreases in intracellular Ca^{2+} influence HIF-1 α expression. Interestingly, both the calcium ionophore (A23187) and the intracellular calcium chelator (BAPTA-AM) were demonstrated to accumulate HIF-1 α under normoxia but through different mechanisms. A23187 acted via stimulating HIF-1 α mRNA transcription since A23187 increased HIF-1 α mRNA levels and actinomycin D (Act D) significantly inhibited the A23187-dependent HIF-1 α induction. On the other hand, BAPTA-AM only transiently induced HIF-1 α through protein stabilization but not via stimulation of HIF-1 α mRNA expression because its mRNA expression was not induced by BAPTA-AM, and Act D did not inhibit the induction of HIF-1 α by BAPTA-AM. It was further proved by in vitro HIF-prolyl hydroxylation assays and VHL-GST-HIF1 α TADN pull-down assay that BAPTA-AM significantly inhibited prolyl hydroxylase activity and inhibited binding of VHL. Concomitant, with the accumulation of HIF-1 α , both of these compounds up-regulated expression of the HIF-1 target gene PAI-1.

Together, the ER-based $\text{OH}\bullet$ -generating Fenton reaction appears to have an impact on the expression of hypoxia-responsive genes via HIF-1 α stabilization and co-activator recruitment. The hypoxia-induced gene expression in HepG2 cells is further dependent on proper ER function and intracellular calcium since the calcium ionophore (A23187) and the intracellular calcium chelator (BAPTA-AM) accumulate HIF-1 α .

1. Introduction

Oxygen (O_2) is essential for the life of all aerobic organisms. During the combustion of organic compounds for generation of energy in form of ATP it serves as the final electron acceptor during mitochondrial electron transfer. In mammals, at the whole body level, oxygen supply is optimized by tight regulation of ventilation, arterial blood hemoglobin saturation and systemic oxygen transport. Even a slight reduction in normal oxygen concentration (hypoxia) can elicit a wide range of adaptive responses at the systemic, tissue and cellular levels. These include (a) induction of tyrosine hydroxylase, which facilitates the control of ventilation through the carotid body; (b) the induction of VEGF, which promotes capillary growth (Bunn and Poyton, 1996); and (c) increased production of erythropoietin (EPO), which augments the rate of erythrocyte formation. In addition, the oxygen tension has been demonstrated to be a key regulator to optimize specific organ functions. For example, the zonal expression of genes encoding metabolic enzymes in the liver acinus is dependent on the oxygen gradient between the periportal (about 65 mmHg) and perivenous (about 35 mmHg) area. In common, all these responses require an oxygen sensing system to detect the decrease in oxygen and a subsequent signaling pathway to transmit the O_2 -signal and to allow the execution of the adaptive responses.

1.1 Oxygen sensing

Systemically, oxygen sensing is originally attributed to specialized chemoreceptor cells in carotid and airway neuroepithelial bodies that regulate cardiovascular and ventilatory rates, respectively (Lopez-Barneo, 1996). However, the cellular oxygen sensors, which may be shared by all mammalian cells, has not been definitively identified yet. The search for a physiological oxygen sensor represents an important and exciting area of research because of its role in development, in cell survival and in tumor cell biology.

1.1.1 The heme oxygen sensor hypothesis

Up to now, virtually all proteins capable of binding molecular oxygen contain iron, often in the center of a heme moiety. Thus, it is reasonable to assume that the mammalian oxygen sensor could be a heme protein. Initially it was shown that treatment of Hep3B cells with cobalt chloride is able to induce EPO mRNA and protein expression similar to that observed with hypoxia (Goldberg et al., 1988). This appears to occur by replacing the iron ion in the heme moiety by cobalt ions thus locking the oxygen sensor in the deoxy conformation. Further

evidence is provided by the finding that iron chelators, such as desferrioxamine, are also capable of mimicking the responses to hypoxia (Ho and Bunn, 1996; Wang and Semenza, 1993). Moreover, experiments utilizing carbon monoxide (CO) have also provided strong support for the hypothesis that the oxygen sensor is a heme protein. The induction of EPO expression in Hep3B cells following exposure to hypoxia was markedly inhibited by the presence of 10% CO. In contrast, CO did not inhibit the induction of EPO expression by cobalt or nickel (Goldberg et al., 1988). This result is fully consistent with the inability of cobalt substituted heme to bind CO. Similar results have been shown in experiments investigating other O_2 -modulated genes, such as phosphoenolpyruvate carboxykinase and VEGF (Kietzmann et al., 1992, 1993; Goldberg et al., 1994).

It was proposed from spectrophotometric investigations in HepG2 cell spheroids and gene expression experiments that the heme protein acting as the O_2 -sensor might be an enzyme with similarity to the NADPH oxidase from neutrophils. This enzyme produces superoxide anion radicals ($O_2^{\cdot-}$) which are then converted to H_2O_2 either spontaneously or by superoxide dismutase. Due to its ability to freely diffuse within the cell and to participate in one or two electron transfer reactions, H_2O_2 may be a suitable candidate for being the second messenger of the O_2 signal.

However, it appeared that the classical leucocyte NADPH oxidase was not the only O_2 sensor since normal oxygen-regulated gene expression was found in cell lines derived from patients suffering from chronic granulomatous disease, an inherited disease in which one of the subunits of the b_{558} /NADPH oxidase complex is defective (Wenger et al., 1996). Furthermore, in knock-out mice deficient in the gp91_{phox} subunit of the b_{558} /NADPH oxidase complex, hypoxic responses of pulmonary vasoconstriction and whole-cell K^+ current remain at the same level as compared with wild-type mice, though a marked reduction in superoxide production could be detected (Archer et al., 1999). Therefore, it was proposed that a NADPH oxidase isoform functioning as a "low output" oxidase might be involved in O_2 sensing. This is supported from the recent identification of different gp91 NADPH oxidase subunit isoforms (Nox 1,3,4,5) (Sorescu et al., 2002) as well as of the p47 and p67 subunit isoforms (Gu et al., 2003). Furthermore, the role of H_2O_2 as mediator of the O_2 signal was substantiated in studies showing that the hypoxia-dependent induction of EPO (Wang et al., 1993), tyrosine hydroxylase, aldolase A (Semenza et al., 1994), glucokinase (Kietzmann et al., 1996) was inhibited when the cells were treated with H_2O_2 . Thus, it is possible but still open whether there is a heme protein oxygen sensor.

1.1.2 Role of mitochondria in O₂-sensing

As the principal oxygen-consuming organelle of the cell, the mitochondrion itself is an apparently promising candidate to be the oxygen sensor. However, the oxygen tension in mitochondria is far too low and too dependent on metabolic fluctuation to make it a useful site for oxygen sensing. This argument is supported by the finding that the respiratory electron transport chain blocker potassium cyanide cannot induce EPO gene expression (Goldberg et al., 1988; Tan and Ratcliffe, 1991). Moreover, the oxygen-dependent expression of phosphoenolpyruvate carboxykinase was unaffected by the respiratory chain uncoupler 2,4-dinitrophenol (Kiezmann et al., 1993). In addition, neither nuclear nor mitochondrial genes that are involved in critical mitochondria functions appear to be regulated by the signaling system responsive to hypoxia and cobalt (Ebert et al., 1996). Although mitochondria are a major source of superoxide anion radicals (O₂^{-•}), which may serve as signal transducers (described in 1.3), the presence of abundant mitochondria-specific superoxide dismutase is likely to markedly limit egress of superoxide to the cytosol. These considerations make mitochondria an unlikely initiating site for O₂ signaling.

In contrast, recent researches utilizing ρ^0 cells depleted of mitochondrial DNA suggested that mitochondria do play a role in oxygen sensing. The DNA in mitochondria encodes specific subunits that are required for a functional electron transport chain, so these ρ^0 cells cannot respire and are forced to survive purely by anaerobic glycolysis. It was first reported that ρ^0 cells lost their response to hypoxia though they still retained their ability to respond to cobalt or desferrioxamine (Chandel et al., 1998; Chandel et al., 2000). However, these results were later challenged by other groups that found ρ^0 cells retained the ability to stabilize the hypoxia-inducible transcription factor-1 α (HIF-1 α) under near-anoxic conditions (0.1% O₂) (Srinivas et al., 2001; Vaux et al., 2001). Further research comparing hypoxic responses in ρ^0 cells under different conditions of oxygen (Schroedl et al., 2002) showed that ρ^0 cells selectively lost the ability to respond to hypoxia but retained the ability to stabilize HIF-1 α under anoxic conditions. These results suggest that multiple oxygen sensors might exist in the same cell and the respiratory chain component in mitochondria is one of them. Clearly, many questions remain to be further clarified regarding the mechanisms by which mitochondria contribute to the process of oxygen sensing.

1.1.3 The new oxygen sensor: a family of novel protein hydroxylases

Although the hunting for the oxygen sensors has been elusive, it has been clear that many

processes involved in oxygen homeostasis are mediated by hypoxia-inducible factors (HIFs). Most of the genes that are activated during hypoxia are regulated by these transcription factors (the detailed information about HIFs is described in 1.2). The nature of the oxygen sensor responsible for HIFs activation has remained enigmatic for a long time, while the breakthrough experiments were performed by two research groups headed by Ratcliffe and Kaelin. They discovered a group of oxygen-dependent hydroxylases, prolyl hydroxylases domain (PHD) protein, which take the responsibility of HIFs stabilization in response to hypoxia (Ivan et al., 2001; Jaakkola et al., 2001). Just for important, the requirement of oxygen as a substrate for these enzymes may make them suitable oxygen sensors.

These PHDs were characterized as non-heme iron enzymes, whose activity requires Fe^{2+} , oxygen, ascorbate and 2-oxoglutarate as cosubstrates. Under normoxia, the PHDs transfer one oxygen atom onto the proline residues of HIF α -subunits, the second oxygen atom reacts with 2-oxoglutarate, yielding succinate and carbon dioxide as products. The modified HIF α -subunit is then specifically bound by the von Hippel-Lindau protein (VHL) which targets it for ubiquitinylation and proteasomal degradation (Huang et al., 1998). By contrast, under hypoxia, the activity of PHDs is limited by the lack of oxygen and thereby HIFs are stabilized. The relatively labile binding of Fe^{2+} at the 2-his-1-carboxylate center of the PHDs results in striking sensitivity to inhibition by iron chelators and metals such as Co^{2+} that could exchange Fe^{2+} at this site. These properties can also additionally explain the hypoxia-mimicking effects of desferrioxamine and cobalt ions which were described above.

More recently, it was discovered that an asparagine residue within the carboxyl-terminal transactivation domain (C-TAD) of HIF α -subunits could also be hydroxylated in an oxygen-dependent manner (Lando et al., 2002a). This modification prevents interaction of the HIF α C-TAD with the CH-1 domain of the coactivator p300, thus blocking the transactivation of HIF (Hewitson et al., 2002). This hydroxylase was then found to be identical to the factor inhibiting HIF-1 (FIH-1), which was previously shown to interact with HIF (Lando et al., 2002b; Mahon et al., 2001). Similar to PHDs, FIH-1 is also a Fe^{2+} - and 2-oxoglutarate-dependent oxygenase, which requires oxygen as substrate. The involvement of at least two distinct types of hydroxylases in oxygen-regulated transcription suggests that these enzymes may be well suited to a role in cellular oxygen sensing.

Although there is little doubt that these hydroxylases are central participants regulating the stabilization and function of HIFs, they may not account for the effects of some hypoxia “mimics” such as carbon monoxide, and many responses to hypoxia including neurotransmitter release in the carotid body and smooth muscle cells contraction in the

pulmonary artery, which do not require activation of HIFs. Furthermore, it has been demonstrated that many growth factors could trigger HIF activation during normoxia (Karni et al., 2002; Laughner et al., 2001; Treins et al., 2002). It is conceivable that the activity of these hydroxylases is regulated by some signaling pathway, making them a downstream target of a separate oxygen sensor. The factors that regulate these hydroxylases still need to be further investigated. So the discovery of these hydroxylases does not close the search for oxygen sensors, but opens another new field for investigation.

All in all, multiple O₂ sensors might be important in adapting cells to hypoxia. Different oxygen tensions might trigger distinct responses by inducing specific oxygen sensing and signaling cascades, then allowing graded responses.

1.2 Hypoxia-inducible transcription factors (HIFs)

The discovery of HIFs has been regarded as a main milestone in the studies of oxygen sensing and signaling. HIF-1 was first identified on the basis of its ability to bind to a hypoxia-response element (HRE) in the 3' flanking region of the EPO gene (Wang and Semenza, 1995). Now this factor is recognized as a global regulator of oxygen homeostasis in a wide range of multicellular organisms. In mammals, a large number of target genes for HIF have been identified, as shown in Table 1. The expression of these genes has important consequences for regulation of cellular metabolism, proliferation, survival, cardiovascular functions, and iron homeostasis and erythropoiesis. Thus, HIF may represent the link between oxygen sensors and effectors at the cellular, local, and systemic level.

1.2.1 HIF-1 structure and the HIF family

Biochemical purification of the HIF-1 protein from Hep3B cells has yielded a heterodimer composed of a 120 kD α -subunit and a 91-94 kD β -subunit (Wang and Semenza, 1995). Further characterization has revealed HIF-1 α is a novel protein containing 826 amino acids, while HIF-1 β is a previously identified heterodimerization partner of the dioxin receptor (aryl hydrocarbon receptor, AhR), called AhR nuclear receptor translocator (ARNT) (Wang et al., 1995; Hoffman et al., 1991). The two subunits share homology of their amino terminal sequences, which contain basic helix-loop-helix (bHLH) and PER-ARNT-SIM homology (PAS) domains (Fig. 1). Whereas the basic domain is essential for DNA binding, the HLH domain and N-terminal half of the PAS domain are necessary for herterodimerization and DNA binding. Moreover, there are two transcriptional activation domains in HIF-1 α , one is referred

to as N-terminal transactivation domain (N-TAD), and the other as C-terminal transactivation domain (C-TAD). In contrast, HIF-1 β contains only one transcriptional activation domain (TAD) at the C terminus. Furthermore, HIF-1 α possesses a unique oxygen-dependent degradation domain (ODDD) that critically controls protein stability. A portion of the ODDD overlaps with the N-TAD.

In addition to the ubiquitously expressed HIF-1 α , two other members of this family, HIF-2 α (also called EPAS1, MOP2, HLF or HRF) and HIF-3 α , have been identified that show a more restricted tissue expression pattern (Ema et al., 1997; Flamme et al., 1997; Gu et al., 1998). HIF-2 α and HIF-3 α contain domains similar to those in HIF-1 α and exhibit similar biochemical

Table 1. HIF-1 target genes.

HIF-1 target gene (function)	References
<i>Oxygen transport: erythropoiesis and iron metabolism</i>	
Erythropoietin (erythropoiesis)	Wang et al., 1993; Firth et al., 1994
Transferrin (iron transport)	Rolfs et al., 1997
Transferrin receptor (iron uptake)	Tacchini et al., 1999; Lok and Ponka, 1999
Ceruloplasmin (iron Oxidation)	Mukhopadhyay et al., 2000
<i>Oxygen transport: vascular regulation</i>	
VEGF (angiogenesis)	Liu et al., 1995; Forsythe et al., 1996
Flt-1 (VEGF-receptor-1)	Gerber et al., 1997
PAI-1 (angiogenesis)	Kietzmann et al., 1999
iNOS (NO production)	Melillo et al., 1995; Jung et al., 2000
Heme oxygenase 1	Lee et al., 1997
Adrenomedullin (vascular tone)	Nguyen and Claycomb, 1999
Endothelin-1 (vascular tone)	Hu et al., 1998
<i>Anaerobic energy: glucose uptake and glycolysis</i>	
Glucose transporter 1 (glucose uptake)	Ebert et al., 1995; Okino et al., 1998
Phosphoglycerate kinase 1 (glycolysis)	Semenza et al., 1994
Aldolase A (glycolysis)	Semenza et al., 1994; 1996
GAPDH (glycolysis)	Graven et al., 1999
Lactate dehydrogenase A (glycolysis)	Firth et al., 1995
<i>Various</i>	
Retrotransposon VL30	Estes et al., 1995
P35srj (HIF-1 feedback regulation)	Bhattacharya et al., 1999
Collagen prolyl-4-hydroxylase α (I)	Takahashi et al., 2000
ETS-1 (transcription factor)	Oikawa et al., 2001
IGFBP-1 (growth factor)	Tazuke et al., 1998

properties, such as heterodimerization with HIF-1 β and DNA-binding to the same DNA sequence in vitro (Semenza, 1999), but HIF-3 α contains only one transactivation domain (TAD). Despite these similarities, neither HIF1 $\alpha^{-/-}$ nor HIF2 $\alpha^{-/-}$ embryos can survive, suggesting the lack of functional complementation in vivo within the HIF- α family.

Moreover, several HIF-1 α variants have been reported. Of particular interest are splice variants HIF-1 α^{516} , HIF-1 α^{557} , HIF-1 α^{735} that terminate respectively at codon 516, 557, and 735, resulting in the absence of both N-TAD and C-TAD or of C-TAD only (Chun et al., 2002; 2001). However, the biological significance of these isoforms is unclear yet. In addition, a novel inhibitory PAS protein (IPAS) (Fig. 1), a splice variant of HIF-3 α has recently been identified (Makino et al., 2001). IPAS lacks a transactivation domain, but remains the capability to dimerize with HIF-1 β , thus serving as a natural HIF antagonist. IPAS is strongly expressed in the corneal epithelium of the eye, an organ where HIF-dependent angiogenesis is suppressed despite profound tissue hypoxia. By contrast, in the mouse heart and lung tissues *IPAS* mRNA is hypoxia regulated, indicating a negative feedback mechanism that controls HIF-1 α activity (Makino et al., 2002).

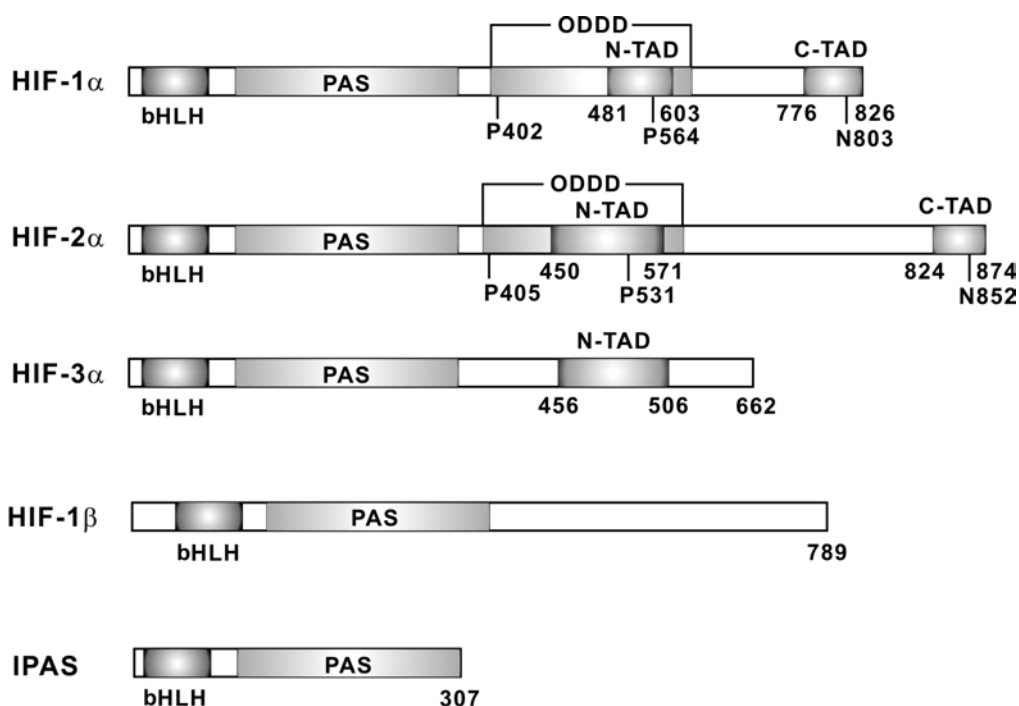


Figure 1. Schematic representation of HIF-1 α , HIF-2 α , HIF-3 α , HIF-1 β , and IPAS. HIF, hypoxia inducible factor; bHLH, basic helix-loop-helix domain; PAS, Per-ARNT-Sim; ODDD, oxygen-dependent degradation domain; N-TAD, N-terminal transactivation domain; C-TAD, C-terminal transactivation domain; P, proline, which can be hydroxylated by PHDs; N, asparagine, which can be hydroxylated by FIH.

The close structural homologues of the ARNT molecule, ARNT2 and ARNT3 (also called member of PAS3, MOP3 or brain and muscle ARNT-like protein-1, BMAL-1), may also play roles as β -class partners of the HIF α -subunits. The ARNT2 protein shares 81% identity with ARNT in the bHLH-PAS domains (Hirose et al., 1996) and has been shown to be able to substitute for ARNT directing HIF to HREs in DNA binding assays (Hogenesch et al., 2000). Thus, ARNT2 was predicted to be a second partner of HIF α -subunits *in vivo*. ARNT3 was originally cloned in EST screens for novel PAS encoding cDNAs (Hogenesch et al., 1997). It has homology with the ARNT protein in both bHLH and PAS domains for about 66% and 40% identity, respectively. Although ARNT3 and HIF-1 α are coexpressed in a number of tissues, ARNT3 is a fairly weak dimerization partner of the HIF α -subunits (Hogenesch et al., 1998). Thus, it is unclear if ARNT3 plays a significant role in hypoxia signal transduction.

1.2.2 Regulation of HIF-1

Both HIF-1 α and HIF-1 β mRNA appears to be uniquely expressed in mammalian cells. By contrast, the HIF-1 α protein responds to changes in oxygen tension, while HIF-1 β is insensitive to hypoxia. So, the biological activity of HIF-1 is determined by the protein level and activity of the HIF-1 α subunit. In addition to the physiological trigger, hypoxia, HIF-1 α activity is also known to be evoked by certain transition metals (Co²⁺, Ni²⁺, Mn²⁺), iron chelation, and certain growth factors and cytokines. Thereby, the regulation of HIF-1 α occurs at multiple levels, including mRNA expression, protein stabilization, trans-activation and nuclear translocation.

HIF-1 α mRNA regulation: It is believed that HIF-1 α mRNA is constitutively expressed in cultured cells independent of oxygen tensions (Wenger et al., 1996; 1997). The regulation of HIF-1 α expression occurs mainly on the post-translational level. However, many growth factors and cytokines such as insulin, interleukin 1 β (IL-1 β), tumor necrosis factor α (TNF- α), endothelial growth factor (EGF), transforming growth factor-1 β (TGF-1 β) and hepatocyte growth factor (HGF) were found to activate HIF-1 α under normoxia via up-regulating its mRNA expression (Bilton and Booker, 2003). Of note, the induction of HIF-1 α by hypoxia is far greater than by growth factors and cytokines, and effects of the two stimuli are additive (Fukuda et al., 2002). Given that the prolyl (and presumably the asparaginyl) hydroxylase enzymes (PHDs and FIH-1) are believed not to be at high concentration within the cell (Epstein et al., 2001), increasing the availability of their HIF-1 α substrate may easily titrate them out, thereby leading to HIF-1 α target gene expression. Moreover, *in vivo* studies have also shown that HIF-1 α mRNA expression is induced by hypoxia or ischemia indicating that

the regulation of HIF-1 α at the transcriptional level is needed for its full activation under such conditions (Yu et al, 1998).

HIF-1 α stabilization: Under normoxia HIF-1 α usually remains undetectable as its half-life is less than 5 min. Proteasomal inhibitors or mutation of the ubiquitin-activating enzyme E1 stabilize HIF1 α , demonstrating that HIF-1 α is degraded through the ubiquitin-proteasome pathway (Salceda et al, 1997). Furthermore, the degradation of HIF-1 α is dependent on the intact ODDD. The ODDD-deleted HIF-1 α is stable and constitutively active (Huang et al., 1998). Interestingly, HIF-1 α is also stable in cells lacking a functional von Hippel-Lindau tumor suppressor protein (pVHL), and expression of wild-type *VHL* restores HIF-1 α instability (Maxwell et al., 1999). Therefore, the specific HIF-1 α degradation under normoxia requires binding of VHL, which, in a complex with elongin B, elongin C, and Cul2, acts as the particle recognition protein for an E3 ubiquitin ligase in HIF-1 α polyubiquitination and followed proteolysis (Ohh et al., 2000; Tanimoto et al., 2000).

As mentioned before, prolyl residues (Pro402 and Pro564) in the ODDD of HIF-1 α can be modified through hydroxylation by PHDs in the presence of oxygen. Structures of HIF-1 α -VHL complexes have elucidated a strict requirement for HIF-1 α hydroxyproline in VHL binding (Hon et al., 2002; Min et al., 2002). Both Pro402 and Pro564 occur in the sequence Leu-X-X-Leu-Ala-Pro, but the two leucines and the alanine are not required for hydroxylation. Mutation of either proline alone only partially stabilizes HIF-1 α , whereas mutation of both prolines markedly increases its stability (Yu et al., 2001). So far, VHL-mediated degradation is regarded as the most critical mechanism for physiological regulation of HIF-1 α (Fig. 2). In addition, recent research has suggested that different mechanisms exist in cells for the regulation of HIF-1 α stability. Arrest-defective 1 (ARD-1), as a protein acetyltransferase, has been shown to directly bind to HIF-1 α and regulate its stability (Jeong et al., 2002). ARD-1 acetylates Lys532 in the ODDD of HIF-1 α and thereby accelerates HIF-1 α interaction with VHL. It has also been demonstrated that ARD-1, as a negative regulator of HIF-1 α stability, functions mainly under normoxic conditions due to decreased ARD-1 mRNA and a decreased affinity to HIF-1 α under hypoxia.

HIF-1 α transcriptional activity: Transcriptional activation is another key step that regulates HIF-1 α activity. HIF-1 α possesses two transcriptional activation domains, N-TAD and C-TAD. They confer transcriptional activation of target genes mainly by the recruitment of general transcriptional co-activators including p300/CBP, SRC-1, or TIF-2 (Arany et al., 1996; Carrero et al., 2000). The transcriptional activity of the C-TAD is hypoxia-inducible. This response is, at least in part, attributable to hypoxia-induced p300/CBP binding, which is governed by

hydroxylation of Asn803 in HIF-1 α (Dames et al., 2002; Lando et al., 2002). As mentioned before, the asparaginyl hydroxylation is catalyzed by FIH-1. Under normoxia, hydroxylated Asn803 prevents p300/CBP binding, whereas hypoxia inhibits the activity of FIH-1, thereby enhancing p300/CBP interaction and up-regulating target gene expression (Fig. 2).

However, this hypothesis is difficult to reconcile with the observation that a stable HIF-1 α mutant under normoxia is able to transcriptionally activate target genes in both cell cultures and animal models (Elson et al., 2001). Furthermore, over-expression of FIH-1 inhibits HIF-1 α transcriptional activity under both normoxic and hypoxic conditions, indicating that other mechanisms may be involved in this process, i.e. FIH-1 could recruit histone deacetylases, directly or via pVHL, hence counteracting the recruitment of the histone acetylase p300/CBP (Mahon et al., 2001). In addition, the redox-sensitive cysteine residue Cys800 in the C-TAD of

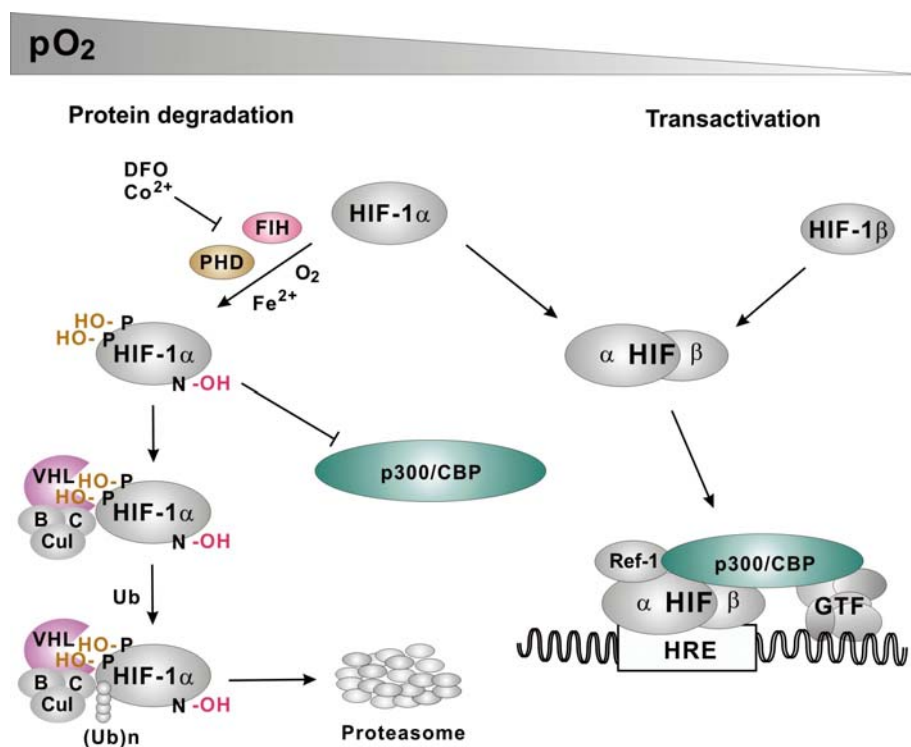


Figure 2. Regulation of HIF-1 α by hydroxylases. Under normoxia, the key proline and asparagine residues are hydroxylated by PHD and FIH, respectively. The hydroxylated proline residues permit the VHL binding, thereby triggering the ubiquitin conjugation and proteasomal degradation of HIF-1 α . The hydroxylated asparagine prevents the binding of p300/CBP to HIF-1 α . Under hypoxia, HIF-1 α is stabilized, translocates into the nucleus and interacts with HIF-1 β to form HIF-1. HIF-1 binds to the HRE in the target genes. Together with the other GTF, it starts the transcriptional machinery. PHD, prolyl hydroxylase domain; FIH, factor-inhibiting HIF-1; VHL, von-Hippel-Lindau; Ub, ubiquitin; DFO, desferrioxamine; GTF, General transcription factor; HRE, hypoxia responsive element; P, proline; N, asparagine; B, elongin B; C, elongin C; Cul, Cullin-2.

HIF-1 α also affects its transactivity (Ema et al., 1999; Lando et al., 2000). Under hypoxia, reduced thioredoxin may translocate into the nucleus and transmit the redox signal to the redox factor Ref-1, which in turn modifies the cysteine in HIF-1 α C-TAD to facilitate the recruitment of the transcriptional coactivators SRC-1, TIF-2 and p300/CBP (Carrero et al., 2000). Indeed, overexpression of thioredoxin/Ref-1 has been shown to amplify the hypoxic signal (Huang et al., 1996). However, the specificity of thioredoxin/Ref-1 in maintaining HIF-1 α in the reduced state as part of the hypoxia-signaling mechanism awaits further clarification.

Nuclear localization of HIF-1 α : A number of studies have observed that HIF-1 α shifts to the nucleus only under hypoxia, implying a distinct oxygen-regulated step (Kallio et al., 1998; 1999). HIF-1 α contains two nuclear localization signals (NLS) which are located at the N-terminus (aa 17-74) and within the C-terminus (aa 718-721), respectively. It was found that the C-terminal NLS motif plays a critical role in mediating hypoxia-inducible nuclear import of HIF-1 α , whereas the N-terminal one may be less important (Kallio et al., 1998, Luo and Shibuya, 2001). Hypoxia might activate nuclear translocation of HIF-1 α by a so far unknown mechanism, but overexpressed HIF-1 α constitutively localizes to the nucleus under normoxic conditions (Hofer et al., 2001). The p14^{ARF} tumor suppressor protein was reported to sequester HIF-1 α into the nucleolus, thereby inhibiting its transactivation function (Fatyol et al., 2001). Therefore, nuclear translocation might be regulated by normoxic inhibition rather than hypoxic activation, and overexpression of HIF-1 α might saturate this inhibition mechanism (Groulx and Lee, 2002; Kallio et al., 1998).

HIF-1 DNA binding and transcriptional complex: Once stabilized and activated under hypoxia, HIF-1 binds to the core sequence R(A/G)CGTG present in the HREs of many oxygen regulated genes (Camenisch et al., 2001). One HRE is necessary but not sufficient for efficient hypoxic gene activation. Multimerization of HREs has been found in the genes encoding several glycolytic enzymes such as glucose transporter 1 (Wenger, 2000). In fact, a functional HRE usually contains neighboring DNA binding sites for additional transcription factors. Although these elements are not involved in the hypoxic induction procedure, they might amplify the hypoxic response or confer tissue-restricted activity to a HRE. Examples include HIF-1 cooperation with the ATF-1/CREB-1 factor at the lactate dehydrogenase A gene (Firth et al., 1995), and with AP-1 at the VEGF gene (Damert et al., 1997), as well as with the orphan receptor hepatic nuclear factor-4 (HNF-4) at the EPO gene (Galson et al., 1995). The molecular mechanism of the interaction between these distinct transcription factors is manifested by the cooperative binding of p300/CBP because high-affinity binding of p300/CBP requires more than one protein-protein interaction (Ebert et al., 1998). Thus, only

the HRE confers hypoxic inducibility, the other elements are required to form a fully functional transcriptional enhancer complex.

1.3 Reactive oxygen species (ROS) as messengers

Reactive oxygen species (ROS) such as superoxide anion radicals and hydrogen peroxide are known to serve as signal transducers in several systems. Because oxygen is the main component of these molecules, it seems obvious that their concentration depends upon the environmental oxygen concentration. It has been reported that the hydrogen peroxide (H_2O_2) concentration is higher under normoxia and lower under hypoxia in hepatocytes and hepatoma cells (Kietzmann et al., 1996, Fandrey et al., 1994). Exogenous H_2O_2 could destabilize HIF-1 α , which led to inhibition of the hypoxic induction of EPO (Huang et al., 1996; Fandrey et al., 1997). Our previous studies also confirmed that ROS might serve as messengers in the O_2 -dependent expression of several enzymes involved in glucose metabolism, such as phosphoenolpyruvate carboxykinase 1 (PCK1) and glucokinase (GK) (Kietzmann et al., 1996; 1997). This model is compatible with the finding that treatment of healthy human volunteers with the antioxidant N-acetylcysteine (NAC) enhanced the hypoxic ventilatory response (HVR) and blood EPO concentration, which is similar to a typical response to hypoxia (Hildebrandt et al., 2002).

Moreover, H_2O_2 , which is a noncharged molecule, can freely cross the membranes and participate in one- and two-electron transfer reactions. Although it has been predicted to be an ideal candidate for an intracellular second messenger from the O_2 sensor, H_2O_2 itself is a relatively inert reaction partner, and cellular H_2O_2 levels are usually tightly controlled. Therefore, its degradation products are of great importance. H_2O_2 is degraded by glutathione peroxidase in the cytosol and mitochondria or by catalase in peroxisomes. In addition, H_2O_2 can be nonenzymatically converted into hydroxyl anions (OH^-) and hydroxyl radicals ($\text{OH}\bullet$) in the presence of Fe^{2+} in a Fenton reaction ($\text{H}_2\text{O}_2 + \text{Fe}^{2+} \rightarrow \text{Fe}^{3+} + \text{OH}^- + \text{OH}\bullet$). Since glutathione peroxidase ($K_m = 100 \mu\text{M}$) and catalase ($K_m = 100 \text{mM}$) require relatively high H_2O_2 concentrations, it appears conceivable that lower concentrations of H_2O_2 may be nonenzymatically converted into OH^- and $\text{OH}\bullet$. The $\text{OH}\bullet$ is highly reactive, with a diffusion area of only a few Angstrom and could be generated in the ultimate vicinity of Fe-containing residues of proteins or even transcription factors and directly react at its site of generation with Fe-S clusters or cysteine residues of regulatory proteins (Porwol et al., 1998). Thus, the Fenton reaction is potentially of great importance in the O_2 signaling cascade (Fig. 3). According to this model, hydroxyl radical concentrations achieved under normoxia would

inactivate HIF-1 α , which is relieved from suppression following a decrease in radical concentrations under hypoxic conditions. A prototype factor for such a mechanism is the iron regulatory protein 2, which is oxidized in an oxygen-dependent manner, ubiquitinated and degraded by the proteasomes in iron-depleted cells (Iwai et al., 1998).

The involvement of such a Fenton reaction in the oxygen signaling pathway has been suggested in studies investigating the hypoxia-dependent EPO gene expression in HepG2 cells (Fandrey et al., 1997) and in the reciprocal modulation by O₂ of the PCK and GK expression (Kietzmann et al., 1998). Furthermore, using confocal laser microscopy and three-dimensional reconstruction, such a Fenton reaction has been localized in a perinuclear space, where granules with high iron concentrations could also be detected. However, it remains open in which cellular compartment the Fenton reaction takes place and whether transcription factors regulating the O₂-dependent gene expression, such as HIF-1 α , are also located in this compartment.

1.4 Aim of the work

Based on the possible involvement of ROS and a Fenton reaction in the oxygen signaling pathway and the crucial role of HIF-1 α in hypoxia inducible gene expression, it was the aim of this study to identify the compartment in which the Fenton reaction takes place and to investigate whether HIF-1 α is localized in the same compartment. Furthermore, the effects of a compartment-specific inhibition of OH• generation or interference with the integrity of the compartment should then be studied with respect to the HIF-1-dependent gene expression.

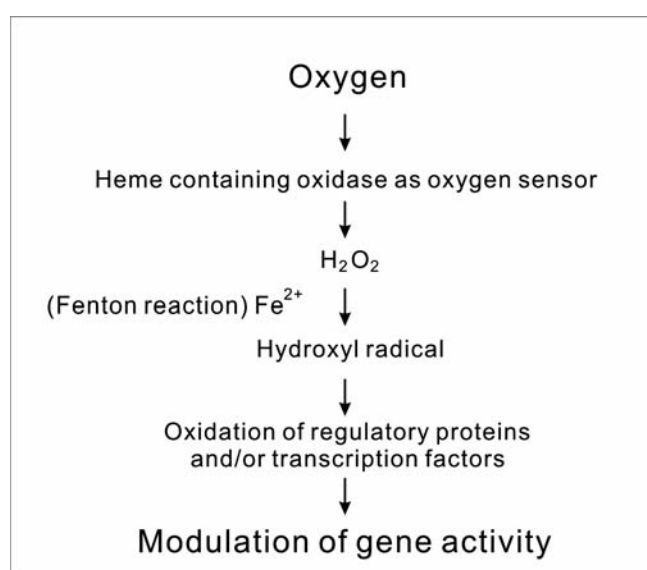


Figure 3. Oxygen sensing for the modulation of gene activation (hypothesis).

2. Materials

2.1 Animals

Male Wistar rats (180-280 g body weight) (Winkelmann, Borchten/Westfalen) were used for the preparation of hepatocytes. Animals were kept according to the German legislation on the protection of animals with a 12 h day and night rhythm (dark phase: 19 h - 7 h) at least 6 days before used for experiments. They had free access to water and food (rat diet "ssniff", Fa. Spezialitäten GmbH, Soest/Westfalen) at a room temperature of 19 - 23°C. They usually had a 30-40 g gain of weight per week. The preparation of hepatocytes was performed during the first 3 h of the light phase after rats were anesthetized by intraperitoneal injection of nembutal (80 mg/kg body weight).

2.2 Bacterial strains, vectors and plasmid constructs

2.2.1 Bacterial strains

Two bacterial *E. coli* K 12 strains DH5 α and XL1-blue (Stratagene) were used for plasmid transformation and *E. coli* BL21 (DE3) was used for protein expression.

2.2.2 Vectors

pBS-KSII vector

The vector pBluescript (pBS-KS II) (Stratagene, Heidelberg) was used for the cloning and sequencing of DNA fragments as well as for *in vitro* transcription of RNA. It contains ColE1 ori for the replication in *E. coli*; the ampicillin resistance gene for antibiotic selection; f1 ori for single strand DNA production; the LacZ gene encoding β -galactosidase which provides the possibility for blue/white color selection of recombinant clones; a multiple cloning site (MCS); T3 and T7 RNA polymerase promoters for the *in vitro* transcription; and primer sequences (universal and reverse primers) for DNA sequencing (Fig. 4).

pCRII-TOPO vector

The vector pCRII-TOPO (Invitrogen) was used in the experiments for the cloning and sequencing of PCR products as well as for *in vitro* transcription of RNA. Similar to pBS-KSII, pCRII-TOPO also contains ColE1 ori, f1 ori, MCS and LacZ gene. The difference is that pCRII-TOPO contains Sp6 and T7 RNA polymerase promoters for *in vitro* transcription and both an ampicillin resistance gene (Amp^r) and a Kanamycine resistance gene (Kan^r) for antibiotic selection (Fig. 5).

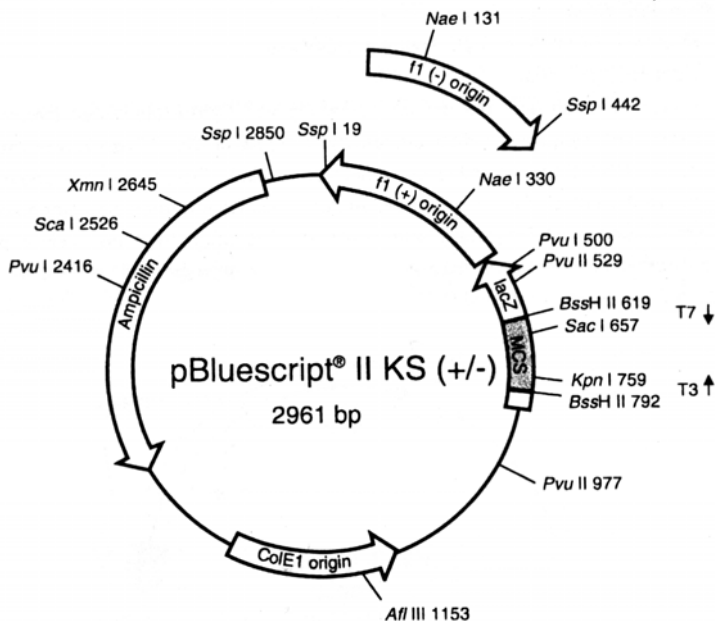


Figure 4. Structure of the pBluescript vector (pBS-KSII). Amp^r, gene conferring ampicillin resistance in *E. coli*; f1 ori, origin of replication derived from filamentous phage; ColE1 ori, origin of replication in *E. coli*. LacZ, gene encoding β -galactosidase for blue/white selection; MCS, multiple cloning sites. Arrows with the Amp^r gene, LacZ gene, T3 and T7 promoters indicate the direction of transcription; the arrow in the f1 ori indicates the direction of ssDNA strand synthesis.

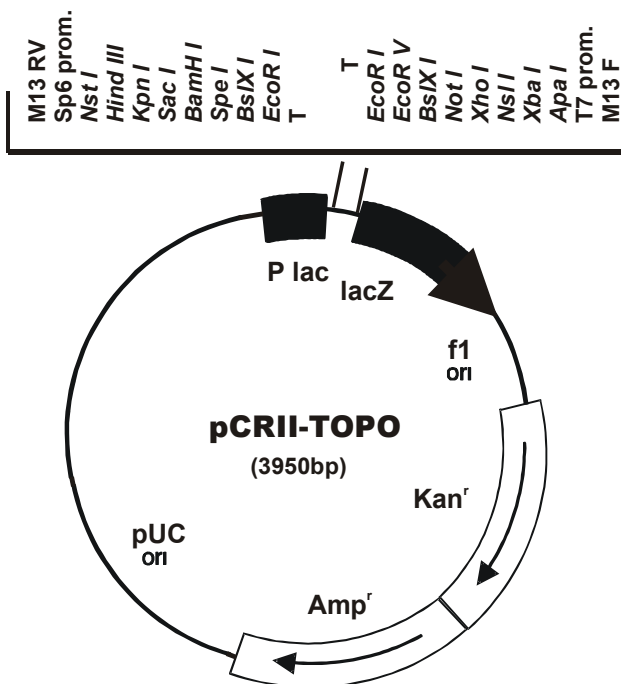


Figure 5. Structure of the plasmid pCRII-TOPO. Amp^r and Kan^r, the ampicillin and kanamycin resistance genes; P lac, lac promoter; LacZ, gene encoding β -galactosidase. The multiple cloning site is flanked by Sp6 and T7 promoters and by the sequences for universal and reverse sequencing primers.

2.2.3 pECFP and pDsRed mammalian expression constructs

pECFP-Golgi, pECFP-Mito, pECFP-ER

Plasmids pECFP-Golgi, pECFP-Mito and pECFP-ER (Clontech) were used for fluorescent labeling of Golgi apparatus, mitochondria and endoplasmic reticulum (ER) in mammalian cells, respectively. In these constructs, there are specific signal sequences which can target the expressed fusion protein to the respective intracellular compartments. In pECFP-Golgi, the Golgi targeting sequence encodes the N-terminal 81 amino acids of human 1,4-galactosyltransferase (GT) (Fig. 6). In pECFP-Mito, the mitochondrial targeting sequence is from 29 amino acids of human cytochrome c oxidase subunit VIII (Fig. 7). In pECFP-ER, the ER targeting sequence of 16 amino acids from calreticulin and 8 amino acids from ER retrieval sequence KDEL, are encoded (Fig. 8). ECFP's fluorescence excitation maxima is from 433 nm to 453 nm and the emission maxima is from 475 nm to 501 nm.

The expression of the fusion protein is guaranteed by the immediate early cytomegalovirus promoter ($P_{CMV\ IE}$) and SV40 polyadenylation signals in these constructs. In addition, the vector backbone also contains a neomycin resistance cassette (Kan^r/Neo^r) consisting of the SV40 early promoter, the neomycin/kanamycin resistance gene of Tn5, and polyadenylation signals from the herpes simplex virus thymidine kinase (HSV-TK) gene which allows selection of stably transfected eukaryotic cells by G418. A bacterial promoter upstream of this cassette drives expression of the kanamycin resistance gene in *E. coli*. The backbone also provides a pUC origin of replication for propagation in *E. coli* and f1 origin for production of single-strand DNA.

pDsRed-Golgi, pDsRed-Mito, pDsRed-ER

Plasmids pDsRed-Golgi, pDsRed-Mito and pDsRed-ER were also used for the fluorescent labeling of Golgi apparatus, mitochondria and endoplasmic reticulum (ER) in mammalian cells, respectively. These constructs were generated by replacing the ECFP-sequence in pECFP-Golgi, pECFP-Mito and pECFP-ER with the DsRed-sequence from pDsRed1-1 (Clontech). For the construction of pDsRed-Golgi and pDsRed-Mito, the replacement was achieved by excising the ECFP-sequence with the restriction endonuclease BamHI/NotI and subsequent ligation of the BamHI/NotI DsRed-fragment. For the construction of pDsRed-ER, the DsRed cDNA fragment was amplified by PCR using pDsRed1-1 as template (Primers were described in 2.3.2, method was described in 3.1.1). The PCR product was ligated into the NheI/BglIII sites of pECFP-ER, thereby replacing the ECFP. DsRed's fluorescence excitation maximum is 558 nm and the emission maximum is 583 nm.

pDsRed2-Peroxi and pDsRed-lysosome

The plasmid pDsRed2-Peroxi (Clontech) was used for the fluorescent labeling of peroxisomes in mammalian cells. It is a mammalian expression vector that encodes a fusion of *Discosoma* sp. Red fluorescent protein (DsRed 2) and the peroxisomal targeting signal 1 (PTS 1) at the 3' end. The PTS1 sequence encodes the tripeptide SKL, which targets the DsRed2-PST1 fusion protein to the matrix of peroxisomes. The backbone of this construct is the same as in the other fluorescent constructs described above (Fig. 9).

The plasmid pDsRed-lysosome was a kind gift from Dr. Stefan Höning. It was used for fluorescent labeling of lysosomes in mammalian cells. It is a mammalian expression vector that encodes a fusion of DsRed protein and 351 amino acids from the lysosomal targeting signal. The backbone of this construct is the same as in the other fluorescent constructs described above.

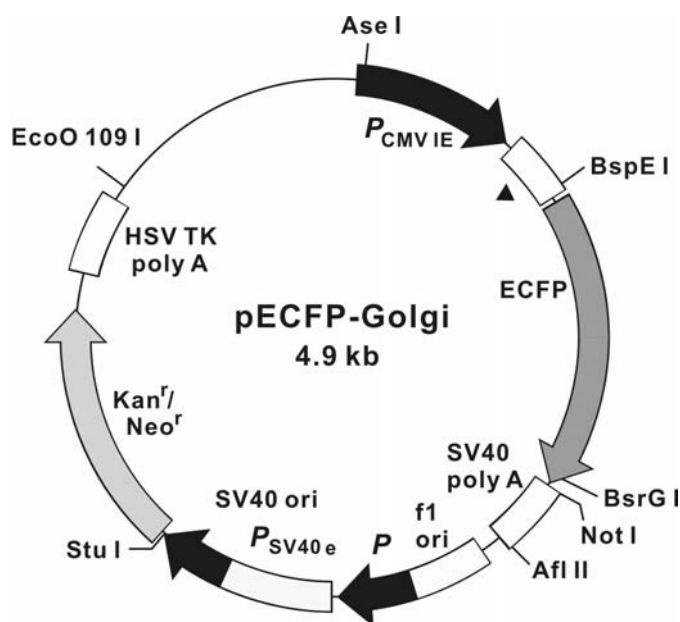


Figure 6. Structure of the construct pECFP-Golgi. This construct encodes a fusion protein consisting of ECFP and the Golgi targeting sequence from the N-terminal 81 amino acids of human 1,4-galactosyltransferase at the 5'-end (\blacktriangle). $P_{CMV IE}$, immediate early cytomegalovirus promoter; SV40 poly A, SV40 polyadenylation signal; P_{SV40} , SV40 promoter; Kan^r/Neo^r , the neomycin/kanamycin resistance gene of Tn5; HSV TK poly A, polyadenylation signals from the herpes simplex virus thymidine kinase; Arrows with the ECFP gene and Kan^r/Neo^r gene indicate the direction of transcription; the arrow in the f1 ori indicates the direction of single-strand DNA synthesis.

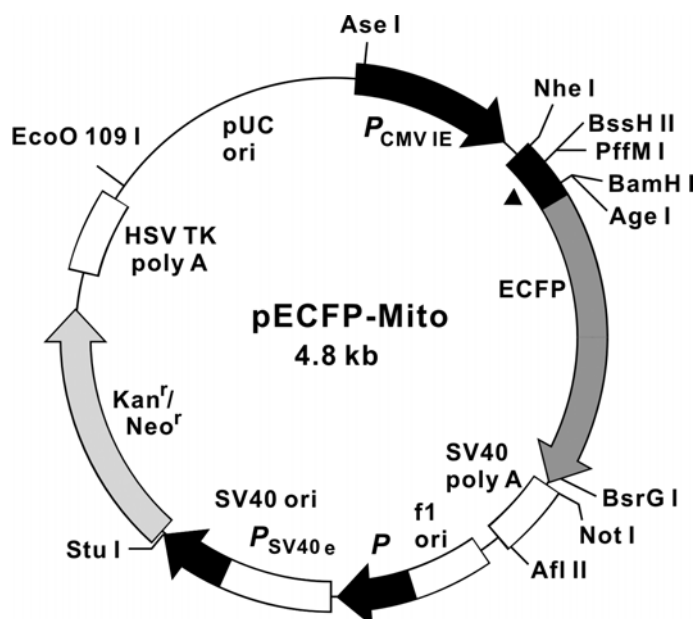


Figure 7. Structure of the construct pECFP-Mito. The construct encodes a fusion protein consisting of ECFP and the mitochondrial targeting sequence from subunit VIII of human cytochrome c oxidase (\blacktriangle). $P_{CMV IE}$, immediate early cytomegalovirus promoter; SV40 poly A, SV40 polyadenylation signal; P_{SV40} , SV40 promoter; Kan^r/Neo^r, the neomycin/kanamycin resistance gene of Tn5; HSV TK poly A, polyadenylation signals from the herpes simplex virus thymidine kinase; the arrow in the f1 ori indicates the direction of single-strand DNA synthesis.

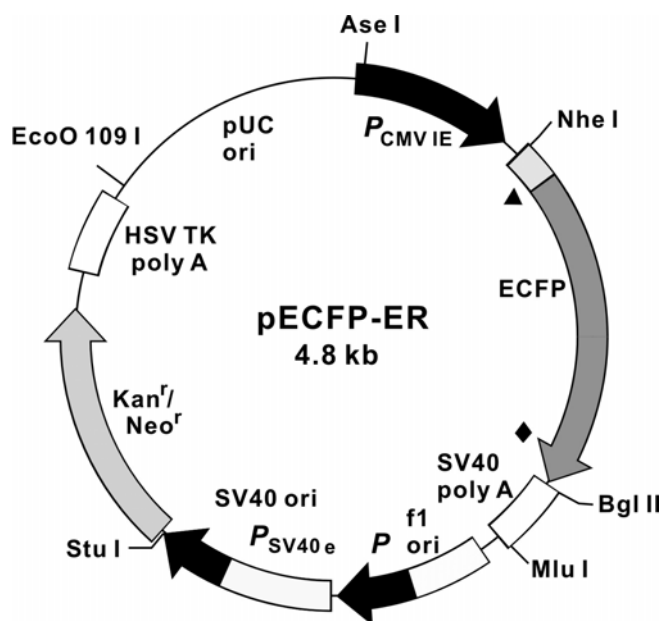


Figure 8. Structure of the construct pECFP-ER. The construct encode a fusion protein consisting of ECFP, the ER targeting sequence of calreticulin cloned at the 5' end (\blacktriangle), and the sequence encoding the ER retrieval sequence, KDEL, cloned at the 3' end (\blacklozenge). $P_{CMV IE}$, immediate early cytomegalovirus promoter; SV40 poly A, SV40 polyadenylation signal; Kan^r/Neo^r, the neomycin/kanamycin resistance gene of Tn5; HSV TK poly A, polyadenylation signals from the herpes simplex virus thymidine kinase; the arrow in the f1 ori indicates the direction of single-strand DNA synthesis.

2.2.4 pGL3-basic constructs

pGL3-hPAI-Luc and pGL3-hPAI-M2-Luc

The pGL3-basic vector (Promega, Fig. 10) was used for the construction of the human PAI-1 promoter constructs pGL3-hPAI-luc and pGL3-hPAI-M2-Luc. The corresponding regions of the human PAI-1 promoter with or without HRE-2 mutation (Fig. 11) were cloned in the MCS of pGL3-basic vector and were already used in the laboratory. The vector contains the firefly luciferase gene (*luc +*) as a reporter gene to quantitatively estimate the promoter activity; polyadenylation signals to stabilize the expressed *luc* mRNA; the gene responsible for ampicillin resistance and *f1 ori* for the production of single-stranded DNA (ssDNA) *in vitro*.

2.2.5 pGL3-Promoter constructs

pGL3-Epo-HRE, pGL3-Epo-HREm

The pGL3 promoter vector (Promega, Fig. 12) was used for the construction of pGL3-Epo-HRE and pGL3-Epo-HREm. The vector contains the SV40 promoter and firefly luciferase gene with the polylinker in front of them. It provides the basis to quantitatively analysis the activity of inserted enhancers. Three copies of either the HRE or a mutated HRE from the erythropoietin gene (Fig. 13) were cloned in the polylinker of the vector to construct pGL3-Epo-HRE (Semenza et al., 1992) and pGL3-Epo-HREm (Goerlach et al., 2003) which were already used in the laboratory.

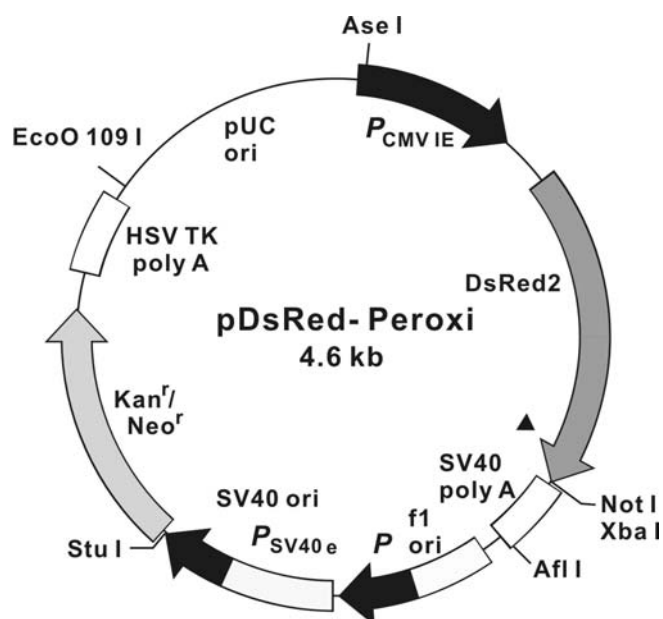


Figure 9. Structure of the construct pDsRed2-Peroxi. The construct encodes a fusion protein consisting of DsRed2 and the peroxisomal targeting signal (PST 1) at the C terminus (▲). The vector backbone in this construct is the same as in p ECFP-Golgi.

2.2.6 Other constructs used in the experiments

pGFP-HIF1 α

The construct pGFP-HIF1 α (Kallio et al., 1998) was used to identify the localization of HIF-1 α under both normoxia and hypoxia. This construct contains a fusion of the green fluorescent protein (GFP) cDNA at the 5'-end and the HIF1 α cDNA at the 3'-end. The expression of the fusion protein is enabled by the CMV promoter, SV40 enhancer, and SV40 poly (A) signal. It was constructed as follows: the BamH I-Not I (Not I site filled in with Klenow) fragment of HIF-1 α was ligated into the BamH I-Nhe I (Nhe I site filled in with Klenow) opened GFP vector (Fig. 14).

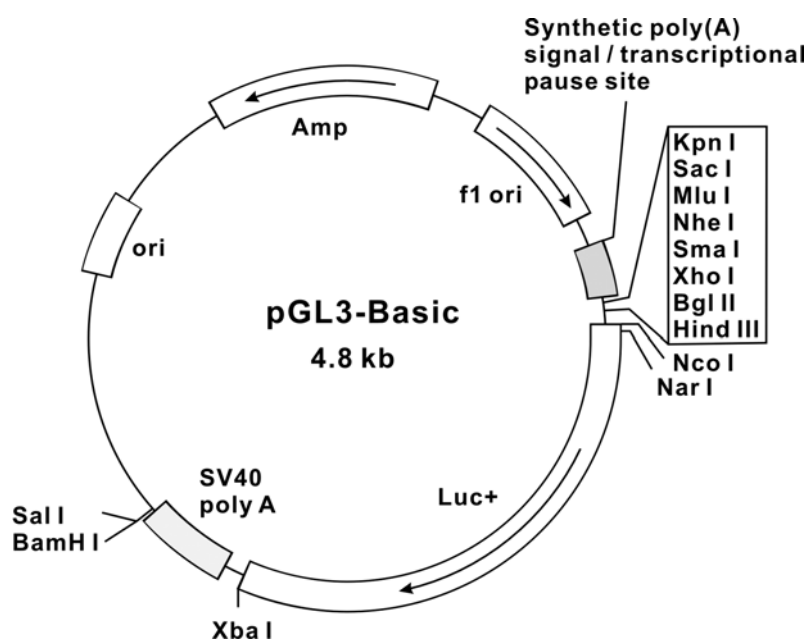


Figure 10. Structure of the pGL3-basic vector. luc⁺, cDNA encoding the modified firefly luciferase; Amp^r, gene conferring ampicillin resistance in *E. coli*; f1 ori, origin of replication derived from filamentous phage; ori, origin of replication in *E. coli*. Arrows within luc⁺ and the Amp^r gene indicate the direction of transcription; the arrow in the f1 ori indicates the direction of single-strand DNA (ssDNA) strand synthesis.

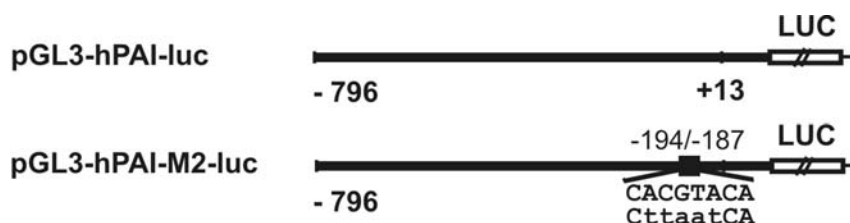


Figure 11. The fragments of human PAI-1 promoter. The human PAI-1 promoter (-806 - +19, according to the transcription start point) was cloned into the pGL3-basic vector. In the construct pGL3-hPAI-M2-Luc, the sequence (-194/-187) corresponding to the hypoxia responsible element is shown on the upper strand in capital letter, mutations are in lowercase letters.

pCMV-HA-VHL

The construct pCMV-HA-VHL (Fig. 15) was used to translate the von Hippel-Lindau (VHL) protein in a reticulocyte lysate system (Promega). It is a kind gift from Dr. Patrick Maxwell. The construct encodes a HA-VHL fusion protein driven by the CMV promoter. In addition, it also contains a neomycin resistance cassette (Kan^r/Neo^r) consisting of the SV40 early promoter, the neomycin/kanamycin resistance gene of Tn5, and polyadenylation signals from the herpes simplex virus thymidine kinase (HSV-TK) gene which allows the selection of stably transfected eukaryotic cells by using G418. A bacterial promoter upstream of this cassette drives expression of the gene encoding kanamycin resistance in *E. coli*. The backbone also provides a ColE1 origin of replication for propagation in *E. coli*.

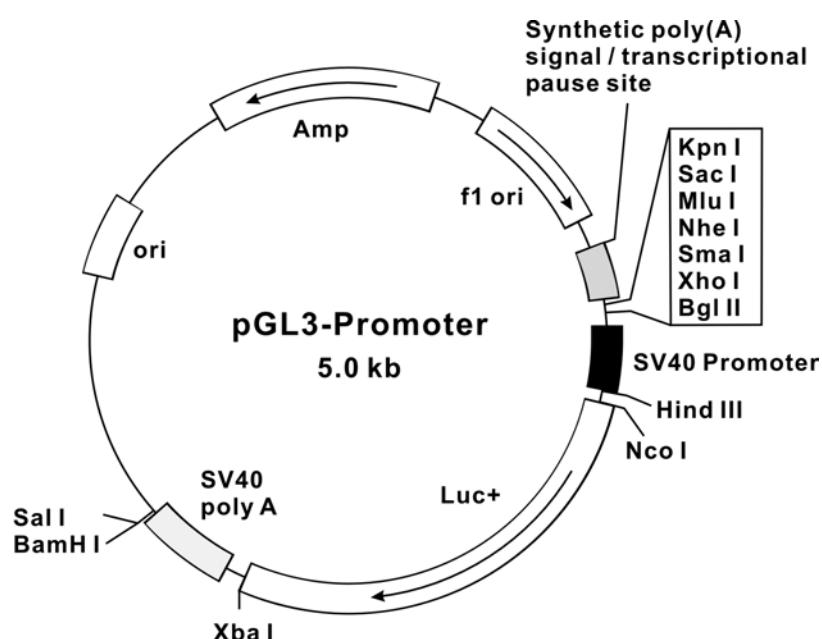


Figure 12. Structure of the pGL3-Promoter vector. *luc+*, cDNA encoding the modified firefly luciferase; Amp^r , gene conferring ampicillin resistance in *E. coli*; *f1 ori*, origin of replication derived from filamentous phage; *ori*, origin of replication in *E. coli*. Arrows within *luc+* and the Amp^r gene indicate the direction of transcription; the arrow in the *f1 ori* indicates the direction of ssDNA strand synthesis.



Figure 13. Sequences of HRE and HREm from the EPO gene. HRE, hypoxia responsive element; HREm, HRE with mutation. The essential sequence for HIF-1 binding is indicated in capital letters and the mutated sites in HREm are underlined. CACAG that is double underlined is necessary help-sequence for HIF-1 action.

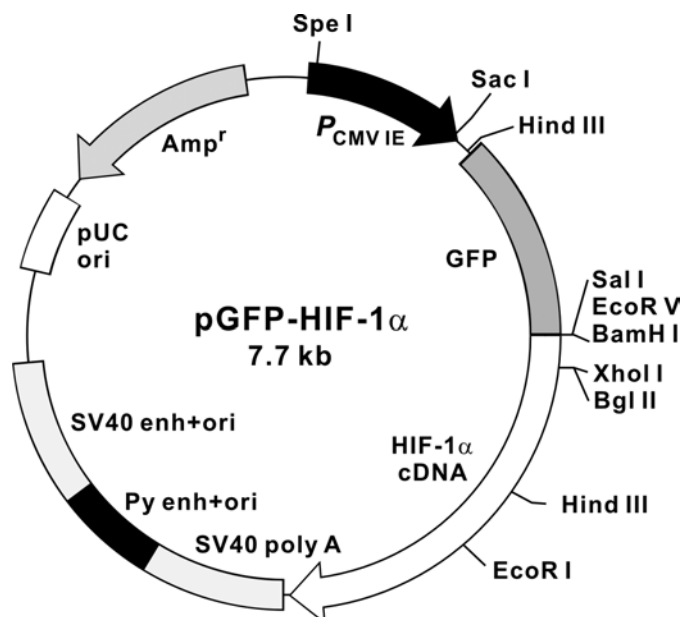


Figure 14. Structure of the pGFP-HIF-1 α construct. $P_{CMV IE}$, CMV promoter including enhancer; GFP, green fluorescent protein; SV40 enh+ori, SV40 enhancer with origin of replication in mammalian cells; Amp^r, gene conferring ampicillin resistance in *E. coli*; pUC ori, origin of replication in *E. coli*. Arrows with GFP-HIF-1 α and the Amp^r gene indicate the direction of transcription.

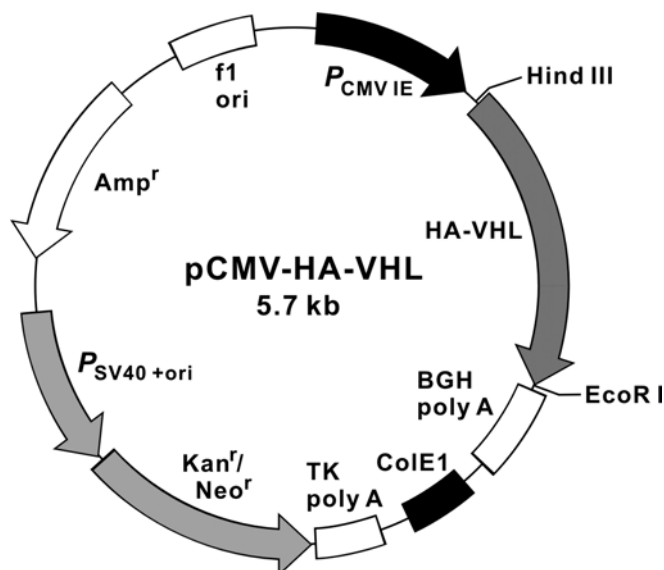


Figure 15. Structure of the pCMV-HA-VHL construct. P_{CMV} , CMV promoter; HA-VHL, HA tagged von Hippel-Lindau, $P_{SV40+ori}$, SV40 promoter with origin of replication in mammalian cells; Amp^r, gene conferring ampicillin resistance in *E. coli*; f1 ori, origin of replication derived from filamentous phage; Arrows within HA-VHL, Kan/Neo^r and the Amp^r gene indicate the direction of transcription; the arrow in the f1 ori indicates the direction of single-strand DNA (ssDNA) strand synthesis.

pGEX-HIF-1 α -TADN

To express the HIF-1 α -TADN protein in *E. coli*, the vector pGEX-5X-1 (Amersham, Fig.16) was used. The pGEX vector provides the basis for inducible, high-level intracellular expression of genes as fusions with *Schistosoma japonicum* glutathione S-transferase (GST) in *E. coli*. Protein expression is under the control of the *tac* promoter, which can be induced by using the lactose analog isopropyl β -D-thiogalactoside (IPTG). An internal *lac I^q* gene contained in the vector guarantees its usage in any *E. coli*. In addition, a Factor X protease recognition site is also included in the vector for cleaving the desired protein from the fusion product. The PCR-amplified 219 bp DNA fragment of rat HIF-1 α -TADN encompassing amino acids 531 to 604 was cloned into the BamH I/Sal I site of pGEX-5X1 for the construction of pGEX-HIF-1 α -TADN (Primers were described in 2.3.2). It has already been used in the laboratory.

pcDNA6-Gal4-HIF1 α TADN, pcDNA6-Gal4-HIF1 α TADNm, pcDNA6-Gal4-HIF1 α TADC, pcDNA6-Gal4-HIF1 α TADCm

The pcDNA6 vector (Invitrogen) was used for the construction of pcDNA6-Gal4-HIF1 α TAD constructs. The vector provides the basis to express foreign proteins in mammalian cells, using the CMV promoter and BGH poly (A) signals. In addition, it also contains the blasticidin resistance gene, which is driven by the EM-7 promoter, for selection of stable transfectants;

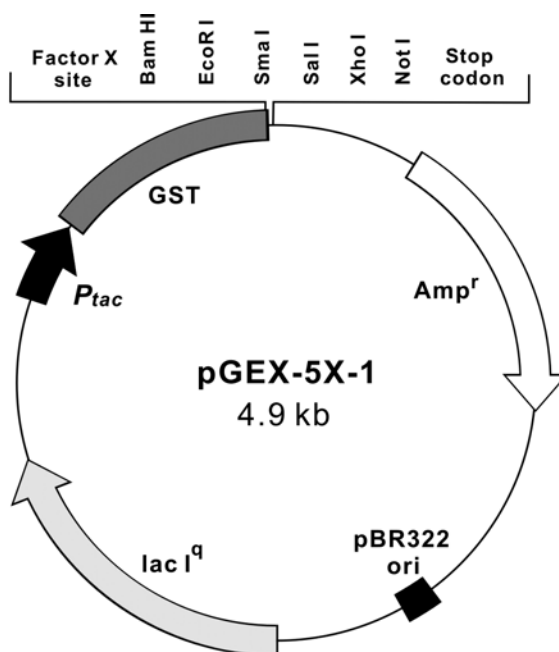


Figure 16. Structure of the pGEX-5X vector. *P_{tac}*, *tac* promoter; GST, Glutathione S-transferase sequence; *Amp^r*, gene conferring ampicillin resistance in *E. coli*; pBR322 ori, origin of replication in *E. coli*; Arrows with *P_{tac}*, *Amp^r* and *lac I^q* indicate the direction of transcription.

the ampicillin resistance gene; the ColE ori, for replication in *E. coli*; the SV40 ori, for replication in mammalian cells; and the f1 ori, for single stranded DNA synthesis *in vitro* (Fig. 17). In pcDNA6-Gal4-HIF1 α TADN, the cDNA encoding a fusion protein of the Gal4 DNA binding domain (aa1-147) and HIF-1 α TADN (aa531-584) was cloned into the MCS of the vector. The pcDNA6-Gal4-HIF1 α TADNm was generated from the wildtype pcDNA6-Gal4-HIF1 α TADN by mutation of proline (P) 564 into alanine (A). In pcDNA6-Gal4-HIF1 α TADC, the cDNA encoding a fusion protein of the Gal4 DNA binding domain (aa1-147) and HIF-1 α TADC (aa772-822) was cloned into the MCS of the vector. The pcDNA6-Gal4-HIF1 α TADCm1 and pcDNA6-Gal4-HIF1 α TADCm2 were generated from the wildtype pcDNA6-Gal4-HIF1 α TADC by mutation of cysteine (C) 800 to serine (S) or asparagine (N) 803 to alanine (A), respectively (Fig. 18). These constructs were already used in our laboratory.

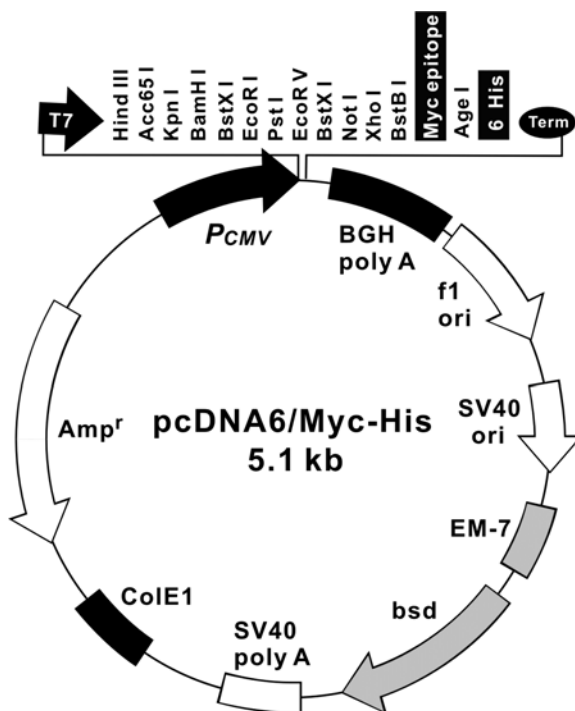


Figure 17. Structure of pcDNA6/Myc-His. P_{CMV} , CMV promoter; bsd, gene conferring blasticidin resistance in mammalian cells; Amp^r , gene conferring ampicillin resistance in *E. coli*; f1 ori, origin of replication derived from filamentous phage; Arrows within the promoters and genes indicate the direction of transcription; the arrow in the f1 ori indicates the direction of ssDNA strand synthesis.

pG₅E1B-luc

The plasmid pG₅E1B-luc was used as reporter construct in the co-transfections with pcDNA6-Gal4-HIF1 α TAD constructs. It contains five Gal4 response elements in front of a weak promoter from the adenovirus E1B gene and the luciferase sequence as the reporter gene. The pG₅E1B-luc provides the basis for functional analyses of transactivities from the expressed protein from pcDNA6-Gal4-HIF1 α TAD constructs (Fig. 18)

2.3 Oligonucleotides

The oligoneocleotides were obtained from NAPS (Göttingen) and were HPLC purified.

2.3.1. Oligonucleotides for sequencing of the plasmidespBS vector

M13 forward: 5'-TGTAACGACGGCCAG-3'

M13 reverse: 5'-ACAGCTATGACCATGATT-3'

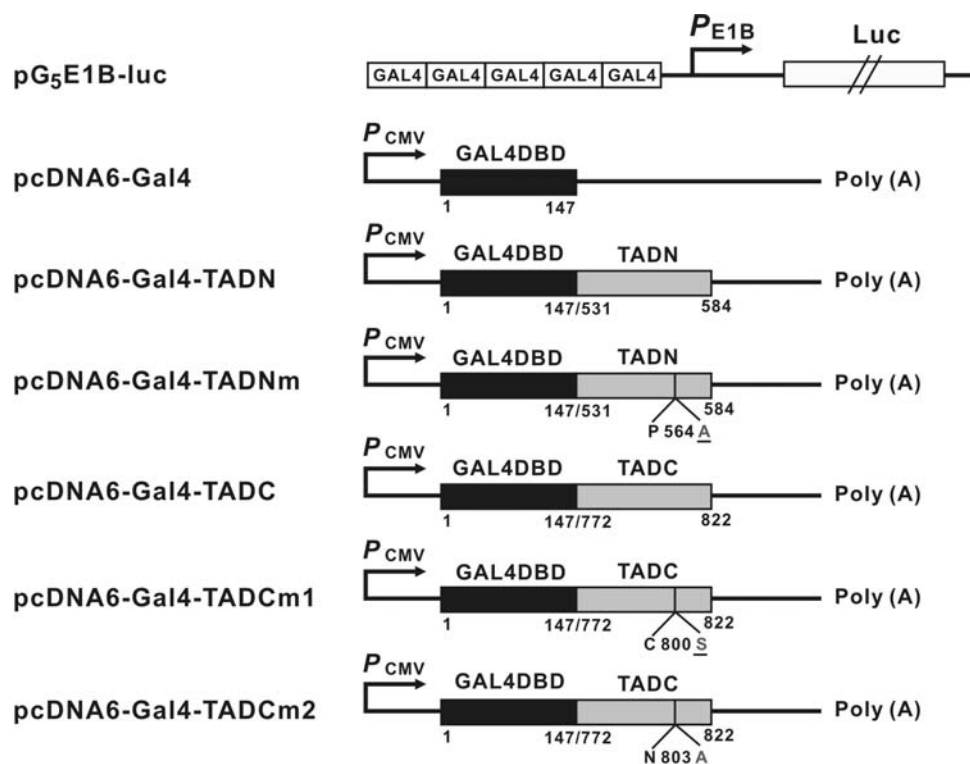


Figure 18. Structure of pG₅E1B-luc and pcDNA6-Gal4-HIF1 α TAD constructs. P_{E1B} , adenovirus E1B promoter; luc, luciferase gene; P_{CMV} , CMV promoter; GAL4DBD, GAL4 DNA binding domain; TADN, N-terminal transactivation domain; TADNm, N-terminal transactivation domain with mutation (proline 564 to alanine). TADC, C-terminal transactivation domain; TADCm, C-terminal transactivation domain with mutation (cysteine 800 to serine, asparagine 803 to alanine).

pGL3 basic vector, pGL3 promoter vector

Forward primer (GL2 primer): 5'-CTTTATGTTTTTGGCGTCTTCC-3'

Reverse primer (RV primer): 5'-CTAGCAAATAGGCTGTCCC-3'

2.3.2. Oligonucleotides for PCR reaction

For the cloning of DsRed-ER fragment:

Forward primer: 5'-AGATCCGCTAGCATGCTGCTATCCGTGCCCGTTGCTGCTC
GGCCTCCTCGGCCTGGCCGTCGCCGTGCGCTCCTCCAAGAACGTCA
TC-3'

Reverse primer: 5'-TTGAATTCGAGATCTTTAACAGCTCGTCCTTGGATCCCAGGAACAG
GTGGTGGCGGCCCTC-3'

For the cloning of HIF1 α TADN fragment in the construct pGEX-HIF1 α TADN:

Forward primer: 5'-CGTGGGATCCTCAAGTTGGAAGTGGTGGAA-3'

Reverse primer: 5'-CCGCTCGAGTCGACTTGTCGTCGTCGTCCTTGTAGTCCGGCTG
TAACTGGGTCTGCTGGAA

2.4 Enzymes

Restriction endonucleases:

All restriction endonucleases were obtained from Takara (Taufkirchen). Their activity were optimized in according buffers provided by the company. The charaters of restriction endonucleases were described as follows:

Enzyme	Specificity	Buffer
<i>Bam</i> <i>Hl</i>	G [^] GATCC	K
<i>Bgl</i> <i>II</i>	A [^] GATCT	H
<i>Nhe</i> <i>I</i>	G [^] CTAGC	M
<i>Not</i> <i>I</i>	GC [^] GGCCGC	H with 0.1% BSA and 0.1% TritonX-100
<i>Sal</i> <i>I</i>	G [^] TCGAC	M

DNA and RNA modifying enzymes:

Taq DNA-Polymerase

The *Taq* DNA polymerase is a temperature resistant 5'-3'-DNA-polymerase, isolated from the thermophilic eubacterium *Thermus aquaticus* BM. which has no 3'-5'- and 5'-3'-exonuclease activity. The *Taq* polymerase possesses the highest activity at pH 8-9 and a temperature of 70-75°C. It could also use modified dNTPs as substrates and can be used for radioactive labeling of DNA fragments as well as for the labeling of DNA fragments with digoxigenin or biotin. The high process capability of *Taq* DNA Polymerase, the lack of exonuclease activity and the high temperature optimum make it possible to be used in PCR and DNA sequencing (product information).

ProofSprinter™ DNA polymerase is a mixture of *Taq* and *Pwo* polymerases. The mixture combines the proofreading capacity of *Pwo* with the high process capability of *Taq*, making it a good choice for cloning or sequencing of PCR products. ProofSprinter has robust performance, owing to its high DNA polymerase activity. Thus, in contrast to many other proof-reading enzymes, ProofSprinter increases PCR yields for both long and short templates. It could also work efficiently with templates that cause problems with *Taq* and other DNA polymerases.

Klenow fragment of DNA polymerase I

DNA Polymerase I, large (Klenow) fragment, is a proteolytic product of *E. coli* DNA polymerase I which retains polymerization and 3'-5' exonuclease activity, but has lost 5'-3' exonuclease activity. Klenow retains the polymerization fidelity of the holoenzyme without degrading 5' termini. It could be used for fill-in of 5' overhangs to form blunt ends, for removal of 3' overhangs to form blunt ends, for second strand cDNA synthesis and second strand synthesis in mutagenesis protocols. The enzyme was purified and free of contaminating endonucleases and exonucleases.

T4 DNA ligase

The T4 DNA catalyzes the formation of a phosphodiester bond between the 5' phosphate of one strand of DNA and the 3' hydroxyl group of the other. This enzyme is used to covalently

link or ligate fragments of DNA together. Most commonly, the reaction involves ligating a fragment of DNA into a plasmid vector.

T3- and T7 DNA-dependent RNA polymerases

Bacteriophage T3 and T7 RNA polymerases are DNA-dependent RNA polymerases with high sequence specificity for T3 or T7 promoters. Both T3 and T7 RNA polymerases synthesize RNA from 5' to 3' and can incorporate ^{35}S , ^{32}P and ^{33}P ribonucleotides. They are used for the generation of strand-specific RNA sequences that may be used as probes for hybridization. The polymerases are Mg^{2+} -dependent and need the four ribonucleoside triphosphates ATP, CTP, GTP and UTP for RNA synthesis. The product has three phosphate groups at the 5'-end and a 3'-OH group at the 3'-end (Sambrook & Russell 2001).

Other enzymes:

Collagenase

The collagenase was used for the preparation of rat primary hepatocytes. It is a protease which degrades collagen fibrils. The collagen is the major fibrous component of animal extracellular connective tissue. Collagenase has no specific activity for any single substrate (single protein) but could recognize specific structural patterns inside protein chains.

Lysozyme

Lysozyme is a muramidase that destroys bacterial cell walls by hydrolyzing the glycoside bond of the bacterial mureine.

RNase A

Bovine pancreatic ribonuclease A (RNase A) is a small monomeric enzyme of 124 amino acids and a molecular weight of 13.7 kDa. The function of this enzyme is to hydrolyze single-stranded RNA by cleaving the phosphodiester bond. It results in formation of nucleoside 5'-monophosphates. RNase A has a pH optimum at 7.0 - 7.5 (Sambrook & Russell 2001). It is used in the isolation of DNA. To inactivate DNases the RNase A solution should be heated before use for 10 min at 100 °C.

2.5 Antibodies

Antibodies used in the experiments are all commercially available. Their parameters were described in Table 2.

Table 2. Antibodies used in the experiments

Antibodies	Host	Company	Dilution
<i>For Western blot analysis</i>			
Primary antibodies			
anti-rat PAI-1 (polyclonal)	rabbit	American Diagnostics	1:100
anti-human PAI-1 (polyclonal)	mouse	American Diagnostics	1:100
anti-rat HO-1 (polyclonal)	rabbit	Biomol, Hamburg	1:500
anti-human HIF-1 α (monoclonal)	mouse	BD Biosciences	1:2000
anti-Golgi membrane (polyclonal)	rabbit	Biosciences, Göttingen	1:2000
anti-human β -Actin (monoclonal)	mouse	Sigma, Heidelberg	1:10,000
<i>HRP-conjugated secondary antibodies</i>			
anti-rabbit IgG	goat	Bio-Rad	1:5000
anti-mouse IgG	goat	Bio-Rad	1:5000
<i>For immunofluorescence</i>			
Primary antibodies			
anti-human HIF-1 α (monoclonal)	mouse	Transduction Laboratories	1:50
anti Living Colors A.v. peptide	rabbit	Clontech	1:20
Secondary antibodies			
anti-mouse IgG	goat	Molecular Probes	1:400
anti-rabbit IgG	goat	Dianova	1:200

2.6 Detection, Purification and synthesis systems (“Kits“)

JETstar, Plasmid Purification System	Genomed/ Bad Oeynhausen
QIAEXII Gel Extraction Kit	Qiagen/ Hilden
DIG-Nucleic-Acid Detection Kit	Roche/ Mannheim
Luciferase Assay Kit	Berthold/ Pforzheim
ECL-Kit	Amersham/ Freiburg
TNT Coupled Reticulocyte Lysate system	Promega/ Mannheim

2.7 Stock solutions

The stock solutions were, unless mentioned, prepared with sterile H₂O at room temperature. All solutions for RNA experiments were treated with DEPC.

Ammonium acetate 7.5 M:

NH ₄ Ac	57.8	g/100 ml	Final concentration
			7.5 M

The solution was autoclaved.

APS 10%:

APS	100	mg/ml	Final concentration
			10 %

APS was always made fresh.

Blocking reagent 10%:

50 mg Blocking reagent was diluted with warming in 500 ml 1x maleic acid buffer. The solution was autoclaved and stored at 4°C.

Lithium chloride 4 M:

LiCl	17	g/100 ml	Final concentration
			4 M

The solution was autoclaved.

Sodium acetate 2 M pH 4.1:

3 M NaAc	2	parts	Final concentration
Acetic acid (conc.)	1	part	2 M

The pH was adjusted with concentrated acetic acid to 4.1. The solution was autoclaved.

Sodium acetate 3 M pH 5.2:

NaAc	24.61	g	Final concentration
H ₂ O	to 100	ml	300 mM

The pH was adjusted with concentrated acetic acid to 5.2. It should be mentioned that for the right pH value a large amount of acetic acid was added. The solution was autoclaved.

PBS 10x:

NaCl	81.82	g/l	Final concentration
KCl	2.02	g/l	1.4 M
Na ₂ HPO ₄	16.02	g/l	27 mM
KH ₂ PO ₄	2.04	g/l	90 mM
			15 mM

The pH was adjusted to 7.0. The solution was prepared with DEPC-H₂O and autoclaved.

SDS:

		Final concentration
SDS	10 g/100 ml	10 %

In the case of precipitation of SDS the solution was warmed.

SSC 20x:

		Final concentration
NaCl	175.32 g/l	3,0 M
Sodium citrate	88.25 g/l	0,3 M

The pH was adjusted with HCl to 7.0. The solution was autoclaved.

Tris/HCl 1 M:

		Final concentration
Tris	12.11 g/l	1 M

The pH values of different solutions were adjusted with HCl to pH 7,5; 8,0; 9,0. The solutions were autoclaved.

Tris/HCl 0.1 M:

		Final concentration
Tris	1.211 g/l	0.1 M

The pH values of different solutions were adjusted with HCl to 7.5; 8.0; 9.0. The solutions were autoclaved.

2.8 Chemicals

All chemicals used were of p.a. quality.

Amersham/Braunschweig:	³⁵ S-methionine, [5- ¹⁴ C]2-Oxoglutarate, Glutathione Sephacrose 4B
Biometra/Göttingen:	MOPS
Calbiochem:	A23187, BAPTA, BAPTA-AM, actinomycin D, cycloheximide
Roche/Mannheim:	Anti-DIG antibodies, blocking reagent, collagenase, CSPD, deoxyribonucleotide 5'-triphosphates (dATP, dCTP, dGTP, dTTP), DIG RNA labeling mix, FCS, poly d (I-C), GPT, hexanucleotides, leupeptin, NCS, pepstatin A, RNase A, RNA standards, T3 polymerase, T7 polymerase
Fluka Chemie/Buchs, Schweiz:	Glycerol, guanidinium thiocyanate
Gibco-BRL, Life	Agarose, medium M199, non essential amino acids for

Technologies/Eggenstein:	MEM, T4 DNA ligase, T4 polynucleotide kinase
Hybaid/Heidelberg:	Proof <i>Sprinter</i> TM DNA polymerase mixture
Kodak/Rochester, USA:	Developer and fixative
MBI Fermentas/St.Leon-Rot:	DNA standarts, RNase inhibitor (RNasin)
Merck/Darmstadt:	All usual laboratory chemicals, formamide, H ₂ O ₂
Messer-Griesheim/Düsseldorf:	Nitrogen, CO ₂ , oxygen
Molecular Probes, Eugene/USA	Dihydrorhodamine (DHR), Rhodamine 123 (RH123)
Oxoid/Basingstoke, GB:	Bacto agar, bacto trypton, yeast extract
PAA Laboratories GmbH, Austria:	MEM medium
Pharmacia Biotech/Freiburg:	LMW protein standards
Pierce/Rockford, USA:	peroxidase buffer
Promega/Mannheim:	Luciferase cell lysis reagent (lysis buffer)
Roth/Karlsruhe:	Rotiphorese [®] Gel 30 (30% acrylamid stock solution with 0.8% bisacrylamid in proportion 37.5:1), Hepes, phenol (in Tris buffer pH 7.0 – 7.5)
Serva/Heidelberg:	Ampicilline, ammonium persulfate, bacitracin, bisacrylamid, bromphenol blue, coomassie blue, DePeX, β-mercaptoethanol, paraformaldehyde, ponceau S, penicillin, CSA, SDS, Serva Blue, TEMED, Tween 20
Sigma/München:	Antifoam A, Brefeldin A, CDTA, dexamethasone, dextran sulfate, DMSO, DTE, E.coli DNA, ethidium bromide, formamide, insulin, lysozym, N-lauroylsarcosin, sodium vanadate, nembutal, maleic acid, PEG 4000, PMSF, streptomycin sulfate, Thapsigargin, Tris, Triton X-100, trypsine, 3-amino-1,2,4-triazole (3-AT), Tunicamycin

2.9 Other materials

Amersham/Braunschweig:	Hyperfilm MP and Hybond N nylon membrane
Greiner/Nürtlingen:	Culture dishes, culture flasks, reaction glass cups, pipet tips, polystyrol tubes
Sartorius GmbH/Göttingen:	Sterile filter Nalgene 0.2 µm
Schleicher und Schüll/Melsungen:	3 MM Whatman paper, nitrocellulose, folding filter

2.10 Instruments

Analysis system for microscopic photography	SIS System/Münster
Auto Lumat LB 953	Berthold/ Pforzheim
Automatic pipets, type Varipette 4710	Eppendorf/Hamburg
Automatic pipet, type Pipetman P 20, P 200, P 1000	Abimed Analysen-Technik GmbH/Langenfeld
Automatic DNA Sequencer, modell 373 A	Applied Biosystems/Weiterstadt
Drying cupboard, type U 40	Memmert/Schwalbach
Electric power apparatus, type EPS 500/400	Pharmacia LKB GmbH/Freiburg
Electroblotting instrument	built by institute's workshop
Eppendorf table centrifuge, types 5414 and 5415 C	Eppendorf-Netheler GmbH/Hamburg
Eppendorf thermostate, type 5320	Eppendorf-Netheler GmbH/Hamburg
Gas controlled incubators "Cytoperm 8080" and "B 5060 EK/O ₂ ", Gasmonitor	Heraeus/Hanau
Gel apparatus for EMSA gels	Sigma/Deisenhofen
Gel dryer	Schütt Labortechnik/Göttingen
Glass dishes	Ochs/Göttingen
Halfmicro osmometer	Knauer/Berlin
Hettich centrifuge, type 3850	Hettich/Tuttlingen
Hybridization apparatus OV 3	Biometra/Göttingen
Ice machine	Inco-Ziegra/Isernhagen
Image analysis system	SIS Computersysteme/Münster
Incubator with shaking, modell 3-25	New Brunswick Scientific Co., Inc. /Edison, New Jersey 08818, USA
Labofuge II	Heraeus/Hanau
Liquid scintillation counter, beta V	Raytest Isotopenmeßgeräte GmbH /Straubenhardt
Magnetic mixer with warming, type RCT B	Ika Labortechnik/Staufen
Microscope Zeiss IM (Video camera Hitachi HV-C20)	Zeiss/Göttingen
Microwave oven, type KOR-6105	Daewoo Electronics Deutschland GmbH/Butzbach
Millipore apparatus, " Milli-Q "	Millipore/Neuhausen
pH meter, pH 535 Multi Cal	Schütt Labortechnik/Göttingen
Phosphorimager with screen plates and eraser	Amersham/Freiburg
Photometer, lambda 3 UV/VIS	Perkin-Elmer GmbH/Langen

2-Photon confocal laser microscopy	Nikon/USA
Sartorius scales, type 2254, H 120 and 2434	Sartorius GmbH/Göttingen
Seesaw apparatus	built by institut's workshop
Sigma table centrifuge 3 E-1	Sigma Laborzentrifugen GmbH /Osterode/Harz
Sorvall high speed centrifuges, RC 5 and RC 5 B	Du Pont Instruments/ Bad Nauheim
Sonicator, modell W-220 F	Schütt Labortechnik/Göttingen
Sterile bench, type Lamin Air, TL 2472	Heraeus/Hanau
Sterile bench, type MRF 06.12 – GS	Prettl Laminarflow und Prozeßtechnik GmbH/Bempflingen
Sterile pump, DBP Nr. P 24333991	Schleicher und Schüll/Dassel
Thermocycler	Bio-Med/Theres
Thermostats, type 450 LE and Typ R 10/2	Meßgeräte-Werk Lauda, Dr. R. Wobser KG/Lauda-Königshofen
Tube pump “ Multifix “, Multifix Motoren	Alfred Schwinherr/Schwäbisch
Ultraviolet emitter, type N-90 GL	Konrad Benda/Wiesloch
Ultraviolet emitter, modell C 62	Ultraviolett Productions Inc. /Californien, USA
Ultraviolet stratalinker, Modell 1800	Stratagene/Heidelberg
Vakuum blot chamber	Biometra/Göttingen
Vakuum pump, Univac DM 04 with cooler Unicryo MC 2L-60ØC and centrifuge Univapo 150	
H, Uniequip	Laborgerätebau/Martinsried
Videodensitometer	Biotec Fischer/Reiskirchen
Videodensitometer camera Hitachi KP-140	Biotech Fischer/Reiskirchen
Video camera DNA ES 49	Herolab/Wiesloch
Videoprinter and transilluminator UVP	Herolab/Wiesloch
Water bath, type K2R and type NB/S8	Meßgeräte-Werk Lauda, Dr. R. Wobser KG/Lauda-Königshofen
X-ray film cassettes	Intas/Göttingen

3. Methods

3.1 Molecular biological methods

3.1.1 Polymerase chain reaction (PCR)

The polymerase chain reaction allows to amplify DNA fragments due to repetitive cycles of DNA synthesis. The reaction uses two specific oligonucleotides (primers), which hybridize to sense and antisense strands of the template DNA fragment, four deoxyribonucleotide triphosphates (dNTP's) and a heat-stable DNA polymerase. Each cycle consists of three reactions which take place under different temperatures. First, the double-stranded DNA is converted into its two single strands (denaturation at 94°C). They function as templates for the synthesis of new DNA. Second, the reaction is cooled (50-60°C) to allow the annealing (hybridization) of primers to the complementary DNA strands. Third, DNA polymerase extends both DNA strands at 72°C (DNA synthesis) starting from the primers. Because the DNA molecules synthesized in each cycle can serve as a template in the next cycle, the number of target DNA copies approximately doubles every cycle. After a certain number of cycles, the target DNA fragment between two primers are specifically synthesized. The repeating cycles of heating and cooling take place in a thermocycler.

To obtain the DNA fragment of DsRed-ER, the PCR reaction was performed by using DsRed-ER specific primers (shown in 2.3.2) and plasmid pDsRed1-1 as template. In addition, the *ProofSprinter*TM DNA polymerase (Hybaid, Heidelberg) was used to get rid of the possible mismatching. The PCR mixture was set up as follows:

PCR reactions:

10 ng	template DNA (pDsRed1-1)
30 pmol	forward primer
30 pmol	reverse primer
0.5 µl	10% tween-20
1 µl	DMSO
3.5 µl	MgCl ₂ (25 mM)
5 µl	10 x PCR buffer [500 mM Tris/HCl pH 9,1, 140 mM (NH ₄) ₂ SO ₄]
1 µl	40 mM dNTP mix (10 mM of each dATP, dCTP, dGTP, dTTP)
2.5 U	Taq/Pwo polymerase
Add H ₂ O to 50 µl	

The PCR was performed in a thermocycler programmed as follows:

Pre-denaturation:	3 min at 96°C
Denaturation:	30 sec at 96°C
Annealing	45 sec at 68 °C
Extension:	60 sec at 72 °C
Cycles:	35 cycles
Final extension:	10 min at 72°C

After the amplification, PCR product (10 µl) was electrophoretically analyzed in a 1% agarose gel with ethidium bromide staining and purified.

3.1.2 DNA electrophoresis and purification from agarose gel

The DNA sample was mixed with 5 µl of loading buffer and loaded onto the 1% agarose gel. The electrophoresis was performed for 45-60 min with 5 Volt/cm. The negatively charged DNA migrated from the cathode (-) to anode (+). To visualize DNA, the gel was treated with ethidium bromide (0.5 µg/ml), which intercalated between the bases of DNA double strands forming a complex fluorescent under UV light. The size of DNA fragments was determined by a DNA molecular weight standard.

Ethidium bromide solution:

Ethidium bromide 10 mg/ml

Stored at 4°C, protected from light.

10 x Tris/acetate/EDTA (TAE) buffer:

			Final concentration	
Tris	6.1	g/100 ml	0.5	M
Sodium acetate	1.6	g/100 ml	0.2	M
EDTA	0.7	g/100 ml	0.02	M

The pH was adjusted with acetic acid to 7.4, the buffer was autoclaved.

Loading buffer:

			Final concentration	
Bromphenol blue	0.01	g/100 ml	0.01	%
Glycerol	40	ml/100 ml	40	%
10 x TAE buffer	10	ml/100 ml	1	X

The buffer was autoclaved and stored at 4°C.

The corresponding DNA fragment was excised from the gel and purified with the QIAEX II kit (Qiagen, Germany). Three volumes of binding and solubilization buffer (QX1) and 10 μ l QIAEX II solution were added to 1 volume of gel. To bind DNA, the solution was incubated at 50°C for 10 min with occasionally vortexing. After centrifugation at 13,000 \times g for 30 sec, the pellet was washed once with QX1 buffer and once with PE buffer. After removing the washing buffer of the last step, the pellet was completely dried at room temperature (for about 15 min). Then, the pellet was resuspended in 20 μ l H₂O and incubated for 5 min at room temperature. After centrifugation at 13,000 \times g for 1 min, the supernatant, which contains the DNA fragments, was collected into a new tube.

3.1.3 Cloning of the PCR product

Restriction reaction

The plasmid pECFP-ER as well as the purified PCR product was digested with NheI and BglII restriction endonucleases. The restriction mixture was incubated for 2 hours at 37°C. Then, the DNA fragments were separated in 1% agarose gel and the corresponding DNA bands were purified from the gel as described above.

Restriction mixture:

Plasmid/PCR product	3 μ g/ 15 μ l
Bgl II	1 μ l
Nhe I	1 μ l
10 x buffer	2 μ l
H ₂ O	to 20 μ l

Ligation

The purified DsRed-ER (Bgl II/Nhe I) DNA fragment was ligated into the linearized pECFP-ER (Bgl II/Nhe I) plasmid by T4 ligase. The ligation reaction was incubated overnight at 16°C and then transformed in the competent *E. coli* DH 5 α cells.

Ligation reaction:

DNA fragment	100 ng
Linearized plasmid	50 ng
5 x Ligase buffer (5 mM ATP)	4 μ l
T4 Ligase (1U/ μ l)	0.5 μ l
H ₂ O	to 20 μ l

Preparation of competent E. coli cells:

A single bacterial colony from the *E. coli* DH 5 α or XL1 glycerol culture was cultured in 5 ml LB medium at 37°C overnight. In the following day, the bacterial suspension was diluted into 500 ml LB medium and continually cultured at 37°C till the OD at 550 nm became 0.3-0.4 (for about 3-6 h). The suspension was divided into two 250 ml flasks and centrifuged at 4°C, 4080 \times g for 15 min. The pellets were resuspended each in 5 ml (1/10 vol.) of ice cold TSS buffer and divided in 100 μ l aliquots in an ethanol/CO₂ bath and stored at -70°C. The competence of the bacterial cells was checked by the transformation of an ampicillin or kanamycin resistant plasmid.

LB medium (Luria Bertani):

<i>Trypton</i>	10 g/l
Yeast extract	5 g/l
NaCl	10 g/l

The pH was adjusted with NaOH to 7.3. The medium was autoclaved after preparation.

TSS buffer:

		Final concentration
NaCl	1.0 g/100 ml	1 % (w/v)
Trypton	1.0 g/100 ml	1 % (w/v)
Yeast extract	0.5 g/100 ml	0.5 % (w/v)
MgCl ₂	0.6 g/100 ml	30 mM
PEG 4000	10 g/100 ml	10 % (v/v)
DMSO	5.0 ml/100 ml	5 % (v/v)

The pH was adjusted with NaOH to 6.5, the buffer was sterile filtered and stored at 4°C.

Transformation of E. coli:

The transformation of *E. coli* was performed with the heat shock method. The ligation mixture or the plasmid DNA was gently mixed with one aliquot of the competent cells (100 μ l) and incubated at 4°C for 30 min. Then the mixture was heated in 42°C water bath for exactly 2 minutes followed by immediate cooling on ice. Thereafter, the bacterial cells were cultured in 800 μ l SOC medium without antibiotics at 37°C for 1 h. An aliquot of 300 μ l was spread over an ampicillin- or a kanamycin-containing agar dish and incubated overnight at 37°C.

SOC medium:

	Final concentration
Tryptone	2 %
Yeast extract	0.5 %
NaCl	10 mM
KCl	2.5 mM
MgCl	10 mM
MgSO ₄	10 mM
Glucose	20 mM

The pH was adjusted with NaOH to 7.3. The medium was autoclaved after preparation.

Ampicillin/ Kanamycin agar dishes:

500 ml LB medium containing 6.25 g bactoagar was autoclaved. After cooling to 50°C, 200 µl ampicillin stock solution (final concentration 40 µg/ml) or 300 µl kanamycin stock solution (final concentration 60 µg/ml) was added, mixed and 10 ml of the solution was poured into each sterile petri dish. The dishes were left for drying at RT overnight and then stored at 4°C in the dark.

Ampicillin stock solution:

Ampicillin 100 mg/ml
Dissolved in H₂O and stored at -20°C.

Kanamycin stock solution:

Kanamycin 100 mg/ml
Dissolved in H₂O and stored at -20°C.

3.1.4 Isolation of plasmid DNA (minipreparation)

Bacteria colonies transformed with a ligation mixture or with a plasmid were picked and cultured in 5 ml LB medium with ampicillin (40 µg/ml) or kanamycin (40 µg/ml) at 37°C overnight. 3 ml of the bacterial culture (2 x 1.5 ml in a Eppendorf cup) were centrifuged at 15,800×g for 30 s. After removal of the medium, the bacterial pellet was resuspended in 200 µl STET buffer and then 50 µl lysozyme (10 mg/ml) was added to lyse bacteria. Thereafter, the lysate was heated for 60 s at 95°C followed by cooling on ice. The resulting bacterial lysate was centrifugated for 10 min (15,800×g, 14,000 rpm). The supernatant containing the

plasmid DNA was collected to a new Eppendorf cup and the sediment containing proteins and genomic DNA was left behind. The plasmid DNA was precipitated with 150 μ l isopropanol (10 min at -20°C). After 5 min of centrifugation ($15,800\times g$, 14,000 rpm), the pellet was resuspended in 200 μ l Tris/EDTA/NaCl and the plasmid DNA was again precipitated with 200 μ l isopropanol (-20°C for 10 min). The pellet was washed once with 70% ethanol, air-dried and dissolved in 40 μ l H_2O . The resulting DNA was checked by restriction analysis with according restriction enzymes as described above.

STET buffer:

			Final concentration	
Tris/HCl, pH 8.0	0.61	g/100 ml	50	mM
EDTA	1.86	g/100 ml	50	mM
Triton-X-100	0.5	g/100 ml	0.5	%
Sucrose	8	g/100 ml	8	%

The buffer was autoclaved and stored at RT.

Tris/EDTA/NaCl:

			Final concentration	
Tris/HCl, pH 7.8	0.121	g/100 ml	10	mM
EDTA	37.2	mg/100 ml	1	mM
NaCl	1.75	g/100 ml	300	mM

3.1.5 Isolation of plasmid DNA with silicate columns (maxipreparation)

The maxi-preparation of plasmid DNA was performed with JETstar Plasmid Maxiprep Kit (Genomed) according to manufacturer descriptions.

The transformed *E. coli* DH5 α cells were cultured in 200 ml LB medium to a density about 10^9 per ml (OD at 600 nm of 1-1.5). The cells were pelleted by centrifugation at 4°C , $5860\times g$ (6000 rpm, GSA rotor) for 30 min. The pellet was resuspended in 10 ml of buffer E1, which contained 100 $\mu\text{g/ml}$ of RNase. Then 10 ml of buffer E2 (with NaOH and SDS for bacterial lysis) was added and mixed gently 4-6 times (the mixture should not be vortexed to avoid shearing of genomic DNA). After 5 min incubation at RT (longer incubation could lead to irreversible denaturation of plasmid DNA), 10 ml of buffer E3 was added for neutralization of the solution. The solution was centrifuged at 20°C , $16,300\times g$ (10,000 rpm, SS34 rotor) for 20 min, during which an undense pellet containing bacterial debris, genomic DNA etc. was formed. The supernatant was carefully applied to the column (length 13 cm, \varnothing 2,6 cm), which was equilibrated with 30 ml of buffer E4. When the lysate has been completely run by

gravity flow through the column, the column was washed once with 60 ml of buffer E5 to remove single stranded DNA, RNA and all other impurities such as proteins, metabolites, polysaccharides and NTPs. Afterwards, the double stranded plasmid DNA was eluted with 15 ml of buffer E6 and precipitate by adding 10.5 ml of isopropanol. After incubated at -20°C for 1 h, the plasmid DNA was pelleted by centrifugation at 4°C , $27,000\times g$ (15,000 rpm, SS34 rotor) for 30 min. The DNA pellet was washed with 70% ethanol, to remove salts, air-dried for 30 min and dissolved in $500\ \mu\text{l H}_2\text{O}$.

To determine the DNA concentration and the presence of protein in the probes, the OD at 260 nm (DNA) and 280 nm (protein) was measured. The prepared plasmids were checked by restriction analysis as described above.

Buffers used in maxipreparation:

Buffer E1	50 mM Tris 10 mM EDTA 100 $\mu\text{g/ ml}$ RNase A	pH 8.0, adjusted with HCl E1 with RNase A stored at 4°C
Buffer E2	200 mM NaOH 1% SDS	
Buffer E3	3.1 M potassium acetate	pH 5.5, adjusted with acetic acid
Buffer E4	600 mM NaCl 100 mM sodium acetate 0.15% Triton X-100	pH 5.0, adjusted with acetic acid
Buffer E5	800 mM NaCl 100 mM sodium acetate	pH 5.0, adjusted with acetic acid
Buffer E6	1.25 M NaCl 100 mM Tris	pH 8.5, adjusted with HCl

3.1.6 Sequencing of plasmids

The sequencing was performed by a “dye terminator cycle sequencing” method according to the manual (Perkin Elmer). In this method, the premix solution contains four dideoxynucleotides (ddNTP, each labeled with a different fluorescent dye), unlabeled desoxynucleotides (dNTP) and a temperature resistant DNA polymerase. The template plasmid and one gene specific primer were added to the reaction mixture. During the PCR reaction, the synthesized single strand DNA would be stopped randomly with the incorporation of ddNTP. Thus, DNA fragments of different size were labeled at their 3'-ends with base specific fluorescent dyes, which could be analyzed with the DNA sequencer (ABI, model 373 A).

Sequence reaction:

			Final concentration
Plasmid	X	μl	800 ng/probe
Primer (2.5 pmol/μl)	2	μl	5 pmol/probe
Premix	8	μl	
H ₂ O	to 20	μl	

The sequence reaction was performed under following conditions: denaturation at 96°C for 10 s, primer annealing at 50°C for 5 s, extension at 60°C for 4 min.

After finishing of the sequence reaction the solution was cooled at 4°C and purified as follows: 2 μl 3 M NaAc, pH 5.2 and 50 μl 95% ethanol (RT) were added and the mixture was centrifuged for 20 min at 15,800×g (14,000 rpm, table centrifuge). The pellet was washed with 250 μl of 70% ethanol, centrifuged for 10 min, air-dried and dissolved in 25 μl of water. Then, the probes were loaded on the gel (4.75% polyacrylamide DNA sequence gel) after denaturation for 2 min at 90°C. The DNA fragments were electrophoretically separated in the sequence service laboratory. The fluorescence of dye-containing polynucleotides was stimulated by 40 mW argon laser (488 nm and 514 nm). The fluorescent signal was identified by the detector system of the DNA sequencer and quantified.

3.2 Cell biological methods

3.2.1 Isolation of primary rat hepatocytes

The isolation of primary rat hepatocytes from liver was performed under sterile conditions by the method of collagenase perfusion (Berry & Friend 1969).

Liver perfusion

1. Non-recirculative *in situ* preperfusion of the liver: After laparotomy a braunule (1.3 X 45 mm) was inserted in the vena portae, and the vena cava inferior was ligated above the diaphragma to close the whole body blood circulation. The vena cava inferior was then cut beneath the liver, cannulated with the braunule (22 X 50 mm) and perfusion started with 150-200 ml preperfusion medium (Krebs ringer solution with EGTA) at a flow rate of 30 ml/min until the liver was free from blood.

2. Recirculative perfusion: The perfusion at a flow rate of 30 ml/min with collagenase perfusion medium was performed until consistency of the liver became soft, due to digestion of the connective tissue (about 7-11 min). During perfusion the medium was recirculated through a plastic tube connected to the braunule inserted in the vena cava inferior.

Both preperfusion and perfusion medium were pumped through an oxygenator, from which they were directed into the vena portae with a pressure of 10-15 cm of water.

Preparation of the hepatocyte suspension

After perfusion the liver was removed and transferred into a glass cup filled with culture medium M 199. The Glisson's capsule, e.g. collagen tissue around the liver, was carefully removed and discarded. The obtained paste-like liver substance was further disrupted. Finally, connecting tissue and remainders of the liver capsule as well as big cell aggregates were removed by filtration of the primary suspension through a nylon net (pore size 79 μm). Non-parenchymal cells and cell debris were removed by numerous selective sedimentations (20 \times g, 2 min). After the last centrifugation hepatocytes were suspended in medium M 199. 50 ml of M 199 were added per 1 g (wet weight) of the sedimented cells; the cell suspension had a density of about 10⁶/2.5 ml.

All mediums and solutions for cell culture were prepared in demineralized water, which was further purified by quartz distillation, sterile filtered in autoclaved bottles and stored at 4°C.

Krebs Ringer stock solution:

			Final concentration
NaCl	7	g/l	120.0 mM
KCl	0.36	g/l	4.8 mM
MgSO ₄ x 7 H ₂ O	0.296	g/l	1.2 mM
KH ₂ PO ₄	0.163	g/l	1.2 mM
NaHCO ₃	2.016	g/l	24.4 mM

The solution was equilibrated with carbogen and adjusted to pH 7,35.

Preperfusion medium:

			Final concentration
EGTA	0.1	g/l	0.25 mM

Dissolved in Krebs Ringer stock solution.

Collagenase perfusion medium:

			Final concentration
HEPES	3.356	g/l	15 mM
CaCl ₂ x 2 H ₂ O	0.588	g/l	4 mM
Collagenase	0.500	g/l	

Dissolved in Krebs Ringer stock solution. Before each preparation of hepatocytes, the collagenase was dissolved in perfusion medium, equilibrated with carbogen for 30 min and finally sterile filtered.

Wash medium:

			Final concentration
HEPES/NaOH pH 7,4	4.77	g/l	20 mM
NaCl	7.00	g/l	120 mM
KCl	0.36	g/l	4.8 mM
MgSO ₄ x 7 H ₂ O	0.30	g/l	1.2 mM
KH ₂ PO ₄	0.16	g/l	1.2 mM
Calf serum albumin	4.00	g/l	0.4 %

Medium 199:

			Final concentration
Pulver medium M 199	9.8	g/l	
Glucose x H ₂ O	1.1	g/l	5.5 mM
HEPES	3.6	g/l	15 mM
NaHCO ₃	1.5	g/l	18 mM
Calf serum albumin	4.0	g/l	0.4 %

Solution A was prepared by dissolving 1.5 g NaHCO₃ in 550 ml H₂O and equilibrated with carbogen for 3-4 hours. The pH was adjusted to 7.35. Solution B was prepared from powder medium, bovine serum albumin and HEPES dissolved in 450 ml H₂O and the pH was adjusted to 7.35. Then solutions A and B were mixed and again equilibrated with carbogen until a pH value of 7.35 was reached. Finally, the medium was sterile filtered.

3.2.2 Primary rat hepatocyte culture

Immediately after preparation, fetal calf serum (4 ml/100 ml suspension) was added to the cell suspension of hepatocytes for better attachment to the bottom of the polystyrol dishes. Furthermore, the antibiotics (1 ml of stock solution per 100 ml cell suspension), 10⁻⁷ M dexamethasone and 10⁻⁹ M insulin as permissive hormones were added. The culture of the hepatocytes was performed on dishes of different sizes and at different cell numbers depending on the type of application:

Application	Cell number / vol. suspension plated	∅ of the culture dish
Transfection	1x10 ⁶ /1.5 ml	60 mm
Protein isolation	2x10 ⁶ /3.0 ml	60 mm
RNA isolation	3x10 ⁶ /9.0 ml	100 mm

After the initial 4 h attachment phase (for transfected cells 5 h) the medium was changed, and the hepatocytes were further cultured in medium M 199 with the same concentrations of hormones and antibiotics as before but without fetal calf serum. After 24 h the medium was changed again. The incubation of the hepatocytes was performed in gas controlled incubators in the water vapour saturated atmosphere with 8% O₂ (v/v) or 16% O₂ (v/v), 5% CO₂ and, accordingly, 87% (v/v) or 79% N₂ at 37°C.

Hormone and antibiotics stock solutions

All solutions were sterile filtered and stored at -20°C.

Antibiotics:

Penicillin G, sodium salt	0.64 g/100 ml
Streptomycine sulfate	1.17 g/100 ml
In 0.9% NaCl solution	

Dexamethasone (100 μ M):

Dexamethasone 3.92 g/100 ml
In 0.9% NaCl solution. Dexamethasone was first dissolved in 0.3 ml of ethanol and then filled with 0.9% NaCl solution to 100 ml.

Insulin (10 μ M):

Insulin 6 mg/100 ml
Bovine serum albumin 100 mg/100 ml
In 0.9% NaCl solution. Insulin was dissolved at pH 2.5, neutralized and then bovine serum albumin was added.

3.2.3 Culture of HepG2 cells

The cells frozen in DMSO at -70°C (app. 5×10^6 cells) were thawed at 37°C and then dissolved in app. 10 ml of MEM (PAA Laboratories GmbH, Austria) supplemented with 10% FCS and 1% antibiotics. After centrifugation at 1000 rpm for 10 min, the supernatant was sucked off. The cells were resuspended in 40 ml of medium and plated in a 170 cm^2 tissue culture flask. When the cells became confluent (app. 25×10^6 cells per 170 cm^2 flask), they were trypsinized (3 ml trypsin per 170 cm^2 flask for app. 5 min at 37°C). The reaction was stopped by adding 10 ml of medium with 10% FCS which contained trypsin inhibitors. For the further culture ca. 1/3 of the HepG2 or HeLa cells were transferred to a new flask, the cells usually were confluent again after about 3 days. For transfection, protein or RNA isolation, 2.5 ml of cell suspension (2×10^5 cells/ml) were plated in 60 mm culture dishes.

HepG2 cells were cultured in gas controlled incubators in the water vapour saturated atmosphere with 8% O_2 (v/v) or 16% O_2 (v/v), 5% CO_2 and, accordingly, 87% (v/v) or 79% N_2 at 37°C .

3.2.4 Transfection of hepatocytes and HepG2 cells

The calcium phosphate precipitation method was used for transfection of primary hepatocytes and HepG2 cells. All the protocols for calcium phosphate precipitation, including the protocol used in the present work, are modifications of the protocol from Graham and van der Eb (Graham et al., 1973). The differences are mostly concerning the type of cells used and the time and duration of transfection (Parker et al., 1979) (Chen et al., 1988) (Rippe et al., 1990). The principle of the method is that DNA forms together with calcium phosphate small

precipitates which are taken up by cells via endocytosis. The precipitate is obtained when the DNA/calcium chloride solution is mixed with a solution containing phosphate.

Transfection mixture for one dish (60 mm):

			Final concentration
Plasmid DNA	2.5	μg	
H ₂ O	to 67.5	μl	
CaCl ₂ 2.5 M	7.5	μl	125 mM
2 x Hepes	75	μl	

The transfection mixture was prepared in polystyrol flasks to prevent adhesion of the DNA to the walls of the flask. After dilution of the plasmid DNA with the appropriate amount of water, CaCl₂ was added first. Then the 2x Hepes solution was added while vortexing and the solution was left at RT for 5-10 min. During this time the DNA/calcium phosphate precipitate was formed, which was visible as a light turbidity of the solution. Finally, 150 μl of the mixture was added to 1.5 ml of freshly plated hepatocytes in suspension or to the medium of precultured HepG2 cells (2.5 ml) in 60 mm ∅ dishes.

The HepG2 cells were plated 16-18 h before transfection at a density of $2.8 \times 10^6 / 15.5$ ml medium. For hepatocytes and HepG2 cells, the medium was changed 5 h and 24 h after the transfection.

2 x Hepes:

			Final concentration
Hepes	1.192	g/100 ml	50 mM
NaCl	1.636	g/100 ml	280 mM
Na ₂ HPO ₄	0.267	g/100 ml	1.5 mM

The pH was adjusted with 5 N NaOH to 7.05, the buffer was stored in 10 ml aliquots at -20°C.

Calcium chloride (2.5 M):

			Final concentration
CaCl ₂	36.75	g/100 ml	2.5 M

The solution was autoclaved and stored in aliquots at -20°C.

3.2.5 Luciferase detection

The detection of luciferase activity in the cells transfected with reporter vectors containing the firefly luciferase gene (*Photinus pyralis*) was performed with the Luciferase Assay Kit (Berthold, Pforzheim). The luciferase assay is based on the enzyme-catalyzed chemiluminescence. Luciferin present in the luciferase assay reagent is oxidized by luciferase in the presence of ATP, air oxygen and magnesium ions. This reaction produces light with a wavelength of 562 nm which can be measured by a luminometer.

After washed twice with 1×PBS, the transfected cells were shaken for 15 min in 300 µl of 1×lysis buffer and then scraped in chilled Eppendorf cups. After 15 s of vortexing primary rat hepatocytes, but not HepG2 cells, were frozen in liquid nitrogen and thawed at RT. The cell lysates were centrifuged for 2 min (15,800×g, 14,000 rpm) and 20 µl of the supernatants were automatically mixed in the luminometer with 100 µl luciferase assay reagent, which was freshly prepared by mixing of equal volume of solutions A and B. The reaction was measured 10 times for 2 s each and the results represented the integrated counting in these 20 s. No information about the composition of solution A and B was given by the supplier.

5 x Lysis buffer:

			Final concentration	
Tris	25 ml of	1 M	125	mM
CDTA	10 ml of	200 mM	10	mM
DTT	4 ml of	500 mM	10	mM
Glycerol	115 ml of	85%	50	%
TritonX-100	10 ml of	100%	5	%
H ₂ O	to 200 ml			

After adjustment of the pH to 7.8 with H₃PO₄ the solution was autoclaved.

3.2.6 Detection of OH• generation in living cells by two photon confocal laser microscopy (2P-CLSM)

Intracellular hydroxyl radicals (OH•) generated in a Fenton reaction can be detected by irreversible conversion of the non-fluorescent dye dihydrorhodamine (DHR). Thereby, the OH• rearranges the π -system of DHR, yielding fluorescent rhodamine 123 (RH), which can be visualized by a fluorescence microscope (Ehleben et al., 1997).

The HepG2 cells were transfected with 5 µg of pDsRed or pECFP constructs (pDsRed-ER, pDsRed-Mito, pDsRed-Golgi, pDsRed-Peroxi, pDsRed-Lyso and pECFP-ER, pECFP-Mito,

pECFP-Golgi, pECFP-Peroxi, pECFP-Lyso, respectively), and further cultured for 24 h to allow the expression of fluorescent proteins. Then, the transfected cells were transferred to a culture chamber on the microscope stage enabling observation at 37°C under a variable gas atmosphere. Cells were treated with 30 μ M DHR for 5 min under normoxia or hypoxia, then, washed without altering the pO₂ as controlled by a polarographic pO₂ catheter-electrode (LICOX MCB). With two photon laser confocal microscopy (2P-CLSM), an excitation wavelength of 850 nm was applied to colocalize RH123 fluorescence (emission wavelength 530nm) and ECFP (emission wavelength 470 nm), and 875 nm wavelength excitation was applied to colocalize RH123 fluorescence and DsRed (emission wavelength 580 nm). Fluorescence was registered by a photo multiplier and analyzed by the EZ 2000 software (Version 2.1.4, Cood Automatisering). The signal-to-noise ratio was determined and images were deconvolved with the Huygens System software (Version 2.2.1, Scientific Volume Imaging), using the Maximum Likelihood Estimation (MLE) method. The data were reconstructed with the Application Visualization System (AVS Waltham). Calculation of isosurfaces was performed on a Unix-based Octane workstation (Silicon Graphics, Mountain View) as described (Strohmaier et al., 2000).

3.2.7 Immunofluorescence

HepG2 cells cultured on cover-slips were transfected with pECFP-ER and incubated under normoxia or hypoxia for 60 min. After fixed with ice cold methanal/acetone (1:1) for 10 min, cells were blocked with 3% BSA in PBS for 1 h. Then, cells were incubated with a monoclonal anti-HIF1 α antibody (1:50) and a rabbit Living Colors A.v. peptide antibody (1:20) for 2 h. After washing 1 \times PBS, an Alexa Fluor 568-conjugated goat anti-mouse IgG secondary antibody (1:400) and a Cy2-conjugated goat anti-rabbit IgG secondary antibody (1:200) were applied to detect the binding of the primary antibodies. Images of immunostained cells were captured by using 2P-CLSM and visualized in false colors as described above.

3.2.8 RNA isolation from cultured cells

The isolation of total RNA was performed with a modification of the method described by Chomczynski and Sacchi (Chomczynski et al., 1987), in which the phenol/ chloroform/isoamyl alcohol extraction was used.

Cultured cells (3 x 10⁶ cells in 100 mm culture dish) were washed with 1 x PBS, and scraped into 500 μ l of guanidinium thiocyanate (GTC) buffer with a disposable cell scraper. The cell

lysate was homogenized by pipetting up and down, and then transferred into a 2 ml Eppendorf cup. Thereafter, 50 μ l of 2 M sodium acetate (pH 4.1), 500 μ l of H₂O-saturated phenol and 100 μ l of chloroform/isoamyl alcohol (ratio 49:1) were added with gentle mixing one after another. The solution was incubated on ice for 15 min and centrifuged at 10000 \times g, 4°C for 20 min in a SS34 rotor. The RNA-containing upper phase was collected in a new 2 ml Eppendorf cup. The RNA was precipitated by adding 1 ml of isopropanol and incubated at -20°C for 1 h. After centrifugation at 10,000 \times g, 4°C for 10 min in the SS34 rotor, the RNA pellet was washed once with 200 μ l 75% ethanol. The purified RNA was centrifuged again for 10 min at 10,000 \times g and dried in a vacuum centrifuge at 37°C for 3 min. Finally, the pellet was dissolved in 40 μ l 0.1% SDS. After measuring the RNA concentration the samples were stored at -20°C.

To determine the concentration and purity of the RNA, the extinction at 260 nm and 280 nm was measured. An OD of 1 at 260 nm corresponds to 40 μ g RNA/ml. The ratio of the OD at 260 nm and at 280 nm is a measure of RNA purity. In a protein-free solution the ratio OD₂₆₀/OD₂₈₀ is 2. Due to protein contaminations this coefficient is usually lower. In our experiments it was over 1.7.

All solutions for RNA experiments were prepared with DEPC-H₂O. By addition of DEPC to millipore water for 12 h RNases in water were inactivated. Then the water was autoclaved.

GTC buffer:

			Final concentration
Guanidinium thiocyanate	47.3	g	4 M
Sodium citrate	2.5	ml 1 M	25 mM
N-lauroyl sarcosine	0.5	g	17 mM
2-mercaptoethanol	0.7	ml	0.1 M
30% antifoam A	0.33	ml	0.1 %
DEPC-H ₂ O	to 100	ml	

The solution was warmed for 30 min at 65°C. The pH was adjusted with 1 N NaOH to 7. 2-mercaptoethanol was added at the end.

Phenol (water saturated):

Two volumes of phenol was mixed with one volume of H₂O. After the phase separation the solution was stored at 4°C protected from light.

3.2.9 Preparation of digoxigenin-labeled RNA probes

For Northern blot analysis the digoxigenin labeled, single-stranded RNA probes were used. The RNA probes were generated by *in vitro* transcription with the DIG RNA Labeling Kit. In this process, the plasmids containing the target gene sequence were linearized and then the RNA probes were synthesized by using T7 or T3 polymerases. The linearized plasmids allowed generation of transcripts of uniform length. One digoxigenin-11-uridine-monomophosphate (DIG-UMP) residue is incorporated approximately every 20-25 nucleotides.

For preparation of the digoxigenin-labeled antisense RNA probes for HIF-1 α , PAI-1, HO-1 and β -Actin, the vectors pCRII-HIF1 α , pBS-PAI1, pBS-HOX1 and pBS-Actin were linearized by BamH I, Xho I, and Xba I, respectively.

Linearization of plasmids

Restriction reaction:

Plasmid	5	μ g
Restriction enzyme	1,5	μ l
10x restriction buffer	2	μ l
H ₂ O	to 20	μ l

The solution was incubated for 2 h at 37°C and then treated with RNase for 15 min. After a phenol/chloroform extraction and ethanol precipitation the pellet was dissolved in 33 μ l of DEPC-H₂O.

In vitro transcription

Reaction of in vitro transcription:

Linearized plasmid	11	μ l
10 x transcription buffer	2	μ l
10 x labeling mix	2	μ l
RNasin (40 U/ μ l)	1	μ l
T7/T3 RNA polymerase (20 U/ μ l)	2	μ l
DEPC-H ₂ O	2	μ l

10 x labeling mix:

ATP	10	mM
CTP	10	mM
GTP	10	mM
UTP	6.5	mM
DIG-UTP	3.5	mM

The solution was incubated at 37°C for 1.5 h. Then 0.5 µl RNA polymerase was again added and the incubation was prolonged for another 1 h. Synthesized digoxigenin-labeled RNA was precipitated with 2.5 µl 4 M LiCl and 75 µl absolute ethanol at -20°C for at least 2 h. The solution was centrifuged at 4°C, 12,000×g (10,000 rpm, SS34 rotor) for 10 min, the pellet washed with 80% ethanol and dried in a vacuum centrifuge. The pellet was dissolved in 100 µl DEPC-H₂O and stored at -20°C.

Estimation of the labeling efficiency

The labeling efficiency of probe yield was estimated by comparison of the DIG-labeled probe with a DIG-labeled control DNA provided in the labeling kit. The transcript (1 µl) as well as digoxigenin-labeled control DNA (0.04 - 5 ng) was spotted on a Hybond Nylon membrane. The nucleic acids were fixed to the membrane in the UV stratalinker for 2 min with 1200 µJ. Thereafter, the membrane was washed for 5 min in buffer 1 (described in 3.2.10) and incubated with 1% blocking reagent (10% blocking reagent diluted with buffer 1) for 20 min. The membrane was then incubated for 20 min in 20 ml of anti-digoxigenin antibody solution (1:10,000 dilution in 1% blocking reagent). The unbound antibody conjugate was removed by washing of the membrane twice in buffer 1 for 15 min. After 2 min equilibration in buffer 3 (described in 3.2.10), the color substrate solution containing 45 µl NBT and 35 µl X-phosphate in 10 ml of buffer 3 was added. The color spots started to appear within 3 min. After about 10 min the reaction was stopped by washing the membrane in TE buffer. All steps were performed at RT.

NBT:

NBT	74 mg/ml in 70% DMF	Final concentration 0.41 mM
-----	---------------------	--------------------------------

The solution was stored at -20°C, protected from light.

X-phosphate:

X-phosphate	50 mg/ml in DMF	Final concentration 0.38 mM
-------------	-----------------	--------------------------------

The solution was stored at -20°C.

Other solutions are described in 3.2.11.

3.2.10 Northern blot analysis

Northern blot analysis is a method to quantify the abundance of a specific RNA species in cells. In this process, the RNA is separated in a denaturing agarose gel, transferred by capillary transfer to a nylon membrane (vacuum blot) and fixed to the membrane by UV crosslinking. The RNA of interest is identified by hybridization with a specific probe.

All solutions used for the Northern blot were DEPC treated and autoclaved, the electrophoresis and blot chambers, gel plates and combs were kept in 3% H₂O₂ overnight to inactivate RNases before use.

Denaturation of RNA sample

The RNA sample (20 µg) was denatured in 16.5 µl loading buffer at 68°C for 15 min and subsequently cooled on ice for 2 min. The RNA was loaded to the gel after added 5 µl sample buffer.

Loading buffer:

			Final concentration
Formamide	15	ml	66.6 %
14.3 x MOPS	2.1	ml	26.7 mM
37% formaldehyde	5.4	ml	8.9 %

The buffer was aliquoted and stored at -20°C.

14.3xMOPs:

			Final concentration
MOPS	5.93	g	286 mM
NaAc	0.58	g	7.1 mM
EDTA	0.5	g	1.3 mM
DEPC-H ₂ O	to 100	ml	

The pH was adjusted with NaOH to 7.0 and the solution was autoclaved.

Sample buffer:

			Final concentration
Glycerin	5	ml	50 %
0.5 M EDTA	20	µl	1 mM
Bromphenol blue	10	mg	0.1 %
DEPC-H ₂ O	to 10	ml	

The buffer was aliquoted and stored at 4°C.

Electrophoresis of RNA samples

For electrophoresis, a 1.5% agarose gel was prepared as follows: 0.9 g agarose was dissolved by heating in 49 ml DEPC-H₂O. Then 6 ml 10 x MOPS and 5 ml formaldehyde (to keep the denaturation of RNA) were added. After mixing, the gel was poured into the prepared gel plate (10 x 14 cm). The gel plate and combs were kept in 3% H₂O₂ overnight before use to make them RNase free.

The denaturing agarose gel was placed into an electrophoresis chamber filled with 1 x MOPS buffer (900 ml). After the samples were loaded, the electrophoresis was performed at 100 Volt till Bromphenol blue reached the edge of the gel (about 2 h).

After gel electrophoresis the formaldehyde was washed out by shaking the gel in 150 ml of a 1% glycine solution for 20 min. 5 µl ethidium bromide solution (3.1.2) was added and the gel was further incubated for 5 min. Ethidium bromide formed a complex with RNA which was fluorescent under UV light (254 nm) and two main bands corresponding to 28S and 18S ribosomal RNA were visible. The gel was photographed with a video camera. Finally, the gel was washed in 20xSSC for 20min before membrane transfer.

MOPs 10x:

		Final concentration
MOPS	41.9 g	200 mM
NaAc	4.1 g	50 mM
EDTA	3.7 g	10 mM
DEPC-H ₂ O	to 1 l	

The pH was adjusted with NaOH to 7.0. The solution was autoclaved.

RNA transfer to nylon membrane

RNA separated in the gel was transferred to a nylon membrane by capillary transfer. For this, a nylon membrane (10x15 cm) was washed in 2xSSC for 10 min. The transfer equipment was prepared in the following way: 3 mm thick filter paper (pre-saturated in 20 x SSC), on which the nylon membrane was placed, was put on a vacuum chamber. The gel was then put on the membrane. Also a rubber mat was placed in a way that no free space was left between it and the gel. The vacuum switched on before the chamber was filled with transfer buffer. The transfer was performed for 1-2 h, during which the RNA was transferred onto the nylon membrane by capillary force. Thereafter, RNA was fixed on the membrane by UV crosslinking for 2 min. To check if the transfer was complete the gel was again observed under UV light.

Hybridization of the RNA with digoxigenin-labeled RNA probes

The nylon membrane carrying RNA samples was placed into a hybridization tube containing 10 ml of hybridization solution. To prevent unspecific binding, prehybridization was performed at 65°C for 1 h in a hybridization oven. Then, the solution was removed and replaced with 6 ml hybridization solution containing 100 ng of digoxigenin-labeled antisense RNA probe. The hybridization was performed at 65°C overnight. The unbound probe was removed by washing in 2xSSC/0.1% SDS for 2 x 5 min and in 0.1x SSC/0.1% SDS for 2 x 15 min at 65°C (posthybridization).

Hybridization solution:

			Final concentration	
Deionized formamide	12.5	ml	50	%
10% blocking reagent	6	ml	2.5	%
20% SDS	25	µl	0.02	%
10% N-lauroylsarcosine	250	µl	0.1	%
20 x SSC	6.25	ml	5	X

The solution was stored at 4°C.

Detection and quantification of the RNA expression

The detection was performed with the DIG Nucleic Acid Detection Kit (Roche) according to the manufacturer instructions. The 0.1x SSC/0.1% SDS washed nylon membrane was equilibrated in buffer 1 for 1 min. To prevent nonspecific binding of the DIG antibody the membrane was washed for 30 min in 100 ml of 1% blocking reagent (10% blocking reagent diluted to 1% with buffer 1). Then the membrane was incubated in 20-30 ml of alkaline phosphatase conjugated anti-digoxigenin antibody solution (1:10,000 dilution in 1% blocking reagent) for 30 min at RT. The unbound antibody was removed by washing in buffer 1 for 2 x 15 min. After 2 min equilibration in buffer 3, the membrane was wrapped in film and incubated for 5 min with CSPD solution (25 mM in 1 ml buffer 3). The liquid was removed and the membrane was incubated at 37°C for 10 min and then exposed to a X-ray film for 30-90 min. For quantification of the RNA bands, the videodensitometer (Biotec-Fischer) was used.

Buffer 1 (maleic acid buffer):

			Final concentration	
Maleic acid	11.61	g	0.1	M
NaCl	8.78	g	0.15	M
H ₂ O	to 1	l		

The pH was adjusted to 7.5 with solid NaOH. The solution was autoclaved.

Buffer 3:

			Final concentration
Tris	12.11	g	0.1 M
NaCl	5.84	g	0.1 M
MgCl ₂	10.17	g	50 mM
H ₂ O	to 1	l	

The pH was adjusted with HCl to 9.5. MgCl₂ was added after autoclave.

3.2.11 Western blot analysis*Total protein isolation from the cultured cells*

Cultured cells were washed with ice-cold 1×PBS and scraped off the plate into 150µl lysis buffer. Then, the cells were thoroughly destroyed by ultrasonic in ice bath for 10 min. After centrifugation at 13,000rpm, 4°C for 15 min, the supernatant was collected into a new tube. Protein concentration of cell extract was measured with Bradford method.

Lysis buffer:

	Final concentration
Tris/HCl (pH=8.0)	50 mM
EDTA	5 mM
NaCl	150 mM
NP-40	0.5 %
DTT	5 mM
Protease inhibitors cocktail tablet	1

Lysis buffer without DTT and protease inhibitors can be stored at 4°C. DTT and protease inhibitor cocktail tablet were added freshly before use.

SDS-Polyacrylamide Gel Electrophoresis of protein (SDS-PAGE)

In SDS-PAGE the denatured polypeptides bind SDS and become negatively charged. The amount of SDS bound is always proportional to the molecular weight of the polypeptide and is independent of its sequence, therefore SDS-polypeptide complexes migrate through polyacrylamide gels in accordance with the size of the polypeptide. By using markers of known molecular weight, it is therefore possible to estimate the molecular weight of the polypeptide chains.

Protein sample (100 µg) from medium or cell extract was denatured by heating to 95°C for 5

min in 1×loading buffer, then cooled on ice immediately. The samples were collected by brief centrifugation and then loaded on the corresponding polyacrylamide gel. The electrophoresis was performed with 8V/cm at the beginning. After the dye front moved into the resolving gel, the voltage was increased to 15 V/cm and the gel was run till the bromophenol blue reaches the bottom of the resolving gel (for about 2 h). Then, the gel can be used for western blotting analysis, or fixed and stained with Coomassie Brilliant Blue.

Starking gel buffer:

			Final concentration
Tris (pH 6,8)	7.2	g/100 ml	0.6 M

Resolving gel buffer:

			Final concentration
Tris (pH 8,8)	22.7	g/100 ml	1.875 M

1× SDS gel-loading buffer:

	Final concentration
Tris/HCl (pH 6,8)	50 mM
SDS	2 %
glycerol	10 %
Bromophenol blue	0.1 %
DTT	40 mM

1× SDS gel-loading buffer lacking DTT can be stored at room temperature. DTT was added just before the buffer was used.

Tris-glycine electrophoresis buffer:

	Final concentration
Tris (pH 6,8)	25 mM
Glycine (electrophoresis grade, pH 8,3)	250 mM
SDS	0.1 %

Electroblotting of immobilized proteins

The separated proteins on the SDS-polyacrylamide gel were electronically transferred to a polyvinylidene fluoride (PVDF) membrane by electroblotting. The PVDF membrane was activated by methanol before used. The transfer equipment was prepared in the following way: a whatmann 3MM filter paper washed with anodenbuffer 1, on which two layers filter paper and the activated PVDF membrane washed with anodenbuffer 2 were inserted into the electroblotting chamber. On the PVDF membrane, the gel and the other two layers of filter

paper washed with kathodenbuffer were placed. The kathod and anode from the power supply were connected with the electroblotting chamber. Electroblotting was performed at constant current (1mA / cm²) for approximately 50 min.

After transferring, the PVDF membrane was stained by Ponceau S. To check if the transfer was complete the gel was stained with Coomassie-blue.

Anodenbuffer 1:

			Final concentration	
Tris (pH 11,3)	18.2	g/500 ml	300	mM
Methanol	100	ml/500 ml	20	%

Anodenbuffer 2:

			Final concentration	
Tris (pH 10,6)	1.5	g/500 ml	25	mM
Methanol	100	ml/500 ml	20	%

Kathodenbuffer 1:

			Final concentration	
Tris (pH 9)	1.5	g/500 ml	25	mM
Methanol	100	ml/500 ml	20	%

Ponceau S:

			Final concentration	
Ponceau S (Sigma P-3504)	1.25	g/500 ml		
Methanol	200	ml/500 ml	40	%
Acetic Acid (100%)	75	ml/500 ml	15	%

Fixing solution:

			Final concentration	
Methanol			50	%
Glacial acetic acid			10	%
H ₂ O			40	%

Coomassie-blue:

			Final concentration	
Coomassie Blue (G250)	2.5	ml/l	0.25	% (v/v)
Methanol	400	ml/l	40	% (v/v)
Acetic Acid (100%)	100	ml/l	10	% (v/v)
Glycerin	20	ml/l	2	% (v/v)

Coomassie-blue destaining:

	Final concentration
Methanol	30 %
Acetic Acid (100%)	10 %

Immunological detection of immobilized proteins

The membrane was blocked with 5% non-fat milk in PBS at room temperature for 1 h followed by incubation with primary antibody at 4°C overnight. After washing with 1×PBS + 0,1% Tween 20 for 3 × 10 min, the membrane was incubated with the respective secondary antibody at room temperature for 1 h followed by 3 × 10 min washing. The detected bands were visualized by ECL (Enhanced Chemiluminescence) followed by exposure of the membrane to X-ray film.

3.2.12 Expression and purification of GST-TADN fusion protein*Expression of GST-TADN*

To investigate the interaction between HIF-1 α TADN and VHL, the GST-TADN fusion protein was expressed in *E.coli*. The plasmid pGEX-GST-TADN or pGEX-5X1 was transformed into the competent cells, BL21(DE3), as described in 3.1.3. The single colony of transformed *E.coli* was picked up and cultured in LB medium containing 100 μ g/ml ampicillin at 37°C until the OD at 550 nm reached 0.4-0.5 (for 3-4 h). Isopropyl β -D-thiogalactoside (IPTG, final concentration of 0.1 mM) was then added to induce fusion protein expression. The bacteria were further cultured at 37°C with aeration for additional 3 h. The bacteria were collected by centrifugation at 4000 rpm, 4°C for 10 min and then stored at -20°C before further purification of the protein.

IPTG:

	Final concentration
IPTG	100 mM

Purification of a fusion protein by Glutathione Sepharose 4B

The collected bacteria pellet was placed on ice and completely suspended in 10 ml of ice cold lysis buffer with 10 mg lysozyme. The suspension was gently mixed at 4°C for about 30 min, followed by ultrasonication on ice in short bursts. Triton X-100 was then added into the lysate

to a final concentration of 1%. The lysate was further incubated at 4°C for 30 min with gentle mixing to aid in solubilization of the fusion protein. After centrifugation at 13,000 rpm, 4°C for 10 min, the supernatant containing the expressed fusion protein was incubated with 380 μ l 80% Glutathione Sepharose 4B (about 300 μ l beads) for 2 h at RT. The contaminated proteins were removed by 4 times washing with 10 ml 1 \times PBS. The GST-TADN or GST protein was subsequently eluted with elution buffer (50 mM Tris-HCl, 10 mM reduced glutathione, pH 8.0).

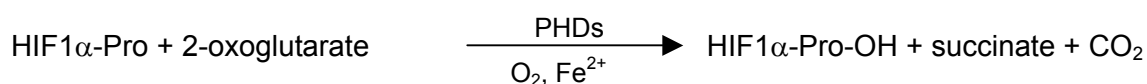
Lysis buffer:

	Final concentration
Tris/HCl (pH 8.0)	20 mM
NaH ₂ PO ₄ /Na ₂ HPO ₄	50 mM
PMSF	1 mM
H ₂ O	to 100 ml

PMSF was added freshly before use. The Complete protease inhibitor cocktail tablet was added to every 10 ml before use.

3.2.13 HIF-1 α peptide hydroxylation assay

HIF-1 α prolyl hydroxylases (PHDs) catalyse the post-translational hydroxylation of specific prolyl residues in HIF-1 α to *trans*-4-hydroxy-prolyl residues. As PHDs are members of the 2-oxoacid- and ferrous ion-dependent dioxygenase family, the hydroxylating reaction requiring 2-oxoglutarate and ferrous ions can be described as:



For the hydroxylation assay, cell extracts from HepG2 cells were prepared as follows: HepG2 cells were cultured for 24 h under normoxia and homogenized at 4°C in lysis buffer [250 mM sucrose, 50 mM Tris-HCl (pH 7.5) supplemented with complete protease inhibitors cocktail tablet]. The homogenate was centrifuged at 1,000 \times g for 10 min. The supernatant was recovered and centrifuged again at 3,000 \times g for 10 min. The supernatant was recovered and centrifuged at 18,000 g for 10 min. The pellet from the last centrifugation was suspended in 40 mM Tris-HCl (pH 7.5).

The cell extracts (about 300 μ g of protein/ml) were then incubated at 37°C for 30 minutes in hydroxylation buffer with either 20 μ g GST or GST-TADN protein in the presence of different concentrations of DHR, RH, or Bapta. The radioactivity associated to succinate was measured in a liquid scintillation counter (Baader et al., 1994). The basal GST-dependent

enzyme activity in each experiment was subtracted from GST-TADN-dependent activity.

Hydroxylation buffer:

		Final concentration	
Tris/HCl (pH 7.5)		40	mM
FeSO ₄		50	μM
ascorbate		1	mM
catalase		0.4	mg/ml
[5- ¹⁴ C]2-oxoglutarate	50,000 dpm		
2-oxoglutarate (unlabeled)		0.1	mM
DTT		0.5	mM
BSA		2	mg/ml

3.2.14 VHL pull-down assay

³⁵S-VHL in vitro translation

For the VHL pull-down assay, ³⁵S-VHL protein was synthesized with the TNT coupled reticulocyte lysate system. The plasmid pCMV-HA-VHL was used as the template and ³⁵S-methionine was used for labelling. The in vitro translation reaction was performed as follows:

TNT lysate reaction:

TNT rabbit reticulocyte lysate	25	μl
TNT reaction buffer	2	μl
TNT T7 RNA polymerase	1	μl
Amino acid mixture(1mM, minus methionine)	1	μl
[³⁵ S]Methionine (>1.000Ci/mmol at 10mCi/ml)	2	μl
RNAsin ribonuclease inhibitor (40u/μl)	1	μl
pCMV-HA-VHL	1	μg
Nuclease-free H ₂ O	to 50	μl

The reaction mixture was incubated at 30°C for 90 min, and then stored at -20°C for VHL pull down assay.

To determine the incorporation of the labelling, 2 μl of the mixture were removed from the reaction and added into 98 μl of 1 M NaOH/2% H₂O₂. After brief vortexing, the solution was incubated at 37°C for 10 min. Each 50 μl was dropped on a small Whatman 3MM filter paper and air-dried. To measure the incorporation of ³⁵S, the filter paper was washed once with 10%

TCA, three times with 5% TCA, two times with ether/ethanol (1:1) and then mixed with 5 ml scintillation mixture after drying. To measure total counts present in the reaction, the filter paper was mixed with 5 ml scintillation mixture without wash. The radioactivity counts were measured with a liquid scintillation counter. The following calculation was used to determine the percent incorporation:

$$\text{percent incorporation} = (\text{cpm of washed filter} / \text{cpm of unwashed filter}) \times 100$$

GST pull-down assay

The purified GST-TADN protein was first incubated with the cell extracts in hydroxylation buffer (without [5-¹⁴C]2-oxoglutarate) in the presence of 0.5 μM DHR, RH or 5 μM BAPTA, as described in 3.2.13. The reaction products were then incubated at 20°C in 200 μl of buffer 1 supplemented with 10 μl Glutathione Sepharose beads and 50,000 dpm of [³⁵S]-labelled human VHL. After 2 h, beads were washed three times with cold buffer 2. The bound proteins were eluted in 10 mM reduced glutathione and loaded on a 15% SDS-polyacrylamide gel. The electrophoresis was performed as described in 3.2.11. After the electrophoresis, the gel was fixed and stained with Coomassie Brilliant Blue. For drying, one side of the gel was covered with film and the other side with two sheets of Whatmann 3MM paper and put in a gel dryer for 2 h at 70°C.

Buffer 1:

	Final concentration	
Tris/HCl (pH 8.0)	50	mM
NaCl	120	mM
NP-40	0.5	%

Buffer 2:

	Final concentration	
Tris/HCl (pH 8.0)	20	mM
NaCl	100	mM
EDTA	1	mM
NP-40	0.5	%

The dried gel was exposed overnight to the europium-covered phosphorimager screen to detect the [³⁵S]-labelled VHL band. Under X-ray irradiation europium electrons are raised to higher energy levels and due to the laser beam of the scanner they return to their original energy levels thereby emitting energy in form of light which is detected by a photomultiplier.

The signal is further processed by a special software (ImageQuant) and shown on the computer screen as black spots or bands so that the resulting picture is very similar to the picture obtained with autoradiography film. This method of detection is much more sensitive than the classical autoradiography and shortens exposure time of the gel app. to 1/10 of the time needed to obtain an autoradiography on film.

3.3 Statistical analysis

Unless indicated otherwise, all data in the figures and text are expressed as means \pm s.e. of n independent observations. Statistical evaluation was performed either by one-way analysis of variance followed by Bonferroni multiple comparisons test (comparison of three or more groups) or paired two-tailed Students t -test (comparison of two groups), where appropriate with the InStat for WindowsTM statistics software package (GraphPad Software). A P value < 0.05 was considered statistically significant.

3.4 Security measures

All the operations with genetically modified organisms and plasmid DNA were performed according to the „Gentechnikgesetz of 1990“ and to the rules prescribed by the „Gentechnik-Sicherheitsverordnung of 1990“. Materials contaminated with bacterial cells were treated with hydrogen peroxide, soap suds and autoclaved.

The chemicals formaldehyde, DEPC, phenol and ethidium bromide are cancerogenic and were carefully managed and disposed.

All the operations with radiochemicals were performed in a C laboratory, the radiochemicals were disposed according to the instructions.

4. RESULTS

4.1 Localization of the OH•-generating Fenton reaction at the endoplasmic reticulum

In order to identify the cellular compartment in which the Fenton reaction takes place, HepG2 cells were transfected with pDsRed-ER, pECFP-ER, pDsRed-Mito, pECFP-Mito, pDsRed-Golgi, pECFP-Golgi, pDsRed-Peroxi or pDsRed-Lysosome to label the according cellular compartments. The transfected cells were then treated with 30 μ M dihydrorhodamine (DHR) for 5 min in the microscope tissue culture chamber under normoxia. It was known that the OH• generated from Fenton reaction could mediate the conversion of DHR to fluorescent rhodamine 123 (RH) which had a different excitation and emission maximum compared to the DsRed and ECFP fluorescent proteins. This allowed to detect RH fluorescence and DsRed or ECFP fluorescence simultaneously by using the emission filter settings in 2P-CLSM without any cross-talk. After the computer programmed deconvolution and reconstruction, the overlap between RH fluorescence and DsRed or ECFP fluorescence indicated the site of OH• generation in the Fenton reaction.

The three dimensional reconstruction of cells revealed that RH fluorescence overlapped only with DsRed fluorescence elicited in the endoplasmic reticulum, but not with the fluorescence in the mitochondria, Golgi apparatus, peroxisomes or lysosomes (Fig. 19). The same result was observed in the cells transfected with pECFP constructs (Fig. 19). Therefore, the OH• generating Fenton reaction was localized in the endoplasmic reticulum but not in the other compartments.

To investigate whether OH• generation in the endoplasmic reticulum is pO₂-dependent, the pDsRed-ER or pDsRed-Mito transfected HepG2 cells were exposed to hypoxia for 60 min before treated with DHR. When keeping the cells under hypoxia within the microscope tissue chamber, the RH fluorescence was not able to be detected at all (Fig. 20, right panel). However, after the cells were changed back to normoxia within the chamber for about 15 min, a clear overlap of OH• generation and DsRed fluorescence was again detected in the ER but not in the mitochondria (Fig. 20, left panel).

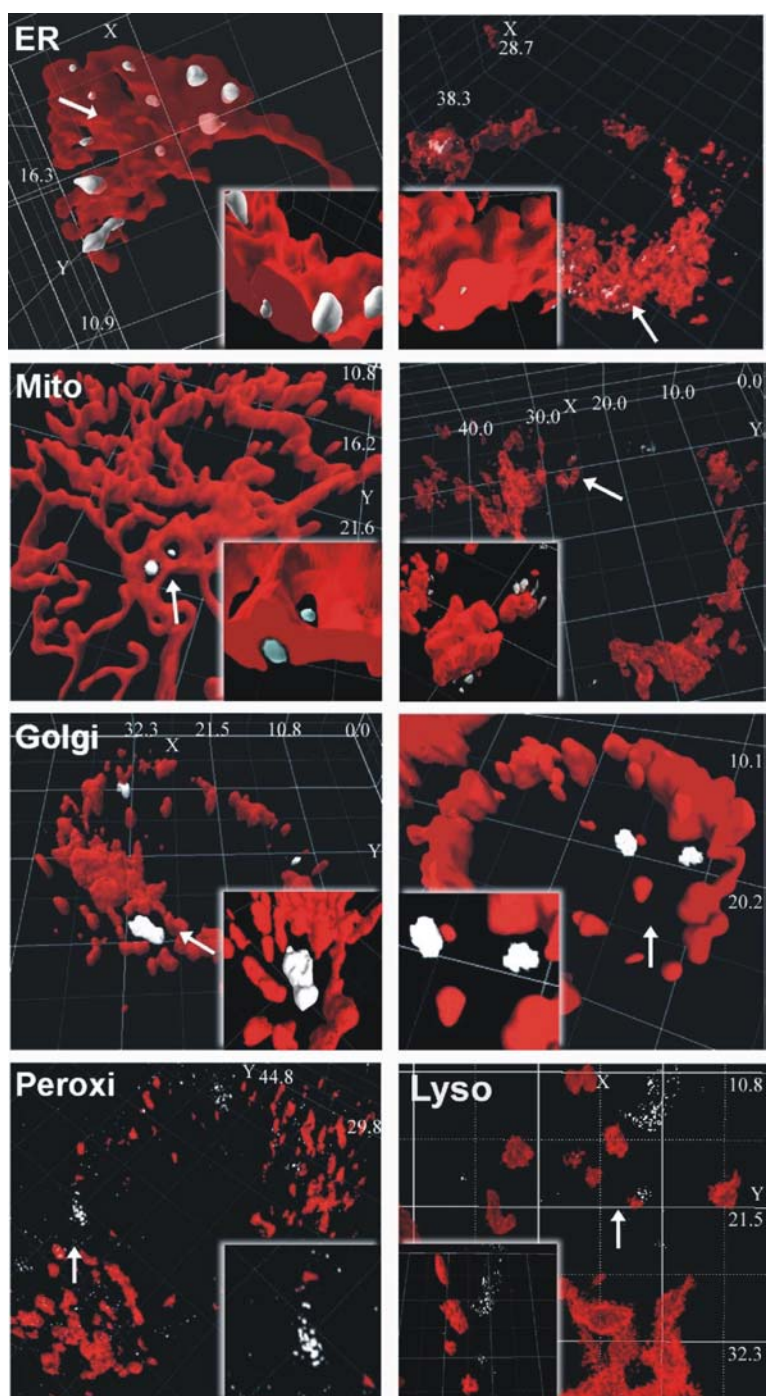


Figure 19. Detection of OH• generation at the endoplasmic reticulum. HepG2 cells were transfected with pDsRed-ER (right panel), pECFP-ER (left panel), pDsRed-Mito (right panel), pECFP-Mito (left panel), pDsRed-Golgi (right panel), pECFP-Golgi (left panel), pDsRed-Lyso (right panel), pDsRed-Peroxi (left panel) constructs. The transfected cells were treated for 5 minutes with 30 μ M dihydrorhodamine (DHR) that is converted into fluorescent rhodamine 123 (RH) by hydroxyl radicals generated in a Fenton reaction. Fluorescence was visualized by 2P-CLSM. The different subcellular compartments are shown in red and the RH fluorescence is shown in gray/white indicating the local OH• generation. The small insets show 20 \times magnified images of the areas with OH• generation indicated by an arrow. Dimensions of the X, Y and Z axis are given in μ m. Representative data from 20 experiments (ER, n=6; Mito, n=5; Golgi, n=5; Peroxi, n=2; Lyso, n=2)

The pO_2 -dependent $OH\bullet$ generation was further supported by applying a photoreduction approach (Hockberger and Skimina, 1999). In this experiment, the pDsRed-ER or pDsRed-Mito transfected cells were challenged with the blue light which initiated a reduction of flavin and concomitantly activated flavin-containing oxidases in the cells. These oxidases could reduce O_2 to H_2O_2 , which was subsequently degraded to $OH\bullet$ by the Fenton reaction. Thus, the photoreduction can serve as a control for intracellular $OH\bullet$ production. After the treatment with DHR, the 2P-CLSM images revealed that O_2 was the major trigger for intracellular $OH\bullet$ production as RH fluorescence in the endoplasmic reticulum was predominantly seen under normoxia but minimal under hypoxia (Fig. 20, insets). However, the photoreduction effect could also be observed in mitochondria since they contain FADH for the generation of electrons. Thus, the O_2 -dependent $OH\bullet$ generation by the Fenton reaction, which may be involved in the O_2 signal cascade, mainly occurred at the endoplasmic reticulum. (Fig. 20, insets).

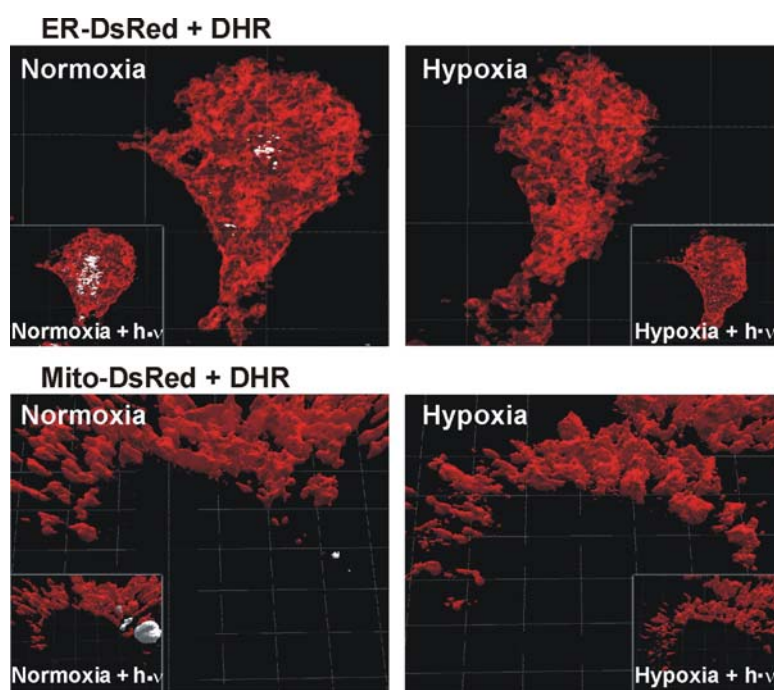


Figure 20. Hypoxia-mediated inhibition of $OH\bullet$ generation at the endoplasmic reticulum. HepG2 cells were transfected with DsRed-ER or DsRed-Mito gene constructs. After 48 h the transfected cells were cultured under hypoxia for 60 minutes and treated for 5 minutes with 30 μ M dihydrorhodamine (DHR) before imaged. Then cells were exposed to normoxia for 15 minutes and were imaged again by 2P-CLSM. Insets: $OH\bullet$ generation mediated by photoreduction. Cells were challenged with light at a wavelength of 450 nm for 5 sec under hypoxia or normoxia and imaged. White, rhodamine123 fluorescence indicating local $OH\bullet$ generation; Red, fluorescence indicating the different subcellular compartments. Representative data from four independent experiments.

4.2 Localization of HIF-1 α at the endoplasmic reticulum under normoxia

Since the O₂-dependent OH• generation by the Fenton reaction was localized in the ER, it would be interesting to investigate whether the transcription factor HIF-1 α could be found in the same cellular compartment. HepG2 cells were transfected with pECFP-ER and incubated under normoxia or hypoxia for 60 min before immunostained with an anti-HIF-1 α antibody. 2P-CLSM results revealed that under normoxia the fluorescence indicating the ER overlapped with the fluorescence indicating the presence of HIF-1 α (Fig. 21 left). In contrast, under hypoxia the ER fluorescence and the HIF-1 α fluorescence were clearly dissociated and the HIF-1 α fluorescence was observed within the nucleus (Fig. 21 right). Thus, under normoxia a substantial amount of HIF-1 α could be localized to the endoplasmic reticulum and therefore it may be a likely target for the generated OH•.

4.3 Modulation of HIF-1 functions by the OH• scavenger Dihydrorhodamine (DHR)

The colocalization of OH• generation by the Fenton reaction with the ER and HIF-1 α implicated that specific scavenging of OH• at the ER by DHR may interfere with HIF-1 functions. This was then studied in the next set of experiments.

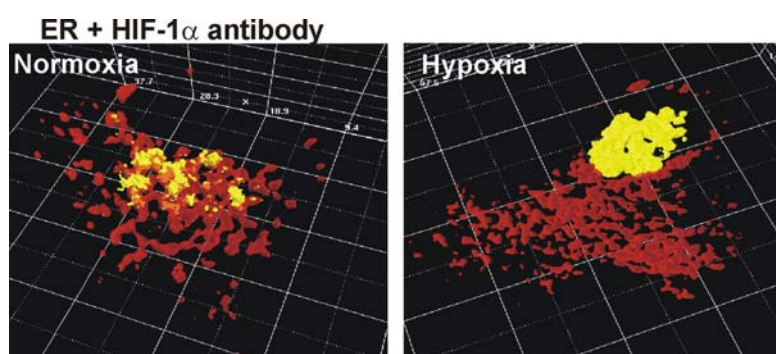


Figure 21 Hypoxia-mediated HIF-1 α translocation from the endoplasmic reticulum to the nucleus. HepG2 cells were transfected with pECFP-ER and exposed to normoxia (60 min) or hypoxia (60 min) and immunostained with an anti-HIF-1 α antibody and a Living colors A. v. peptide antibody. The fluorescence of the secondary antibodies was captured by 2P-CLSM and visualized in false colors. Yellow/orange color indicates HIF-1 α and red color indicates ER. Dimensions of the X, Y, Z axis are given in μm . Representative data from four independent experiments.

4.3.1 Induction of HIF-1 dependent genes by DHR

Previous studies have shown that the expression of plasminogen activator inhibitor-1 (PAI-1) and heme oxygenase-1 (HO-1) in hepatocytes was clearly enhanced under hypoxia and these inductions were mainly mediated by HIF-1 (Kietzmann et al, 1999). Therefore, both PAI-1 and HO-1 were used as read-out for HIF-1 activation in these experiments. Primary rat hepatocytes were cultured under standard conditions for 24 h, and then treated with 6 μ M DHR for 4 h under normoxia or hypoxia. The expression of PAI-1 and HO-1 was detected at both mRNA and protein levels. Hypoxia (8% O₂) induced PAI-1 and HO-1 mRNA expression by about 3.5-fold. Similarly, DHR treatment (6 μ M) under normoxia also induced PAI-1 and HO-1 mRNA expression by 3.5- and 2.5-fold, respectively. The mRNA induction was followed by an induction at the protein level. DHR (6 μ M) induced PAI-1 and HO-1 protein 2- and 3-fold, respectively. No synergistic effects of DHR and hypoxia were observed. The DHR treatment under hypoxia did not further enhance the expression of both genes either at the mRNA level or protein level (Fig. 22).

The finding that DHR induced HIF-1-dependent gene expression was further demonstrated by reporter gene experiments. It is known that HIF-1 activates gene expression by binding to hypoxia response elements (HRE) in regulatory regions of target genes. In the next experiments, HepG2 cells were transfected with constructs containing the wild type human PAI-1 gene promoter (pGL3-hPAI) or a promoter with a HRE mutation (pGL3-hPAI-M2). The luciferase (LUC) activity assay revealed that treatment with DHR as well as hypoxia induced the PAI-1 wild type promoter activity by about 2.4-fold (Fig. 23) while the HRE mutated hPAI-1 promoter did not respond to either DHR treatment or hypoxia (Fig. 23). Moreover, transfection with a construct containing three HRE copies from the EPO gene (pGL3-EPO-HRE) also demonstrated that DHR treatment mimicked hypoxia by inducing LUC activity about 2-fold (Fig. 24). Mutation of the critical nucleotides in the HRE (pGL3-EPO-HREm) abolished both the induction by hypoxia and by DHR (Fig. 24). As a control, the treatment with 6 μ M RH, which is the final product of DHR conversion, had no effects on LUC activity indicating the specificity of the DHR effect (Fig. 23, 24). Therefore, the specific scavenging of OH• by DHR mimicked hypoxia and induced hypoxia-regulated genes via HIF-1.

4.3.2 Induction of HIF-1 α protein levels by DHR

The results from the Northern and Western blots as well as from the transfection experiments supported that DHR may have a direct effect on HIF-1 α . Therefore, it was checked whether the OH• scavenger DHR could modulate HIF-1 α protein expression. The HIF-1 α protein was

hardly detectable under normoxic conditions, while under hypoxia HIF-1 α was significantly induced (Fig. 25). Similarly, the treatment with 6 μ M DHR under normoxia induced the HIF-1 α protein level by about 4-fold, while DHR had no effects under hypoxia. Since the final product of DHR conversion, RH, had no effect on the HIF-1 α protein level, these results verified that DHR induced endogenous HIF-1 α protein expression by specifically scavenging the OH \bullet radicals (Fig. 25).

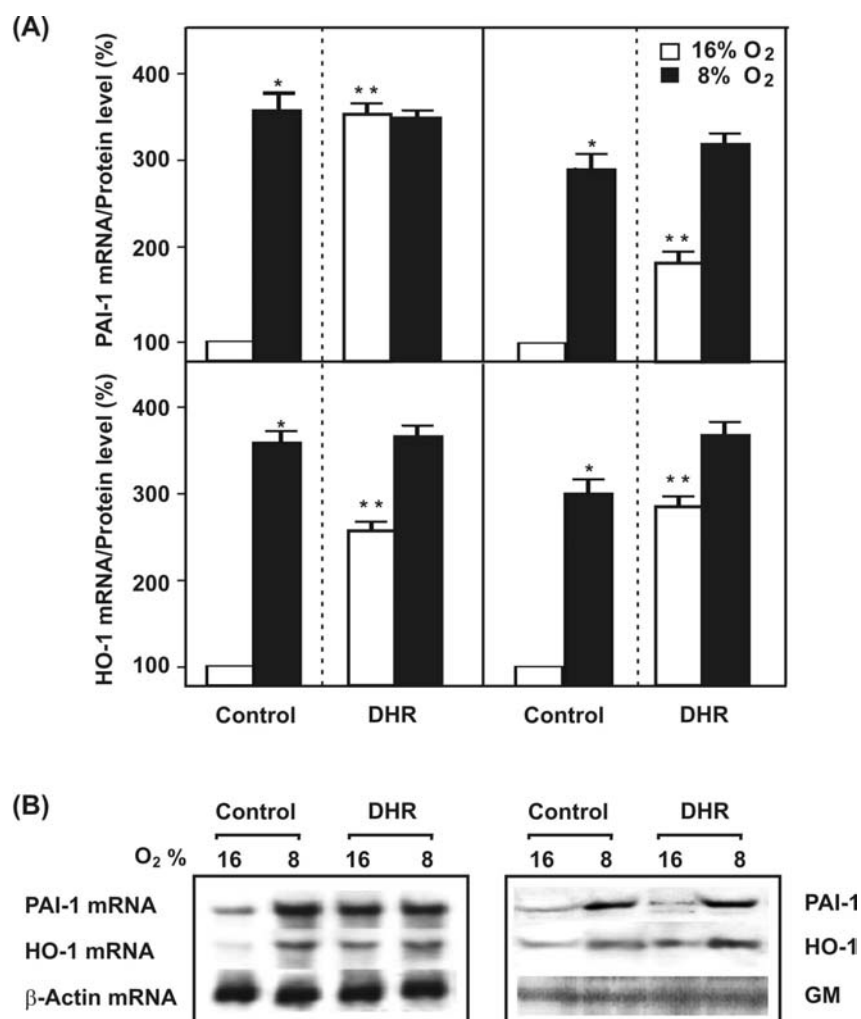


Figure 22. Induction of PAI-1 and HO-1 gene expression by DHR under normoxia. Primary cultured hepatocytes were cultured for 24 h under normoxia (16% O₂) and then treated with 6 μ M DHR and cultured under normoxia or hypoxia (8% O₂) for 4 h. The expression of PAI-1 and HO-1 was detected by Northern blot (left panels) and Western blot (right panel). **(A)** The statistical summary of the PAI-1 and HO-1 expression is shown. Gene expression under normoxia was set to 100%. * $P \leq 0.05$ (16% O₂ vs. 8% O₂); ** $P \leq 0.05$ (16% O₂ vs. 16% O₂ + DHR); $n=3$. **(B)** Representative Northern and Western blot. 20 μ g of total RNA was hybridised with Dig-labeled PAI-1, HO-1 or β -Actin antisense RNA probes. For western blot, 100 μ g protein from medium or cell lysates was analysed with PAI-1 or HO-1 antibodies, respectively. Anti-Golgi membrane antibody (GM) was used as the internal control. Autoradiographic signals were obtained by chemiluminescence and scanned by videodensitometry.

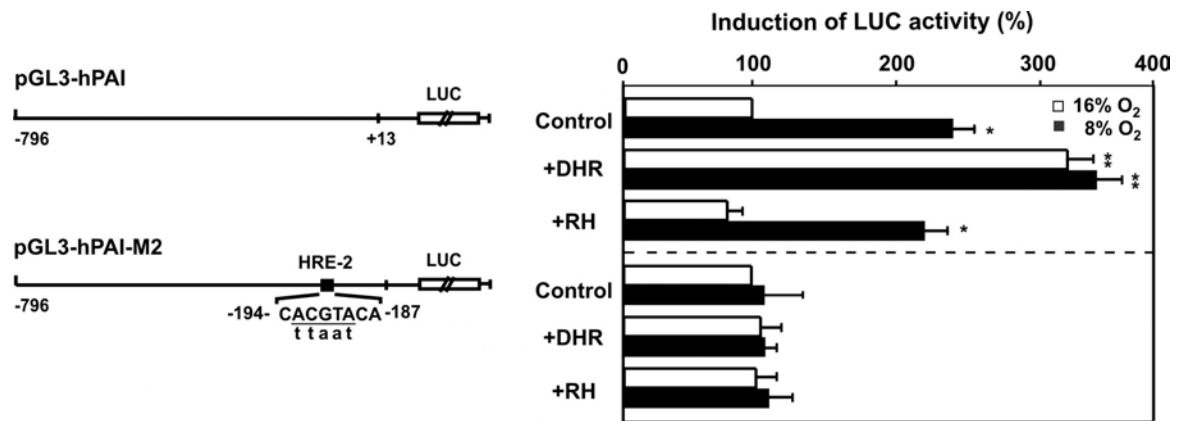


Figure 23. The induction of PAI-1 promoter activity by DHR. HepG2 cells were transfected with either the wild type 806 bp human PAI-1 promoter LUC construct (pGL3-hPAI) or the PAI-1 promoter construct mutated at the HRE-2 site (pGL3-hPAI-M2). The transfected cells were treated with 6 μ M dihydrorhodamine (DHR) or 6 μ M rhodamine (RH) and further cultured 24 h under normoxia (16% O₂) or hypoxia (8% O₂). In each experiment the LUC activity of pGL3-hPAI or pGL3-hPAI-M2 transfected cells at 16% O₂ was set to 100%, respectively. In pGL3-hPAI-M2 the wild type PAI-1 sequence is shown on the upper strand, mutated bases are shown in lower case letters. * $P \leq 0.05$, 16% O₂ vs. 8% O₂; ** $P \leq 0.05$, 16% O₂ vs. 16% O₂ + DHR or 8% O₂ vs. 8% O₂ + DHR, n=3.

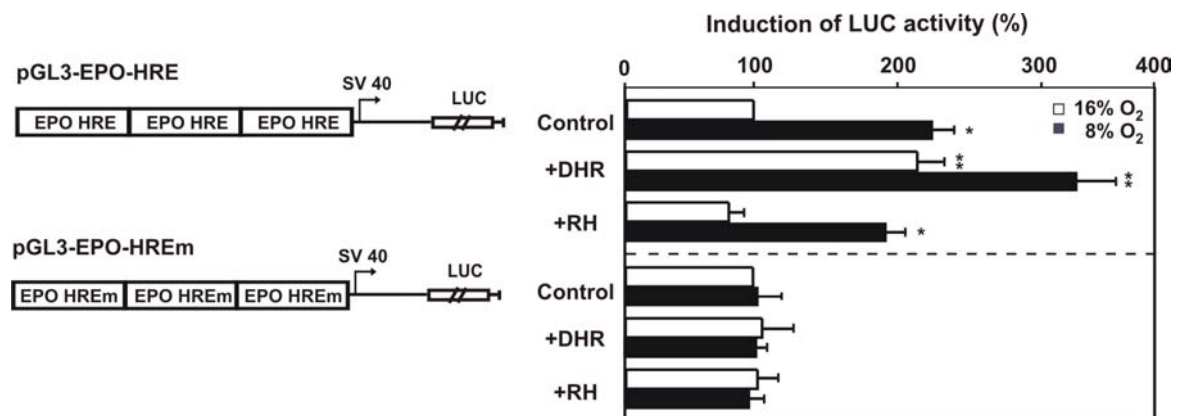


Figure 24. Induction of EPO-HRE Luc gene expression by DHR. HepG2 cells were transfected with the luciferase construct containing three copies of the erythropoietin hypoxia response element (EPO-HRE) or mutated HRE (EPO-HREm) in front of the SV40 promoter and the luciferase. The transfected cells were treated with 6 μ M dihydrorhodamine (DHR) or 6 μ M rhodamine (RH) and further cultured 24 h under normoxia (16% O₂) or hypoxia (8% O₂). In each experiment the Luc activity of pGL3- EPO-HRE or pGL3- EPO-HREm transfected cells at 16% O₂ was set to 100%, respectively. * $P \leq 0.05$, 16% O₂ vs. 8% O₂; ** $P \leq 0.05$, 16% O₂ vs. 16% O₂ + DHR or 8% O₂ vs. 8% O₂ + DHR, n=3.

4.3.3 Induction of HIF-1 α nuclear translocation by DHR

The accumulation of the HIF-1 α protein after treatment with DHR does not necessarily mean that this might have a regulatory function. Since functionally active HIF-1 α is translocated into the nucleus under hypoxic conditions, it was investigated whether DHR may influence HIF-1 α nuclear translocation. Therefore, HepG2 cells were transfected with an expression vector for GFP-tagged HIF-1 α (pGFP-HIF1 α) and treated with DHR. It was found that both hypoxia and DHR treatment could induce the nuclear accumulation of GFP-tagged HIF-1 α as observed by fluorescence microscopy (Fig. 26). In addition, PDTC (100 μ M), which can act also as radical scavenger, also induced nuclear accumulation of HIF-1 α (Fig. 26).

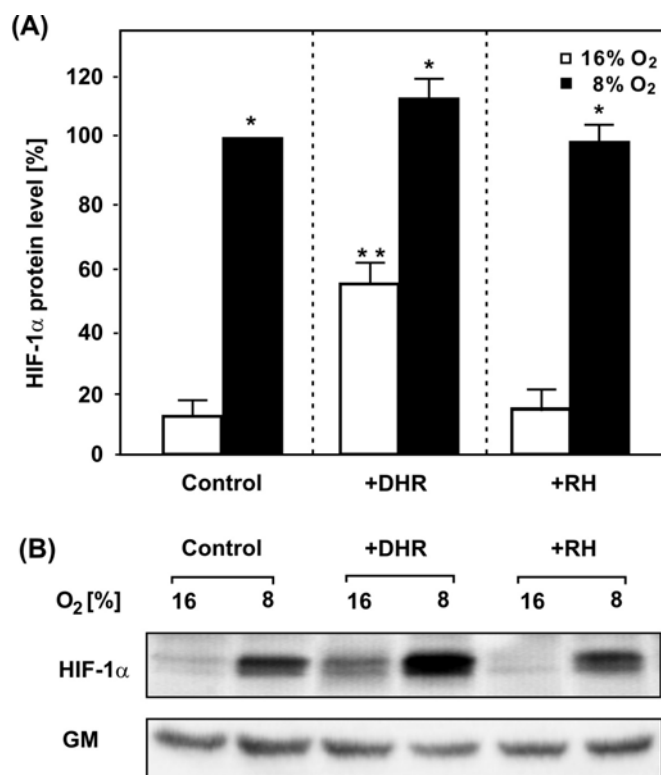


Figure 25. Induction of HIF-1 α protein expression by DHR under normoxia. HepG2 cells were cultured for 24 h under normoxia (16% O₂), the cells were then treated with either 6 μ M dihydrorhodamine (DHR) or 6 μ M rhodamine (RH) and further incubated for 4 h under normoxia or hypoxia (8% O₂). **(A)** The statistical summary of HIF-1 α protein levels measured by Western blot. The HIF-1 α protein level under hypoxia was set to 100%. * $P \leq 0.05$ 16% O₂ vs. 8% O₂, ** $P \leq 0.05$ 16% O₂ vs. 16% O₂ + DHR, $n=3$. **(B)** Representative Western blot. 100 μ g of protein from the whole-cell extract were subjected to Western analysis with an antibody against HIF-1 α or golgi membrane (GM) (as an internal control). Autoradiographic signals were obtained by chemiluminescence and scanned by videodensitometry.

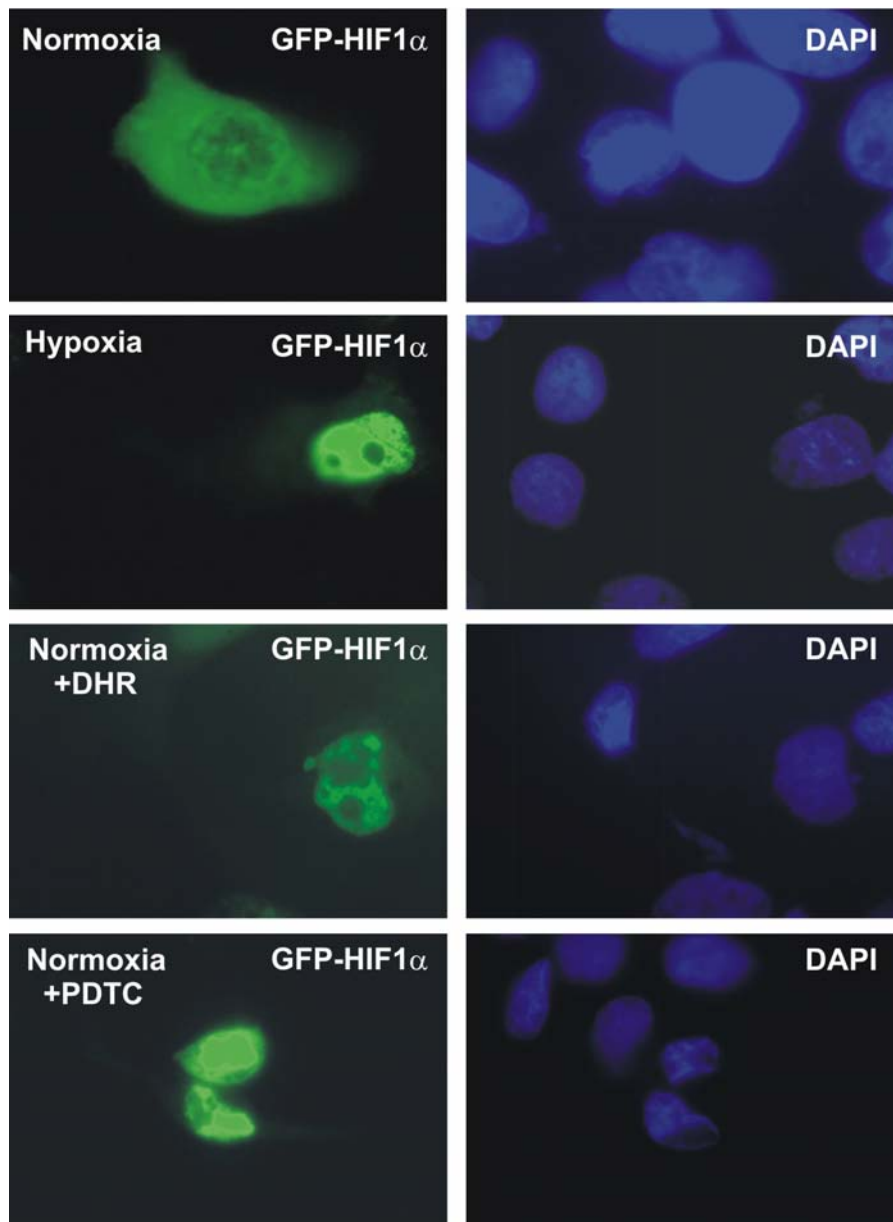


Figure 26. Induction of HIF-1 α nuclear translocation by dihydrorhodamine (DHR) under normoxia. Cells were transfected with GFP-HIF-1 α and cultured under normoxia (16% O₂). After 48 h cells were cultured under hypoxia (4 h) or treated with either 6 μ M dihydrorhodamine (DHR) or 100 μ M PDTC under normoxia. The green fluorescence indicates the accumulation of GFP-tagged HIF-1 α in the left panel; Microscopic images of the same fields are shown in the right panel indicating the DAPI fluorescence of the nucleus. Representative data of three independent experiments.

4.3.4 Induction of HIF-1 α transactivity by DHR

The finding that DHR treatment could induce HIF-1 α protein expression and accumulation in the nucleus supported that DHR may influence HIF-1 α transactivation as well. It is known that HIF-1 α has two transactivation domains, TADN (amino acid 531-575) and TADC (amino acid 786-826). To investigate whether DHR influences HIF-1 α activity on either domain, HepG2 cells were cotransfected with a reporter construct (pG5-E1B-LUC), which contains 5 copies of a Gal4 response element, and constructs, which allow the expression of the Gal4-DNA binding domain (Gal4DBD) or a fusion protein of the Gal4DBD and either TADN or TADC. The cotransfection of pG5-E1B-LUC and the Gal4DBD expression vector (pcDNA6-Gal4DBD) only led to low LUC activities in the cells (Fig. 27). However, in cells cotransfected with pG5-E1B-LUC and the Gal4-HIF1 α -TADN vector (pcDNA6-Gal4-HIF1 α -TADN), LUC activity was enhanced by about 200-fold. This LUC activity could be further increased by hypoxia to about 350-fold and the treatment with DHR but not with RH mimicked hypoxia (Fig. 27). Furthermore, it has been reported that hydroxylation of the proline residue (P564) in HIF-1 α -TADN was crucial for the O₂-dependent degradation of HIF-1 α under normoxia. Mutation of the proline (P564) residue to alanine in the construct led to an enhancement of LUC activity under normoxia and a loss in the induction by hypoxia as well as by DHR (Fig. 27). Similar results were obtained in the cotransfection experiments with pG5-E1B-LUC and the Gal4-HIF1 α -TADC vector (pcDNA6-Gal4-HIF1 α -TADC). Although the LUC activity was lower than with the TADN constructs (Fig. 27), treatment with DHR under normoxia mimicked hypoxia and induced the transactivity of TADC, whereas RH had no such effect. Mutation of the critical site for redox modification within the TADC of HIF-1 α (cysteine 800 to serine) abolished both hypoxia- and DHR-dependent induction of LUC activity (Fig. 27).

4.3.5 Modulation of HIF-1 α stability by DHR

In the experiments above, it was shown that the mutation of the proline residue (P564) abolished the induction of HIF-1 α by both hypoxia and DHR. This proline residue has also been shown to be critical for the degradation of HIF-1 α under normoxia. The normoxic degradation is achieved after this proline residue becomes hydroxylated which enables the binding of VHL. The proline hydroxylation is mediated by a group of newly discovered enzymes named HIF proline hydroxylation domain (PHDs) proteins which are similar to the collagen proline hydroxylase. Thus, the activity of these enzymes, which is dependent on the cosubstrates O₂, iron, ascorbate and 2-oxoglutarate, appears to be critical for HIF-1 α stability. While the PHDs enzyme activity can be directly measured by the conversion of 2-oxoglutarate

to succinate, the detection of bound VHL to TADN by GST-pull down assay is an indirect measurement of HIF-1 α PHDs activity. Scavenging of OH \bullet by DHR may inhibit HIF-1 α /VHL interaction due to the reduction of prolyl hydroxylase activity via ferrous redox chemistry. To prove this, VHL GST pull-down assays and PHDs enzyme activity measurements were performed.

The results from the VHL GST pull-down experiments showed that binding of the radioactive ^{35}S -VHL to the GST-TADN fusion protein could only be detected after the *in vitro* expressed GST-TADN was incubated with the cell extract. The treatment with DHR of the cells and additional DHR in the reaction system clearly reduced the interaction between VHL and GST-TADN indicating a reduced hydroxylation. By contrast, RH did not disturb HIF-1 α /VHL interaction (Fig. 28A). Moreover, the total prolyl hydroxylase activity present in the cell extracts was measured by the formation of ^{14}C -succinate from ^{14}C -2-oxoglutarate in the hydroxylase activity assay. It was found that the addition of DHR to the assay had an inhibitory

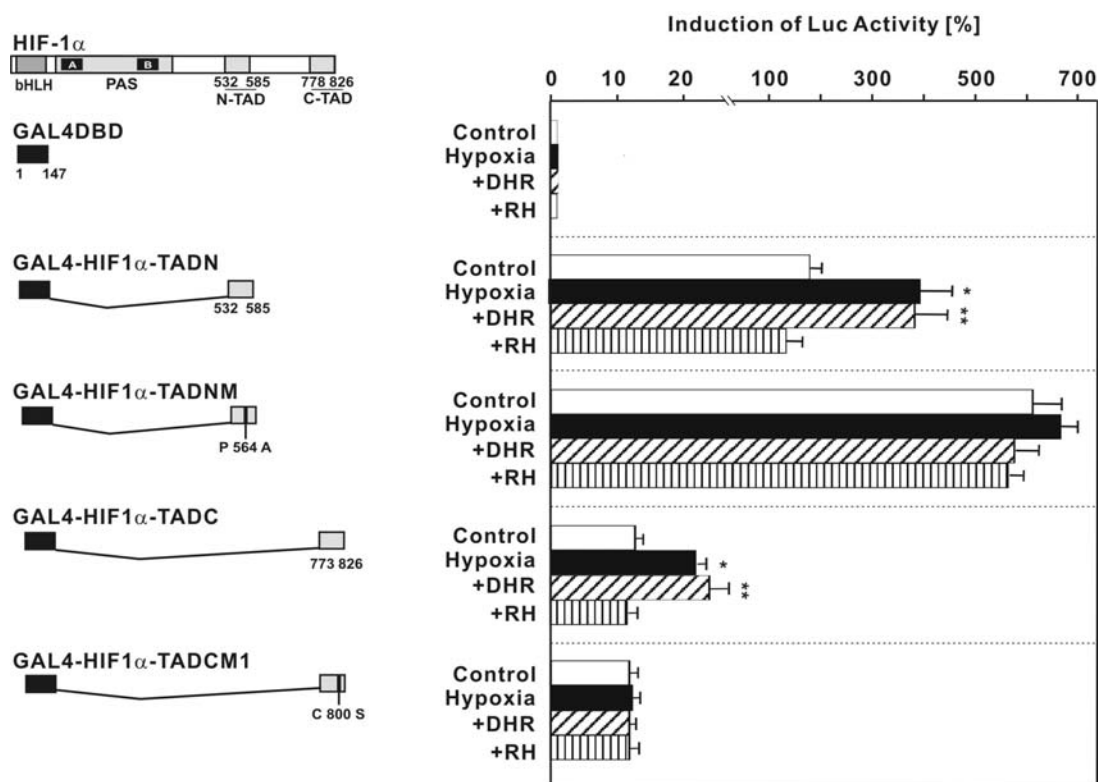


Figure 27. Induction of HIF-1 α transactivation by DHR. HepG2 cells were cotransfected with a luciferase reporter pG5-E1B-LUC and different fusion gene constructs in which the Gal4 DNA binding domain was fused to either the TADN (532-585) or TADC (773-826) of HIF-1 α as shown on the left. The mutations in the constructs are indicated. After 24 h the transfected cells were treated with either 6 μM DHR or 6 μM RH and further cultured for 24 h under normoxia (16% O $_2$) or hypoxia (8% O $_2$). The statistical summary of LUC activity was shown on the right. * $P \leq 0.05$, Control vs. hypoxia; ** $P \leq 0.05$, Control vs. DHR, $n=4$.

effect in a dose-dependent manner whereas the RH treated samples did not display a reduced activity (Fig. 28B).

4.4 Modulation of HIF-1 by endoplasmic reticulum stress

The previous experiments demonstrated that both Fenton reaction and HIF-1 α could be found at the ER. This implicates that ER dysfunction may interfere with O₂ signaling. To investigate this, a variety of pharmacological compounds were used. These included tunicamycin, an inhibitor of protein glycosylation, and brefeldin A, a blocker of protein transport out of the ER. Both of them have been shown to lead to protein accumulation in the ER, which was referred as ER stress (Elbein, 1987). In addition, ER accumulates high levels of Ca²⁺ from the cytoplasm through the endoplasmic reticulum Ca²⁺-ATPase. This pool of Ca²⁺ is important for the translation, folding, glycosylation, disulfide bonding and sorting of secretory proteins in the ER through its direct interactions with a variety of ER-resident molecular chaperones and enzymes (Meldolesi and Pozzan, 1998). Therefore, thapsigargin as an inhibitor of the ER Ca²⁺-ATPase was also included in the experiments.

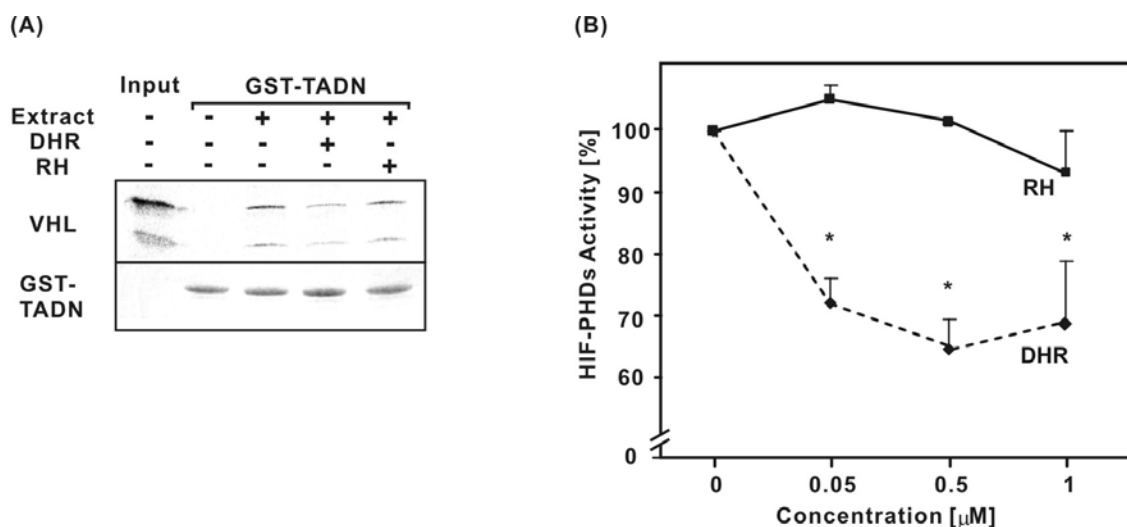


Figure 28. Inhibition of HIF-1 α prolyl hydroxylase activity by DHR. **(A)** GST pull-down assay. The GST-HIF1 α -TADN fusion protein was incubated with or without HepG2 cell extract supplemented with cofactors in the presence of either DHR or RH supplemented with cofactors. Glutathione-Sepharose beads and [³⁵S]VHL were then added and the bound VHL was recovered, subjected to SDS-PAGE, and visualized by phosphoimaging. The input remains from directly loaded [³⁵S]VHL. The two bands represent the 213 and 160 amino acid VHL translation products. **(B)** Dose-dependent inhibition of HIF prolyl hydroxylase activity by DHR. The GST-HIF1 α -TADN fusion protein or the GST protein were incubated with HepG2 cell extract, cofactors and [5-¹⁴C]2-oxoglutarate in the presence of different concentrations of DHR or RH. The radioactivity associated to succinate was determined. In each experiment the basal HIF-TADN-dependent activity which was set to 100% was determined by subtracting the GST-associated activity. * $P \leq 0.05$, DHR vs. RH with the same concentration, $n=3$.

4.4.1 Modulation of LUC activity in EPO-HRE-Luc transfected cells by endoplasmic reticulum stress

The modulation of HIF-1 α -dependent gene expression by ER stress was first investigated by reporter gene analysis. HepG2 cells were transfected with pGL3-EPO-HRE construct, then treated with tunicamycin (10 μ g/ml), brefeldin A (10 μ g/ml) or thapsigargin (2 μ M) under normoxia or hypoxia for about 24 h. It was found that the treatment with these compounds decreased LUC activity under both normoxia and hypoxia. Interestingly, tunicamycin and brefeldin A presented the hypoxia deficient increase of LUC activity while cells still responded to hypoxia in the presence of thapsigargin (Fig. 29). In pGL3-EPO-HRE-mutant transfected cells, LUC activity could not be enhanced by hypoxia. However, all compounds inhibited the LUC activities under both normoxia and hypoxia, which might be due to a more general effect on gene expression (Fig. 29).

4.4.2 Modulation of HIF-1 α protein levels by endoplasmic reticulum stress

To explain the results of the reporter gene analyses, the influence of ER stress on HIF-1 α protein expression was further studied. It is known that the induction of HIF-1 α protein by

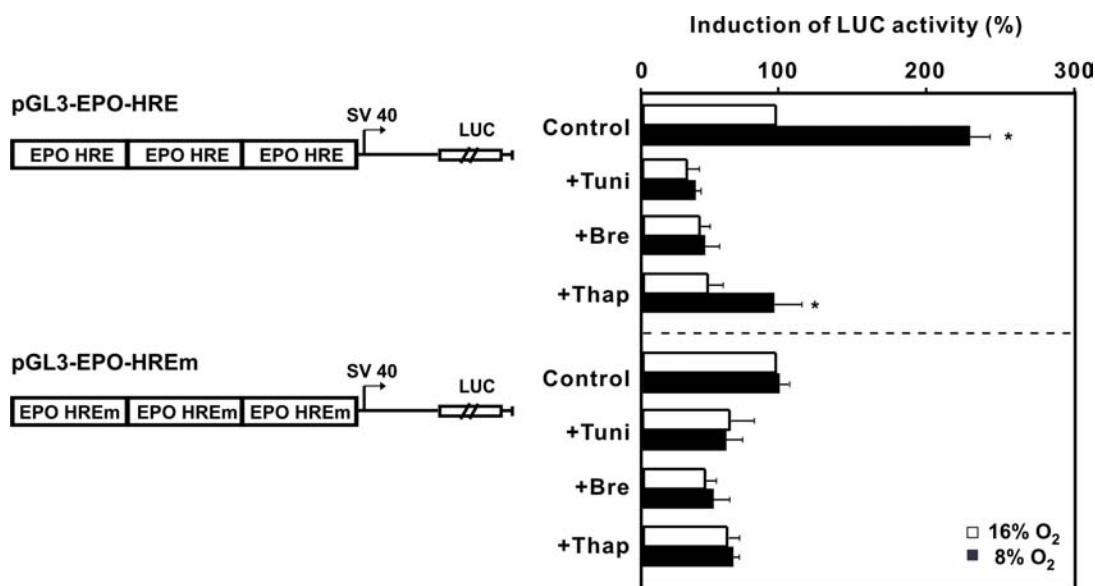


Figure 29. The modulation of EPO-HRE activity by ER stress. HepG2 cells were transfected with the luciferase construct containing three copies of the erythropoietin hypoxia response element (EPO-HRE) or mutated HRE (EPO-HREm) in front of the SV40 promoter and the luc gene. The transfected cells were treated with tunicamycin (10 μ g/ml), brefeldin A (10 μ g/ml) or thapsigargin (2 μ M) and further cultured 24 h under normoxia (16% O₂) or hypoxia (8% O₂). In each experiment the LUC activity of pGL3-EPO-HRE or pGL3-EPO-HREm transfected cells at 16% O₂ was set to 100%, respectively. * $P \leq 0.05$, 16% O₂ vs. 8% O₂ within the same group, n=3.

hypoxia is very fast, and usually occurs within 1 h. However, the induction of ER stress as an accumulative process is relatively slow. Therefore, in these experiments, HepG2 cells were pre-treated with tunicamycin (10 μ g/ml), brefeldin A (10 μ g/ml) and thapsigargin (2 μ M) under normoxia for 24 h, then incubated under either normoxia or hypoxia for 4 h. HIF-1 α protein was detected by Western blot analysis. HIF-1 α protein expression was induced about 5-fold by hypoxia (Fig. 30). Consistent with the results of the reporter gene analysis, the pre-treatment with tunicamycin and brefeldin A but not with thapsigargin inhibited the hypoxia-dependent induction of HIF-1 α . Interestingly, a high level of HIF-1 α protein could be detected after pre-treatment of cells with thapsigargin under normoxia (Fig. 30).

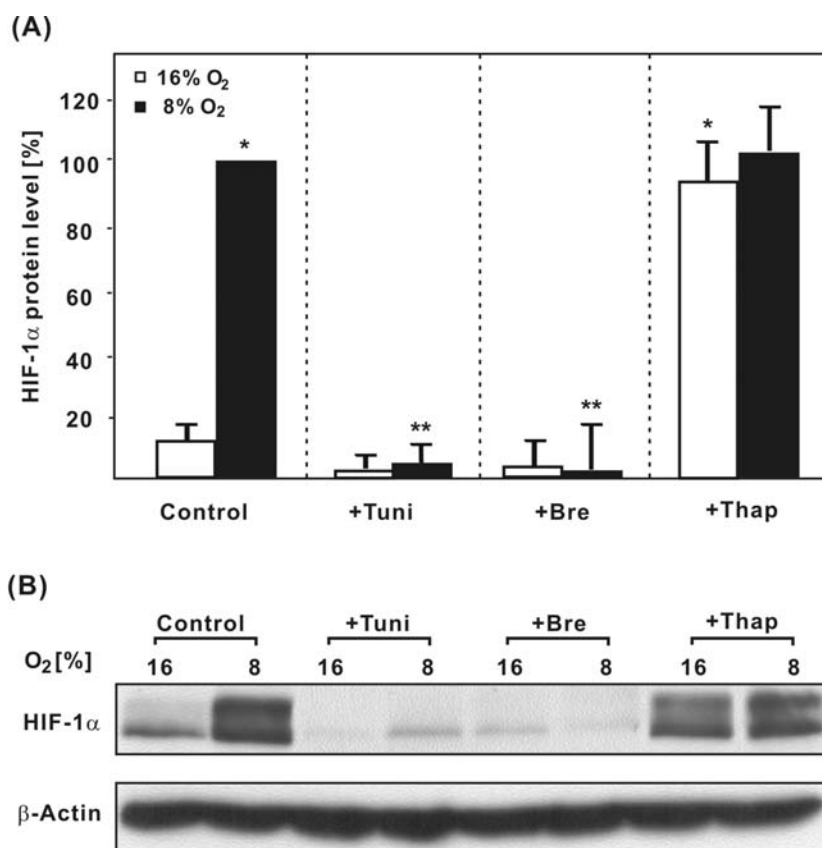


Figure 30. Modulation of HIF-1 α protein expression by ER stress. HepG2 cells were pre-treated with tunicamycin (10 μ g/ml), brefeldin A (10 μ g/ml) and thapsigargin (2 μ M) under normoxia (16% O₂) for 24 h, then incubated under either normoxia or hypoxia (8% O₂) for 4 h. HIF-1 α protein was detected by Western blot analysis. **(A)** The statistical summary of HIF-1 α protein levels. The expression of HIF-1 α under hypoxia was set to 100%. * $P \leq 0.05$ 16% O₂ vs. 8% O₂, 16% O₂ vs. 16% O₂ +Thap, ** $P \leq 0.05$ 8% O₂ vs. 8% O₂ +Tuni, 8% O₂ vs. 8% O₂ +Bre, $n=3$. **(B)** Representative Western blot. 100 μ g of protein from the whole-cell extract were subjected to Western analysis with an antibody against HIF-1 α or β -actin (as an internal control). Autoradiographic signals were obtained by chemiluminescence and scanned by videodensitometry.

As mentioned above, thapsigargin causes ER stress by inhibiting the Ca^{2+} -ATPase on the ER membrane and thus changes also the cytoplasmic Ca^{2+} concentration. This does not only indicate that the ER stress but also cytosolic Ca^{2+} interferes with HIF-1 α protein expression. Therefore, it was further investigated whether Ca^{2+} was involved in the cellular response to hypoxia.

4.5 The role of calcium in HIF-1-dependent responses

4.5.1 Modulation of HIF-1 α protein levels by intracellular calcium

To investigate the role of calcium in oxygen signaling, other agents, which can change the concentration of intracellular calcium, were used besides thapsigargin. These included A23187 (calcium-specific ionophore), BAPTA (cell impermeable extracellular calcium chelator) and BAPTA-AM (cell permeable intracellular calcium chelator). In these experiments, cultured HepG2 cells were treated with the different agents under normoxia or hypoxia for 4 h respectively. HIF-1 α protein expression was checked by Western blot analysis. As it has been described above, the treatment with thapsigargin (2 μM) as well as A23187 (5 μM), which were proposed to increase the cytoplasmic calcium concentration, significantly induced HIF-1 α protein expression under both normoxia and hypoxia (Fig. 31). However, it was surprising that BAPTA-AM (5 μM), the intracellular Ca^{2+} chelator also induced HIF-1 α protein expression under normoxia and hypoxia. As a control, the extracellular calcium chelator, BAPTA, did not influence HIF-1 α protein expression (Fig. 31).

Next, the time-dependent stimulation of HIF-1 α protein expression by A23187 and BAPTA-AM was further investigated. While the HIF-1 α protein remained at a very low level under normoxia; it was already induced by hypoxia within 2 h and reached the maximum after 4 h and decreased at 24 h. Both A23187 and BAPTA-AM increased HIF-1 α already maximally after 4 h under normoxia. HIF-1 α remained at a high level up to 24 h in the presence of A23187 while it dramatically decreased after 4 h in the presence of BAPTA-AM (Fig. 32). This suggests that these two different compounds, which could either increase or decrease the intracellular calcium concentration, might regulate HIF-1 α expression in a different manner.

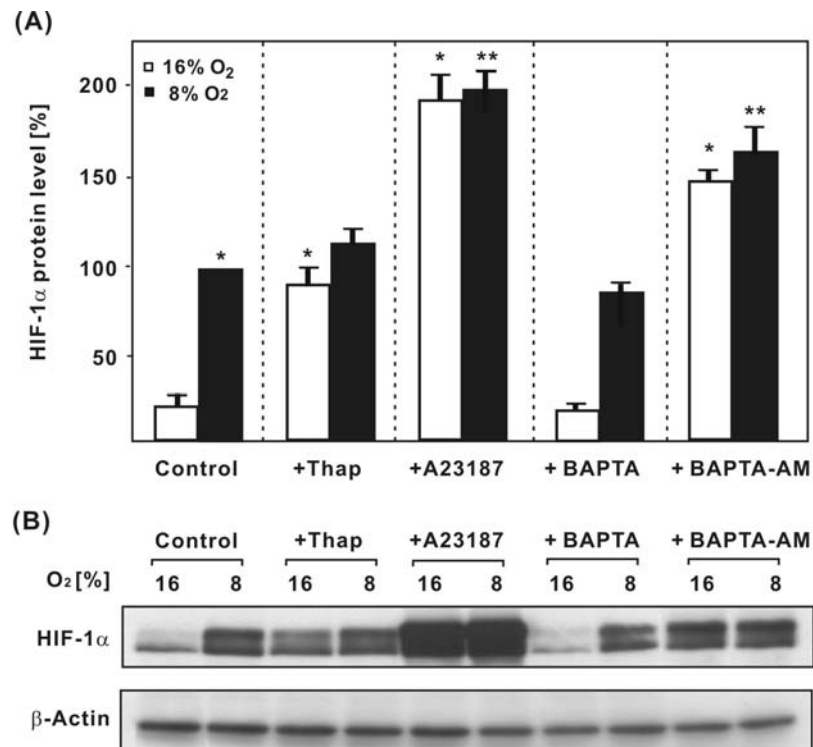


Figure 31. Modulation of HIF-1 α protein expression by intracellular calcium. HepG2 cells were treated with thapsigargin (2 μ M), A23187 (5 μ M), BAPTA-AM (5 μ M) or BAPTA (5 μ M) under normoxia (16% O₂) or hypoxia (8% O₂) for 4 h. HIF-1 α protein was detected by Western-blot analysis. **(A)** The statistical summary of HIF-1 α protein levels. The expression of HIF-1 α under hypoxia was set to 100%. * $P \leq 0.05$ as compared with 16% O₂ Control, ** $P \leq 0.05$ as compared with 8% O₂ Control, $n=3$. **(B)** Representative Western blot. 100 μ g of protein from the whole-cell extract were subjected to Western analysis with an antibody against HIF-1 α or β -actin (as an internal control). Autoradiographic signals were obtained by chemiluminescence and scanned by videodensitometry.

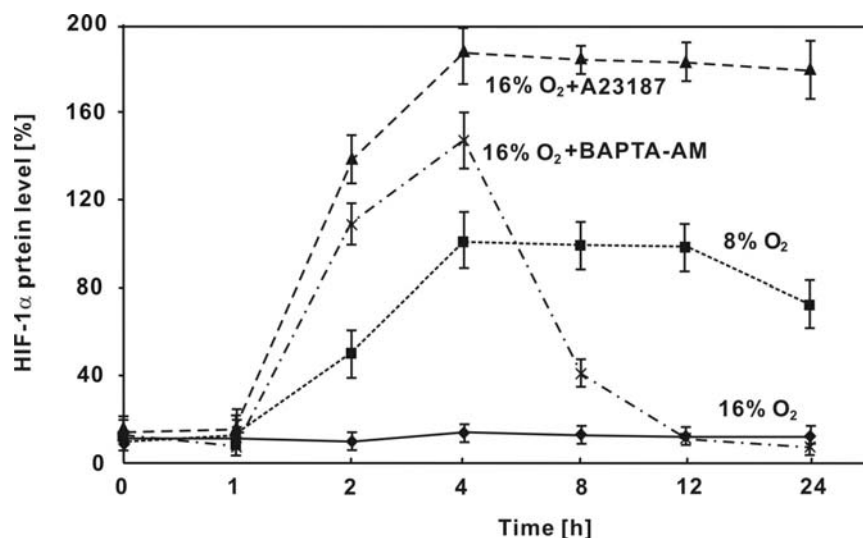


Figure 32. Time-course of the HIF-1 α protein expression after treatment with A23187 or BAPTA-AM. HepG2 cells were incubated under normoxia or hypoxia (8% O₂) or treated with A23187 (5 μ M) or BAPTA-AM (5 μ M) under normoxia (16% O₂) and then harvested at different time points. HIF-1 α protein was detected by Western-blot analysis. The statistical summary of HIF-1 α protein levels is shown. The expression of HIF-1 α under hypoxia at 4h was set to 100%, $n=3$.

4.5.2 The calcium ionophore induces HIF-1 α expression at the transcriptional level

HIF-1 α expression can be regulated at both transcriptional and post-translational levels by hypoxia. To further study the mechanism of HIF-1 α induction by A23187, actinomycin D (Act D) and cycloheximide (CHX) were administered to HepG2 cells for 30 min to block gene expression at the transcriptional level and the translational level, respectively. Then, the cells were treated with A23187 (5 μ M) under normoxia or hypoxia for 4 h. Both Act D and CHX significantly inhibited HIF-1 α protein expression induced by A23187 (Fig. 33). This indicated that the induction of HIF-1 α protein expression by A23187 needed *de novo* synthesis of both mRNA and protein in the cells.

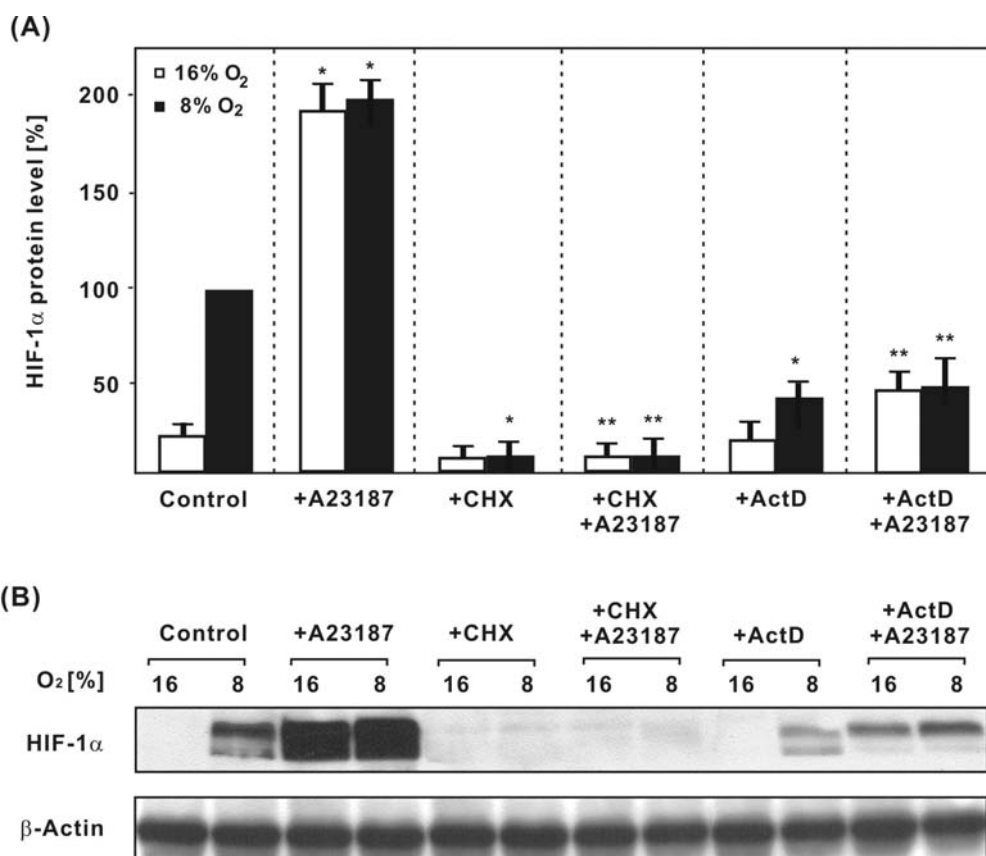


Figure 33. Inhibition of A23187 induced HIF-1 α protein expression by actinomycin D and cycloheximide. HepG2 cells were pre-treated for 30 min with actinomycin D (Act D, 5 μ g/ml) and cycloheximide (CHX, 10 μ g/ml) and then stimulated with A23187 (5 μ M) under normoxia (16% O₂) or hypoxia (8% O₂) for 4 h. HIF-1 α protein was detected by Western blot analysis. **(A)** The statistical summary of HIF-1 α protein levels. The expression of HIF-1 α under hypoxia was set to 100%. * $P \leq 0.05$ as compared to the control under the same pO₂; ** $P \leq 0.05$ as compared to the A23187 treatment group under the same pO₂; n=3. **(B)** Representative Western blot. 100 μ g of protein from the whole-cell extract were subjected to Western analysis with an antibody against HIF-1 α or β -actin (as an internal control). Autoradiographic signals were obtained by chemiluminescence and scanned by videodensitometry.

To further investigate whether A23187 has direct transcriptional effects, HIF-1 α mRNA expression was detected by Northern blot analysis. As expected, under hypoxia HIF-1 α mRNA abundance was upregulated by about 2-fold (Fig. 34). Treatment with A23187 under normoxia induced HIF-1 α mRNA expression even stronger than hypoxia. In addition, a synergistic effect of A23187 and hypoxia was also observed (Fig. 34). These results suggested that the calcium ionophore A23187 induces HIF-1 α expression mainly at the transcriptional level.

4.5.3 The intracellular calcium chelator leads to HIF-1 α protein stabilization

Similar to A23187, the mechanism of HIF-1 α induction by the intracellular calcium chelator BAPTA-AM was also studied. Again, it was found that the pretreatment with CHX inhibited both hypoxia and BAPTA-AM induced HIF-1 α expression (Fig. 35). By contrast to the A23187 treatment, BAPTA-AM could still induce HIF-1 α protein expression in the presence of Act D (Fig. 35). It suggested that BAPTA-AM induces HIF-1 α at the post-transcriptional level. This was further verified by checking HIF-1 α mRNA levels with Northern blot analysis. It was found that the HIF-1 α mRNA abundance did not show significant differences with or without BAPTA-AM treatment under both normoxia and hypoxia (Fig. 36).

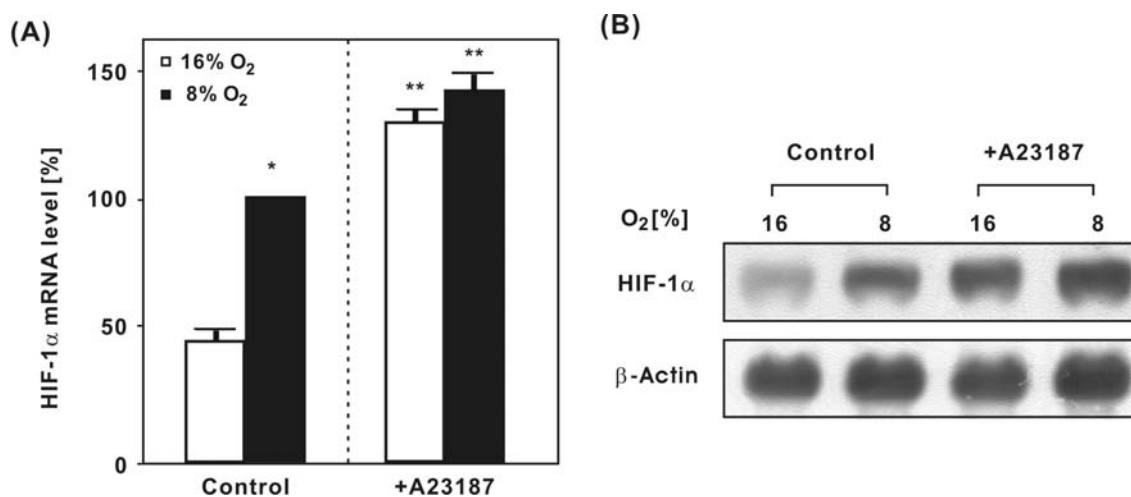


Figure 34. Modulation of HIF-1 α mRNA expression by the calcium ionophore A23187. HepG2 cells were stimulated with A23187 (5 μ M) under normoxia (16% O₂) or hypoxia (8% O₂) for 4 h. HIF-1 α mRNA was detected by Northern blot analysis. **(A)** The statistical summary of HIF-1 α mRNA levels. The expression of HIF-1 α under hypoxia was set to 100%. * $P \leq 0.05$, 16% O₂ vs. 8% O₂; ** $P \leq 0.05$, +A23187 vs. control under the same pO₂ condition; n=3. **(B)** Representative Northern blot. 20 μ g total RNA of each sample was subjected to Northern blot analysis with HIF-1 α or β -actin (as an internal control) antisense RNA probes. Autoradiographic signals were obtained by chemiluminescence and scanned by videodensitometry.

The results from the experiments with Act D and BAPTA-AM led to the hypothesis that the intracellular calcium chelator BAPTA-AM might accumulate HIF-1 α through protein stabilization. Thereby, proline 564 in the N-TAD plays a crucial role while it is hydroxylated by PHDs and thus mediates the interaction of HIF1 α and VHL. In the following experiments, the proline hydroxylation and the subsequent binding of VHL were investigated by *in vitro* prolyl hydroxylase activity assay and GST pull-down assay, respectively. The results showed that the treatment of cells with BAPTA-AM (5 μ M) and additional BAPTA in the reaction clearly reduced the hydroxylase activity and inhibited the interaction between VHL and GST-TADN (Fig. 37). As a positive control, the addition of Co²⁺ which substitutes for the Fe²⁺ necessary for PHD activity in the reaction system also led to the reduction of hydroxylase activity and VHL binding (Fig. 37).

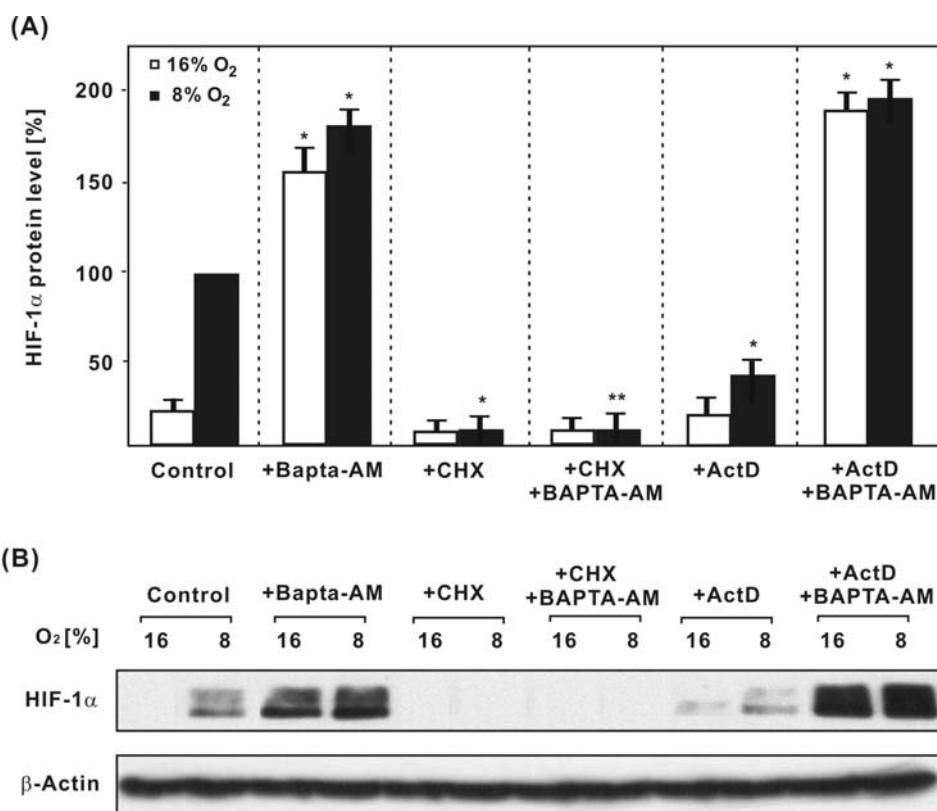


Figure 35. Modulation of BAPTA-AM induced HIF-1 α protein expression by actinomycin D and cycloheximide. HepG2 cells were pre-treated for 30 min with actinomycin D (Act D, 5 μ g/ml) and cycloheximide (CHX, 10 μ g/ml) and then stimulated with BAPTA-AM (5 μ M) under normoxia (16% O₂) or hypoxia (8% O₂) for 4 h. HIF-1 α protein was detected by Western blot analysis. **(A)** The statistical summary of HIF-1 α protein levels. The expression of HIF-1 α under hypoxia was set to 100%. * $P \leq 0.05$ as compared to the control under the same pO₂; ** $P \leq 0.05$ as compared with BAPTA-AM treatment group under the same pO₂; n=3. **(B)** Representative Western blot. 100 μ g of protein from the whole-cell extract were subjected to Western analysis with an antibody against HIF-1 α or β -actin (as an internal control). Autoradiographic signals were obtained by chemiluminescence and scanned by videodensitometry.

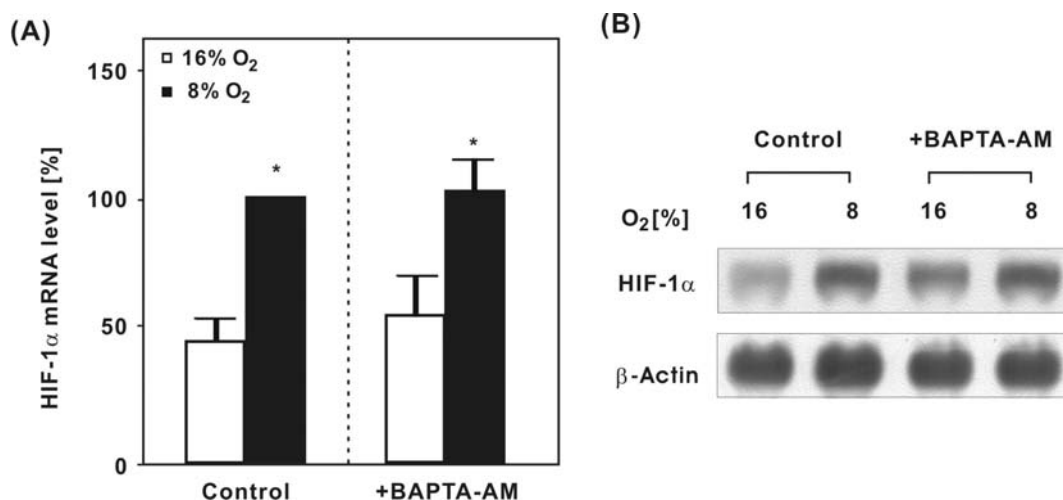


Figure 36. Modulation of HIF-1 α mRNA expression by the intracellular calcium chelator BAPTA-AM. HepG2 cells were stimulated with BAPTA-AM (5 μ M) under normoxia (16% O₂) or hypoxia (8% O₂) for 4 h. HIF-1 α mRNA was detected by Northern blot analysis. **(A)** The statistical summary of HIF-1 α mRNA levels. The expression of HIF-1 α under hypoxia was set to 100%. * P \leq 0.05, 16% O₂ vs. 8% O₂; n =3. **(B)** Representative Northern blot. 20 μ g total RNA of each sample was subjected to Northern blot analysis with HIF-1 α or β -actin (as an internal control) antisense RNA probes. Autoradiographic signals were obtained by chemiluminescence and scanned by videodensitometry.

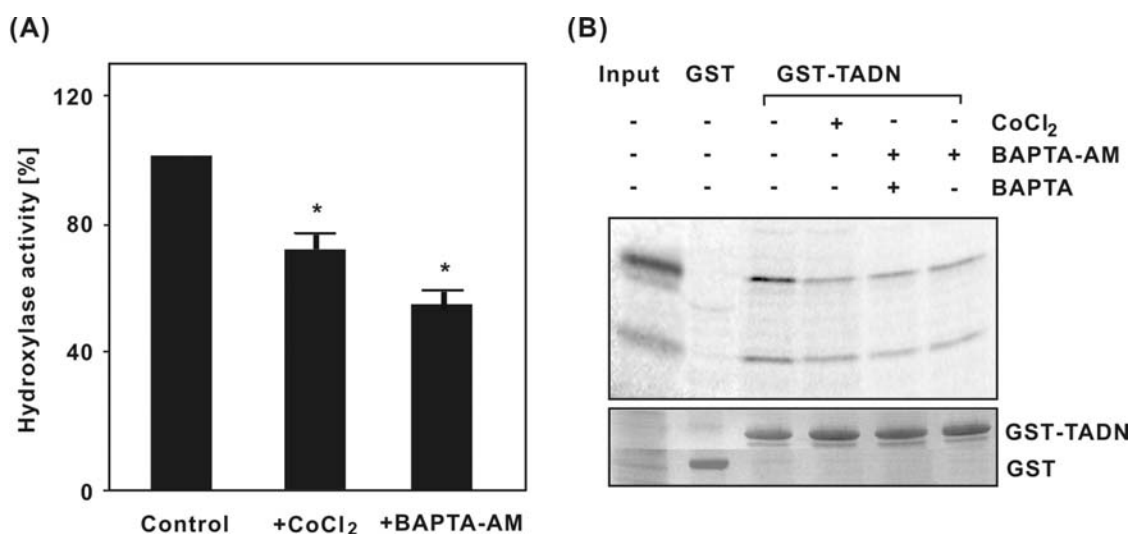


Figure 37. Inhibition of HIF prolyl hydroxylase activity by the calcium chelator BAPTA-AM. **(A)** Prolyl hydroxylase activity assay. The GST-HIF1 α -TADN fusion protein or the GST protein were incubated with HepG2 cell extract, cofactors and [5-¹⁴C]2-oxoglutarate in the presence of CoCl₂ or BAPTA-AM (5 μ M). The radioactivity associated to ¹⁴C-succinate was determined. In each experiment the basal HIF-TADN-dependent activity (control) was set to 100% after normalization to GST-associated activity. * P \leq 0.05 compared with control, n =3; **(B)** VHL pull-down assay. HepG2 cells were treated with or without BAPTA-AM (5 μ M). Cell extracts were prepared and incubated with the GST-HIF1 α -TADN fusion protein the presence of CoCl₂ or BAPTA (5 μ M) supplemented with cofactors. Glutathione-Sepharose beads and [³⁵S]VHL were then added and the bound VHL was recovered, subjected to SDS-PAGE, and visualized by phosphorimaging. The input remains from directly loaded [³⁵S]VHL. The two bands represent the 213 and 160 amino acid VHL translation products. Representative data of three individual experiments.

4.5.4 The calcium chelator but not the calcium ionophore induces HIF-1 α TADN transactivity

The finding that HIF-1 α can be stabilized by the intracellular calcium chelator (BAPTA-AM) but not by the calcium ionophore (A23187) was further supported by functional assays. For this, HepG2 cells were cotransfected with pG5-E1B-LUC and pcDNA6-Gal4-HIF-1 α TADN constructs. As shown before, the HIF-1 α TADN transactivity could be induced by hypoxia. The mutation of the critical amino acid (Pro 564) in TADN, which led to hydroxylation resistance of the protein, caused an increase in its transactivity under normoxia and a loss of the response to hypoxia. The treatment with BAPTA-AM could also increase HIF-1 α TADN activity by about 2-fold under normoxia, while A23187 had no effect (Fig. 38). No induction was observed in pcDNA6-Gal4-HIF-1 α TADNm transfected cells since the Pro 564 mutation inhibited the binding of VHL and subsequent degradation of the fusion protein (Fig. 38). Furthermore, asparagine 803 in HIF-1 α TADC can also be hydroxylated by another hydroxylase named FIH and thus block the interaction of HIF-1 α with p300/CBP. To investigate whether BAPTA-AM could also interfere with FIH activity and thereby promote HIF-1 α TADC transactivity a similar luciferase reporter gene analysis was performed with pG5-E1B-LUC and pcDNA6-Gal4-HIF-1 α TADC constructs. It was found that hypoxia could induce TADC transactivity by about 1.8-fold and this induction was abolished by the mutation of asparagine to alanine (Fig. 38). However, neither BAPTA-AM nor A23187 had any effect on TADC transactivity (Fig 38).

4.5.5 Both the calcium ionophore and the intracellular calcium chelator induce HIF-1-dependent gene expression

After the demonstration that both the calcium ionophore (A23187) and the intracellular calcium chelator (BAPTA-AM) can enhance the amount of HIF-1 α in HepG2 cells, it was investigated whether they could induce HIF-1-dependent genes. In these experiments, PAI-1 was selected as a read-out gene and the influence of A23187 and BAPTA-AM on its expression was checked on both PAI-1 mRNA and protein levels. In line with previous studies, the expression of PAI-1 was significantly enhanced under hypoxia at the mRNA and protein level. The treatment of cells with either BAPTA-AM or A23187 could also clearly induce PAI-1 mRNA and protein expression (Fig. 39)

The induction of HIF-1-dependent gene expression by BAPTA-AM and A23187 was further demonstrated by reporter gene analysis with pGL3-EPO-HRE constructs. Hypoxia induced LUC activity about 2-fold. Treatment with BAPTA-AM could increase the LUC activity even up to 4.5-fold under normoxia and hypoxia. In contrast, the extracellular calcium chelator BAPTA had no effect on LUC activity under both normoxia and hypoxia. Interestingly, although a significant induction of LUC activity under normoxia was also detected after treatment with A23187 (0.1 μ M), this induction was not as strong as that under hypoxia. Mutation of the HRE in pGL3-EPO-HREm abolished all inductions by hypoxia, BAPTA-AM and A23187 (Fig. 40).

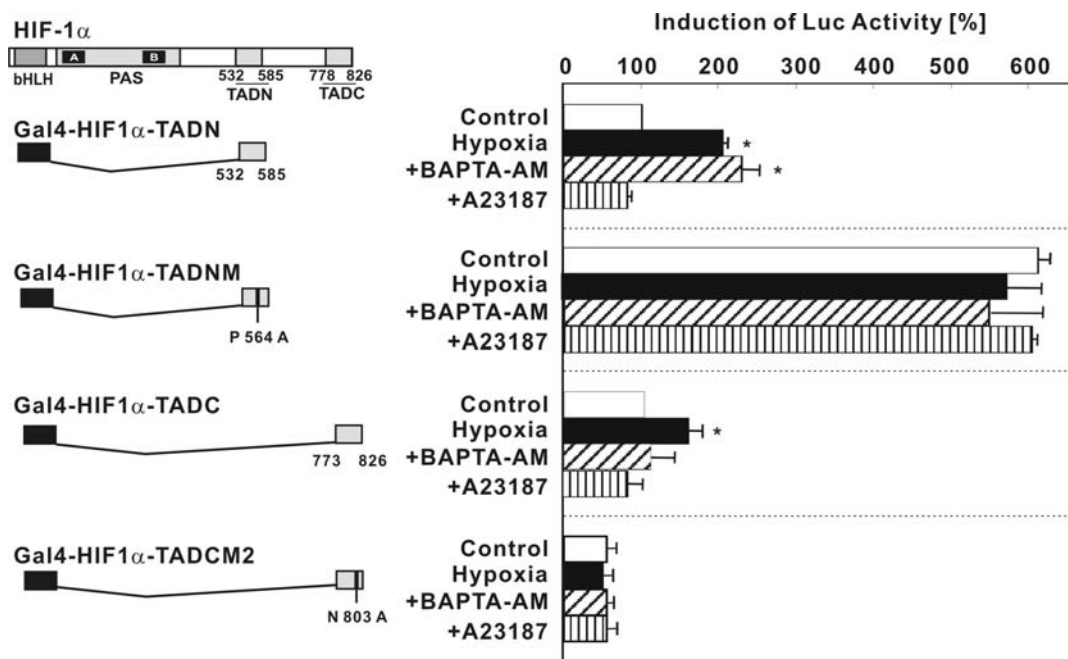


Figure 38. Induction of HIF-1 α TADN transactivation by BAPTA-AM. HepG2 cells were cotransfected with a luciferase reporter construct pG5-E1B-LUC and different fusion gene constructs in which the Gal4 DNA binding domain was fused to either the TADN (532-585) or TADC (773-826) of HIF-1 α as shown on the left. The mutations in the constructs are indicated. After 24 h the transfected cells were treated with either 5 μ M BAPTA-AM or 0.1 μ M A23187 under normoxia (16% O₂) or hypoxia (8% O₂) for 24 h. The statistical summary of LUC activity was shown on the right. * $P \leq 0.05$ compared to the control in the same group, n=4.

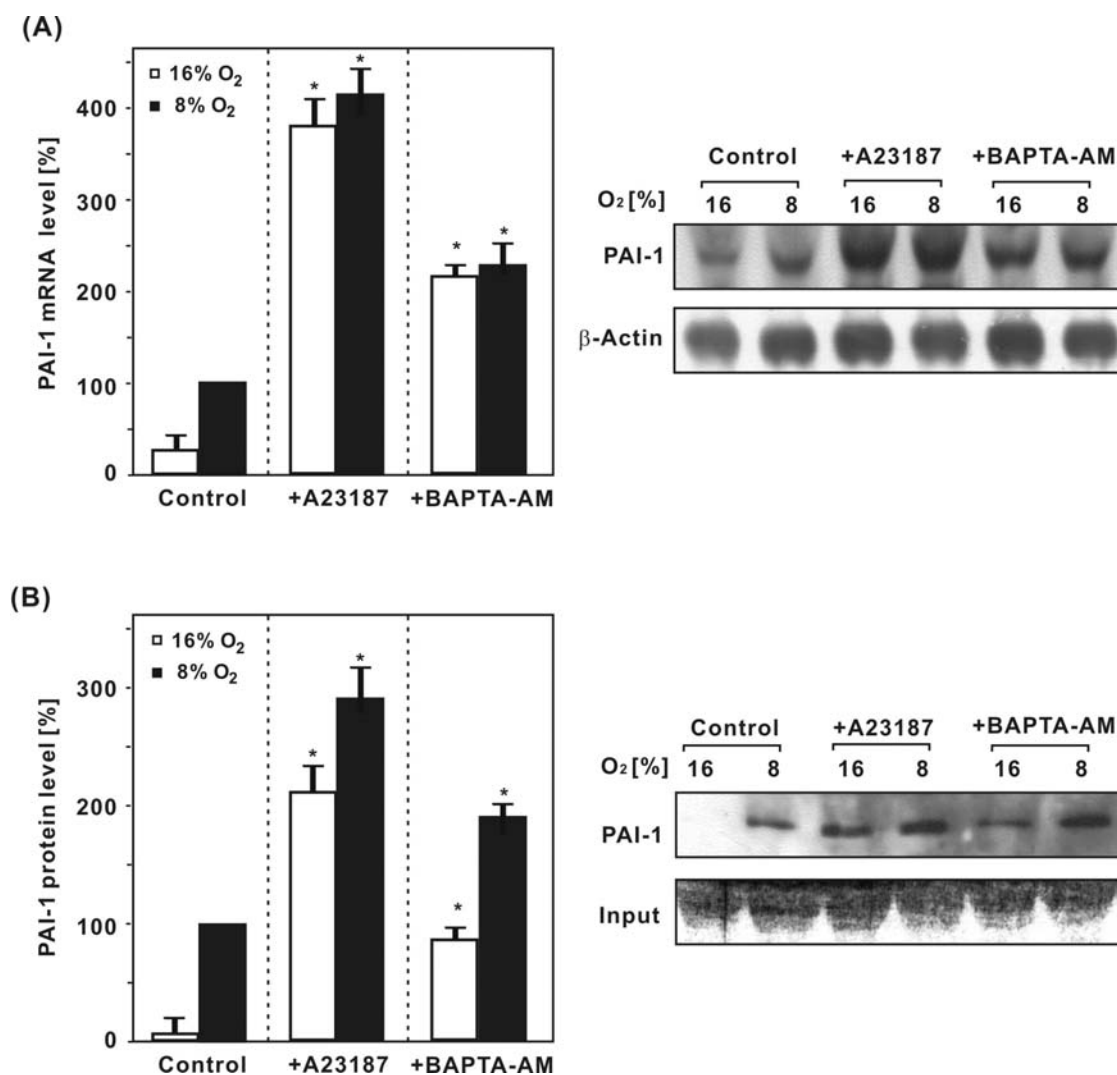


Figure 39. Induction of PAI-1 gene expression by the calcium ionophore A23187 and the calcium chelator BAPTA-AM. Cultured HepG2 cells were treated with 5 μ M A23187 or 5 μ M BAPTA-AM and further cultured under normoxia (16% O₂) or hypoxia (8% O₂). **(A)** Northern blot analysis. The cells were harvested 4 h after treatment. Total RNA was isolated and the expression of PAI-1 was detected by Northern blot analysis. PAI-1 mRNA levels under hypoxia were set to 100%. * $P \leq 0.05$ as compared to the control under the same pO₂. **(B)** Western blot analysis. The PAI-1 protein was analyzed as a soluble protein from the medium 24 h after treatment. PAI-1 protein expression was detected by Western blot analysis. The PAI-1 protein level under hypoxia was set to 100%. * $P \leq 0.05$ as compared to the control under the same pO₂. Representative Northern or Western blots are shown on the right with loading control. Autoradiographic signals were obtained by chemiluminescence and scanned by videodensitometry.

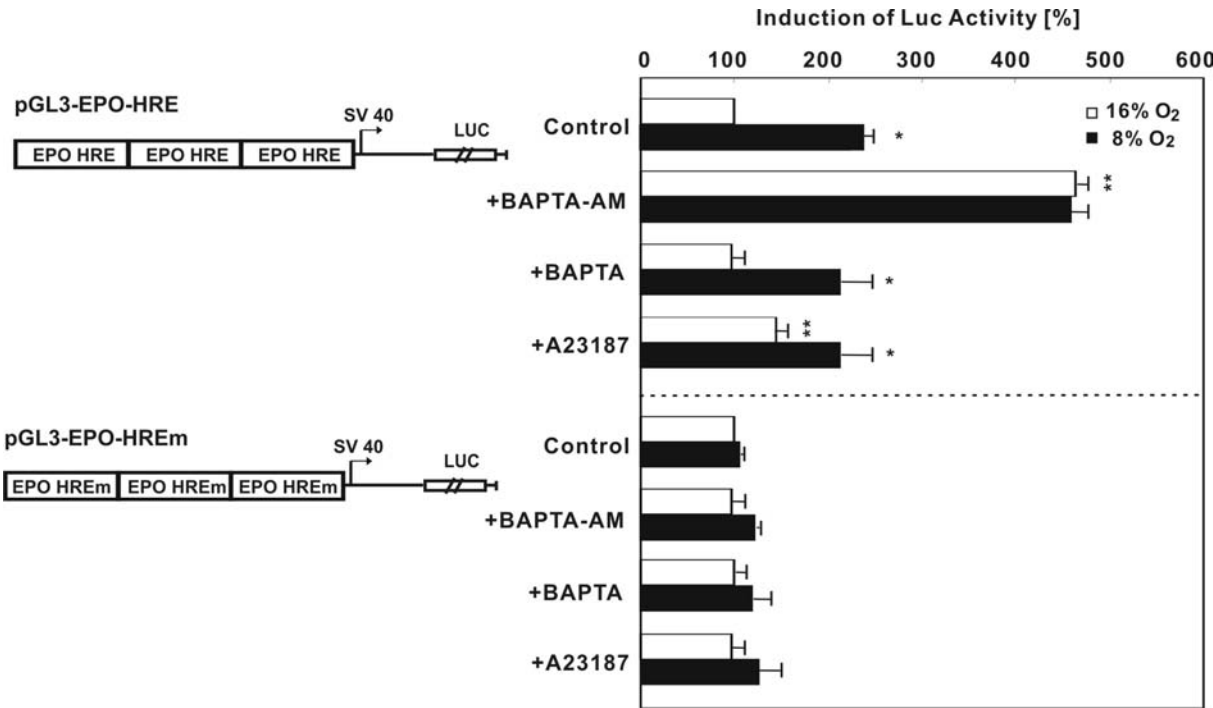


Figure 40. The modulation of EPO-HRE LUC activity by intracellular calcium. HepG2 cells were transfected with the luciferase construct containing three copies of the wild type erythropoietin hypoxia response element (EPO-HRE) or mutated EPO-HREm in front of the SV40 promoter and the luc gene. The transfected cells were treated with BAPTA-AM (5 μ M), BAPTA (5 μ M) or A23187 (0.1 μ M) and further cultured for 24 h under normoxia (16% O₂) or hypoxia (8% O₂). In each experiment the LUC activity of pGL3-EPO-HRE or pGL3-EPO-HREm transfected cells at 16% O₂ was set to 100%, respectively. * $P \leq 0.05$, 16% O₂ vs. 8% O₂, ** $P \leq 0.05$, Control 16% O₂ vs. BAPTA-AM or A23187, n=3.

5. Discussion

In the present study the H_2O_2 degrading Fenton reaction ($\text{H}_2\text{O}_2 + \text{Fe}^{2+} \rightarrow \text{OH}^- + \text{OH}\bullet + \text{Fe}^{3+}$) which could transfer the O_2 signal was localized to the endoplasmic reticulum (ER) by using the $\text{OH}\bullet$ scavenger DHR and gene constructs which express fluorescent proteins specifically in subcellular compartments. It was also demonstrated that the $\text{OH}\bullet$ generation at the ER was O_2 -dependent and scavenging of $\text{OH}\bullet$ by DHR mimicked hypoxia leading to the activation of HIF-1 and HIF-1-dependent PAI-1 and HO-1 gene expression. Furthermore, it was shown that calcium ions which can be released from the ER may affect the HIF-1 α protein levels via transcriptional or post-translational regulation, thus regulating HIF-1-dependent PAI-1 gene expression.

5.1 Reactive oxygen species (ROS) as messengers in O_2 -signaling

Several studies have shown the participation of ROS in O_2 sensing and signaling transduction (Kietzmann et al., 1998; Chandel et al. 1998, 2000), but the knowledge about the precise source, species, and mode of interaction of ROS with the transcriptional system are limited. As mentioned before, H_2O_2 , as a noncharged molecule, has been regarded as an ideal candidate for an intracellular second messenger from the O_2 sensor. In the presence of Fe^{2+} , H_2O_2 can be nonenzymatically converted into hydroxyl anions (OH^-) and highly reactive hydroxyl radicals ($\text{OH}\bullet$). Previous research has shown that the $\text{OH}\bullet$ generating Fenton reaction took place in a perinuclear space where granules with high iron concentrations could also be found (Kietzmann et al. 1998).

5.1.1 Localization of intracellular ROS generation

Any electron-transferring protein or enzymatic system can result in the formation of ROS as “by-products” of electron transfer reactions. The mitochondrion, as the principal oxygen-consuming organelle of the cell, at least under some circumstances, is a major producer of oxygen radical species. It has been assumed that this “unintended” generation of ROS in mitochondria accounts for ~1-2% of total O_2 consumption under reducing conditions (Freeman and Crapo, 1982). Moreover, peroxisomes are an important source of total cellular H_2O_2 production. They contain a number of H_2O_2 -generating enzymes including glycolate oxidase, D-amino acid oxidase, urate oxidase, L- α -hydroxyacid oxidase and fatty acyl-CoA oxidase. Peroxisomal catalase utilizes H_2O_2 produced by these oxidases to oxidize a variety of other substrates in peroxidative reactions. However, due to high concentrations of

mitochondrial SOD, the mitochondria-generated $O_2^{\cdot-}$ is maintained at very low steady state levels and unlikely to escape into the cytoplasm. Similarly, only a small fraction of H_2O_2 generated in peroxisomes appears to escape peroxisomal catalase (Thannickal and Fanburg, 2000). These findings are against the role of these intracellular organelles in the O_2 -signaling pathways but in line with the present study where the ER but not mitochondria or other intracellular organelles was found to be associated with $OH\cdot$ generation. This appears to be specific since the non-fluorescent agent DHR used in the experiments reacts very poorly with H_2O_2 , only in the presence of Fe^{2+} occurs a fast conversion of DHR into fluorescent RH, indicating the generation of $OH\cdot$ in the Fenton reaction (Royall and Ischiropoulos, 1993). However, the RH fluorescence does not indicate the primary site of H_2O_2 production but only the conversion of H_2O_2 . Despite the ER located cytochrome *P*-450 and *b*₅ families of enzymes can oxidize unsaturated fatty acids and xenobiotics and reduce molecular O_2 to produce $O_2^{\cdot-}$ and/or H_2O_2 (Thannickal and Fanburg, 2000), the H_2O_2 utilized by the Fenton reaction might also come from other organelles, as it is capable of diffusing across biomembranes. The cellular H_2O_2 levels are usually controlled by glutathione peroxidase in the cytosol following the reaction: $H_2O_2 + 2GSH \rightarrow GSSG + 2H_2O$. Since glutathione peroxidase (K_M 100 μ M) (Chance, 1979) requires a relatively high H_2O_2 concentration it appears conceivable that H_2O_2 with lower concentrations may be non-enzymatically converted in an ER localized Fenton reaction. The resulting highly reactive $OH\cdot$ can then directly or indirectly modify the activity of transcription factors such as HIF-1 α .

5.1.2 Production of reactive oxygen species under normoxia and hypoxia

In the present study, we showed that $OH\cdot$ generation is decreased under hypoxia. However, these findings appear to be conflicting in terms of the hypothesized increases or decreases in ROS production during hypoxia. It was proposed that hypoxia increases ROS which stabilize HIF-1 α , and application of H_2O_2 to cells may activate HIF-1 and HIF-1 target genes (Chandel et al. 1998; 2000). However, we and others have found the opposite, namely that H_2O_2 destabilized HIF-1 α even under hypoxia and prevented the induction of HIF-1 target genes by hypoxia (Fandrey et al., 1994; Huang et al., 1996; Kietzmann et al., 1998). Direct measurement of H_2O_2 production also revealed a decrease rather than an increase under hypoxia in a variety of cell types (Vaux et al., 2001). These findings have led to the proposal that higher concentrations of ROS such as H_2O_2 , superoxide anion radicals ($O_2^{\cdot-}$) and hydroxyl radicals ($OH\cdot$) are produced under normoxia and might trigger HIF-1 α degradation. This ROS dilemma called for an analytical method to determine the kinetics and dependence

of O_2 -dependent ROS production in cells. Unfortunately, the high reactivity and relative instability of ROS make them extremely difficult to be detected or measured in biological systems. Most methods for identification of specific ROS are based on reactions with various detector molecules that are oxidatively modified to elicit luminescent or fluorescent signals. In this study, DHR which could specifically detect the formation of $OH\bullet$ was utilized to image and localize the hot spots of the Fenton reaction and their response to hypoxia. Its resulting RH fluorescence possesses a different excitation and emission maximum with the intracellular compartment labeled fluorescent protein. This property allowed us to optimize the fluorescence excitation and avoid crosstalk between the two different fluorescences by using the tunable wave-length in 2P-CLSM. In addition, 2P-CLSM excited the fluorescence with infrared light (Hockberger et al. 1999), therefore this non-phototoxic irradiation of the cells avoided unspecific ROS generation. Moreover, several other specific conditions were also carefully set up in this study to avoid artificial results. These included 1) The cells were kept under physiological conditions during the experiments in the microscope culture chamber to minimize the cell stress; 2) The treatment with DHR (30 μ M) for 5 min achieved an optimal dye deposit which allowed the full conversion of DHR to fluorescent RH and minimized secondary RH distribution via diffusion and channel transport; 3) The measurements were started under hypoxic conditions where low levels of ROS were expected since DHR to RH conversion is irreversible. With all of these, it was found that the RH fluorescence at the ER could only be detected when the cells were reoxygenated for about 15 min but not under hypoxia, indicating the Fenton reaction generated $OH\bullet$ was pO_2 -dependent. This indication was further proved by performing the blue light challenge to the cells, which increased RH fluorescence under normoxia as compared with the nearly missing illumination reaction under hypoxia. Therefore, the data of the present study provide another evidence that ROS are generated under normoxia and that decreased ROS would contribute to the hypoxic responses.

5.1.3 Regulation of HIF-1 α by ROS

As mentioned before, HIF-1 plays a crucial role in mediating cellular responses to hypoxia by inducing expression of a large number of hypoxia responsible genes. The HIF-1 α subunit is rapidly degraded under normoxia by a ubiquitin-proteasome pathway, involving the von Hippel-Lindau tumour suppressor protein (pVHL). The pVHL functions as the substrate recognition component of a multi-component ubiquitin E3 ligase in the O_2 -dependent destruction of HIF-1 α (Huang et al., 1998; Kallio et al., 1999; Maxwell et al., 1999; Ohh et al.,

2000). Interestingly, subcellular localization of pVHL by immunofluorescence revealed a cytoplasmic peri-nuclear immunostaining pattern, which colocalized with the markers for the ER (Schoenfeld et al., 2001). Further investigations demonstrated that a 64-amino acid region of pVHL (residues 114 – 177) was responsible for its proper ER subcellular localization and for pVHL-associated ubiquitination functions. Within this study, in addition to the localization of OH• generation by the Fenton reaction at the ER, it was also found that HIF-1 α was associated with the ER under normoxia. The assembling of these critical molecules in the same cellular compartment indicated possibilities for the regulation of HIF-1 α by the local redox state in cells. It was assumed that the generation of OH• in the ER facilitated the modification of HIF-1 α , which was recognized by pVHL. This is further supported by a number of recent reports showing that pretreatment with H₂O₂ inhibited the ability of hypoxia to stabilize HIF-1 α , thereby abrogating hypoxia-induced gene expression in a variety of cell types (Fandrey et al., 1994; Huang et al., 1996; Kietzmann et al., 1998). In the present study, the sensitivity of HIF-1 α activity against the redox state of the cell was demonstrated by using DHR as a specific OH• scavenger. The treatment of the cells with DHR induced HIF-1 α protein expression, nuclear translocation as well as the transcriptional activity, which subsequently enhanced HIF-1-target PAI-1 and HO-1 gene expression. Moreover, it was also demonstrated that the scavenging of OH• by DHR acted mainly on the N-terminal (TADN) and C-terminal (TADC) transactivation domains of HIF-1 α .

The HIF-1 α -TADN contains one of two key proline residues (Pro564) since it overlaps with the oxygen-dependent degradation domain (ODDD). These proline residues can be specifically hydroxylated by a group of recently discovered prolyl hydroxylases (PHDs) which thereby control HIF-1 α -pVHL physical interaction. Single mutation of the Pro564 in TADN led to a significant enhancement of its transactivity and abolished the induction by hypoxia as well as by DHR. This suggested that DHR might also act on this proline residue to induce HIF-1 α transactivity in parallel with PHDs or in an inhibitory way upstream of PHDs. It has been reported that HIF-1 α peptide residues (556 to 574) treated with H₂O₂ plus iron did inhibit the HIF-1 α -pVHL interaction to some extent *in vitro* (Jaakkola et al., 2001). *In vivo*, the PHDs, as members of the 2-oxoglutarate-dependent dioxygenase superfamily, require multiple co-factors and co-substrates indicating the regulatory potential of these molecules. It is now clear that PHD activity is dependent on Fe(II) and their oxidation of the HIF-1 α peptide is believed to occur through the intermediate generation of a highly reactive ferryl species (Prescott and Lloyd, 2000). Therefore, a redox cycle may modulate PHD activity where the electrons may partially arise from OH•. This was supported by the data from the hydroxylation activity assay and GST-pull down assay in the present study, where the OH• scavenger DHR

showed an inhibitory effect on HIF-1 α prolyl hydroxylase activity in a dose-dependent manner and interfered with the binding of pVHL to TADN (Fig. 28).

While HIF-1 α -TADN becomes stabilized under hypoxic conditions, HIF-1 α -TADC function appears to be regulated by the recruitment of coactivators such as CREB-binding protein (CBP)/p300 and SRC-1 (Carrero et al., 2000). Another critical regulator appears to be the redox factor-1 (Ref-1)/thioredoxin system since forced expression of Ref-1 or thioredoxin markedly enhanced TADC transactivation in a hypoxia-responsive manner (Huang et al., 1996; Ema et al., 1999). It was proposed that Cys800, which is essential for TADC transactivation, was reduced by Ref-1 in response to hypoxia and thereby facilitates the recruitment of CBP/p300. Here we found, that specific scavenging the OH \bullet by DHR mimicked hypoxia and induced TADC transactivity while mutation of the Ref-1 target site Cys800 completely abolished transactivation. Therefore, the OH \bullet generated by the Fenton reaction may directly affect the redox state of Cys800 and thus the recruitment of CBP/p300. This mechanism may act together with the Factor-inhibiting HIF (FIH-1) which has been found to hydroxylate Asn803 of the HIF-1 α -TADC under normoxia leading to decreased ability of HIF-1 α to bind CBP/p300 (Lando et al., 2002). However, whether the specific scavenging of OH \bullet by DHR could interfere with the activity of FIH-1 as it did to PHDs remains to be further investigated.

5.2 The involvement of the ER in hypoxic responses

The finding of the co-localization of OH \bullet generation and HIF-1 α in the ER encouraged us to investigate the involvement of ER function in hypoxic responses. In eukaryotic cells, the ER serves as the major organelle for lipid and protein biosynthesis. Approximately one-third of all cellular proteins are translocated into the lumen of the ER where post-translational modification, folding and oligomerization occur (Kaufman, 1999). The ER provides a unique oxidizing compartment for the folding of membrane and secretory proteins that are destined to the cell surface, as well as for proteins destined to other intracellular organelles, such as lysosomes and the Golgi compartment. In addition, the ER is also the calcium pool within the cell and serves as a signaling-transducing organelle that continuously responds to environmental cues to release calcium. The ER is exquisitely sensitive to alterations in homeostasis from a variety of different stimuli, such as glucose starvation, inhibition of protein glycosylation, perturbation of calcium homeostasis, and exposure to free radicals. Under such conditions, perturbation of protein folding and the accumulation of misfolded proteins in the ER induce ER stress and impair the function of the organelle (Kaufman, 1999).

The finding that brefeldin A and tunicamycin, which block protein transport out of the ER and inhibit glycosylation respectively, showed an inhibitory effect on hypoxia-induced HIF-1 α expression and HIF-1-dependent reporter gene expression suggesting that the hypoxic responses of cells were dependent on the proper ER function. It is known that the lumen of ER is much more oxidizing than the cytosol due to the higher ratio of oxidized to reduced glutathione (GSSG/GSH) in the ER. A selective import of GSSG from the cytosol was proposed to generate conditions suitable for protein modification in the ER lumen. The ER stress might disturb this thereby causing misfolding of HIF-1 α . Since the redox-dependent HIF-1 α modification was involved in its stabilization and activation, such misfolding might contribute to HIF-1 α degradation. Additionally, it is not clear whether disulfide bonds exist within the HIF-1 α molecule and whether other ER located redox-sensitive enzymes such as protein disulfide isomerase (PDI) are also involved in the regulation of HIF-1 α activity.

Protein disulfide isomerase (PDI) is particularly interesting since it catalyzes the rate-limiting reactions of oxidative formation, reduction, and isomerization of disulfide bonds within the ER. The expression of PDI is up-regulated by ER stress (Kozutsumi et al., 1988; Dorner et al., 1990) and in response to hypoxia in neuroblastoma cells. Overexpression of PDI in these cells resulted in attenuation of cell viability in response to hypoxia and protected hippocampal CA1 cells from apoptotic cell death in response to brain ischemia (Tanaka et al., 2000). In addition, PDI is also known to function as the β -subunit of prolyl 4-hydroxylase, which catalyzes the formation of 4-hydroxyproline in collagens and other proteins with collagen-like sequences (Kivirikko and Myllyharju, 1998). Since the HIF-PHDs share a high degree of similarity with the collagen prolyl-4-hydroxylase (P4H), it would be particularly interesting to investigate whether the HIF-PHDs may have an interaction with PDI.

5.3 The role of calcium ions in HIF-1 α regulation

It was found in this study that ER stress caused by thapsigargin did not repress the hypoxia-induced EPO-HRE activity, although it inhibited the general reporter gene expression under both normoxia and hypoxia like the other ER stress-inducing reagents including brefeldin A and tunicamycin. Indeed, the treatment of thapsigargin could accumulate HIF-1 α under normoxia in HepG2 cells. Since thapsigargin, as an inhibitor of the ER Ca²⁺-ATPase, can also cause an elevation of intracellular Ca²⁺, this interesting finding initiated to further investigate the involvement of Ca²⁺ in HIF-1 α regulation.

In addition to the important functions of calcium in the ER, it acts also as the most important intracellular messenger. The very low resting Ca²⁺ concentration in the cytosol creates an

ideal condition for its signaling purposes. Upon stimulation usually through generation of inositol trisphosphate (IP₃), Ca²⁺ is rapidly released from the intracellular stores (ER) and mediates a plethora of cellular processes. Recent studies indicate that Ca²⁺ is also involved in the cellular response to hypoxia. Indeed, a significant increase in free intracellular Ca²⁺ was observed in endothelial cells and in HepG2 cells after 2 h of hypoxia (Arnould et al., 1992; Mottet et al., 2003). This increase in cytosolic calcium was also due to the release of Ca²⁺ from intracellular stores (Hampl et al., 1995; Pisani et al., 2000). This would be in line with our finding using thapsigargin. Based on our observation that HIF-1 α accumulated in response to thapsigargin, the involvement of Ca²⁺ in HIF-1 α regulation was further proved with other reagents such as the calcium ionophore (A23187), the cell impermeable calcium chelator (BAPTA) and the cell permeable calcium chelator (BAPTA-AM). Surprisingly, both A23187 and BAPTA-AM, which was proposed to increase and decrease the intracellular Ca²⁺ respectively, showed a significant induction of HIF-1 α protein expression and induced the hypoxia responsive PAI-1 expression. These responses seem to involve different molecular mechanisms including a transcriptional response as well as a post-translational response.

5.3.1 Implication of calcium ions in HIF-1 α accumulation

In this study, it was demonstrated that the accumulation of HIF-1 α by A23187 was due to enhanced transcription since an increased abundance of HIF-1 α mRNA was detected and it could be significantly inhibited by actinomycin D. It was proposed from a study using angiotensin in vascular smooth muscle cells that activation of the protein kinase C (PKC)/ERK pathway played a major role in the increase of HIF-1 α gene transcription (Page et al., 2002). Similarly, this signaling pathway could also be activated by the elevation of intracellular Ca²⁺ in HepG2 cells (Mottet et al., 2002). Therefore, it is reasonable to propose that the A23187 stimulated HIF-1 α gene transcription occurs through activation of the ERK pathway. This was then demonstrated by the finding that accumulation of HIF-1 α by A23187 was totally abolished in the presence of U0126, an inhibitor of the ERK pathway (data not shown).

Furthermore, application of actinomycin D also inhibited hypoxia-induced HIF-1 α accumulation by about 50%, although it was not as strong as with A23187. This also implicates that hypoxia can regulate HIF-1 α mRNA transcription although HIF-1 α mRNA was regarded to be constitutively expressed in cultured cells independent of oxygen tensions (Wenger, et al, 1996; 1997). However, it appeared not to be the fact in HepG2 cells since a clear induction of HIF-1 α mRNA expression was detected under hypoxia. This may be cell-type specific since different cell-types may express a different combination of signaling

proteins and may therefore respond to the same stimuli to a lesser or greater extent. This may also include the MAPK pathway components, which could be activated by hypoxia as well as by the elevation of intracellular Ca^{2+} in HepG2 cells, but not in other cell types such as A549 and Hep3B cells (Metzen et al., 1999; Saltiel and Kahn, 2001). This may be the reason for the contradictory results obtained between this study and other reports which mentioned that elevation of intracellular Ca^{2+} could not induce the HIF-1 α protein levels in Hep3B and A549 cells (Metzen et al., 1999; Salnikow et al., 2002).

Interestingly, BAPTA-AM, which was supposed to decrease the intracellular Ca^{2+} by chelation, could also enhance HIF-1 α protein levels under normoxia but its effect was much more transient compared to A23187. We propose that BAPTA-AM accumulates HIF-1 α protein through its stabilization but not via stimulation of HIF-1 α gene transcription, based on the following findings. First, treatment with BAPTA-AM did not enhance HIF-1 α mRNA expression and accumulation of HIF-1 α protein could not be blocked by actinomycin D. Second, the HIF-1 α prolyl hydroxylation assay and GST-pull down analysis revealed that BAPTA-AM inhibited PHD activity and thus the interaction between HIF-1 α and pVHL.

5.3.2 Involvement of calcium in HIF-1-dependent gene expression

Although the accumulation of HIF-1 α caused by the Ca^{2+} ionophore was not observed in all studies, the involvement of Ca^{2+} in hypoxia responsive gene expression has been well established. Elevation of intracellular Ca^{2+} has been shown to induce the expression of many hypoxia responsive genes, such as vascular endothelial growth factor (VEGF) and NDRG-1/Cap43 (Claffey et al., 1992; Salnikow et al., 1999; Mottet et al., 2002). Additionally, overexpression of a calmodulin dominant negative mutant, as well as the calmodulin antagonist W7 inhibited HIF-1 activity and abolished hypoxia-inducible expression of VEGF. The Ca^{2+} and calmodulin were further proposed to act upstream of ERK to enhance the transactivation of HIF-1 α (Hur et al., 2001; Mottet et al., 2002). Moreover, the elevation of intracellular Ca^{2+} also activates many other transcription factors. Of particular interest is the activator protein-1 (AP-1) which has been reported to be activated by the Ca^{2+} ionophore and to cooperate with HIF-1 in response to hypoxia (Salnikow et al., 2002).

With the accumulation of HIF-1 α protein, both the Ca^{2+} ionophore (A23187) and chelator (BAPTA-AM) were found to stimulate the expression of PAI-1, a hypoxia responsive gene in HepG2 cells. Consistent with the HIF-1 α protein level, A23187 showed the strongest effect compared to hypoxia and BAPTA-AM. However, A23187 could only slightly induce the HIF-1-dependent reporter expression. Three explanations for this discrepancy have to be considered. First, A23187, as a Ca^{2+} ionophore, also depletes the Ca^{2+} pool in the ER and

induces ER stress as Thapsigargin does. This condition would unspecifically inhibit the expression of exogenous genes and lead to a decrease of LUC activity, as it has been demonstrated with other ER stress inducing reagents. Second, it is clear that the HIF-1 transactivity is inhibited by asparaginyl hydroxylation and/or redox modification under normoxia (Ema et al., 1999; Lando et al., 2002). Since A23187 accumulates HIF-1 α by increasing its transcription, these overexpressed HIF-1 α needs first to titrate these inhibitions out. This would cause the existence of dysfunctional HIF-1 α proteins to some extent. Third, several studies have demonstrated that AP-1 is one of the critical transcription factors for PAI-1 expression (Kasza et al., 2002). With activation of this transcription factor, it is convincible to find that A23187 boosted PAI-1 expression with even less functional HIF-1 α under normoxic conditions.

All together, the present study provides further information on the signaling pathway leading to HIF-1-dependent responses in cells (Fig. 41).

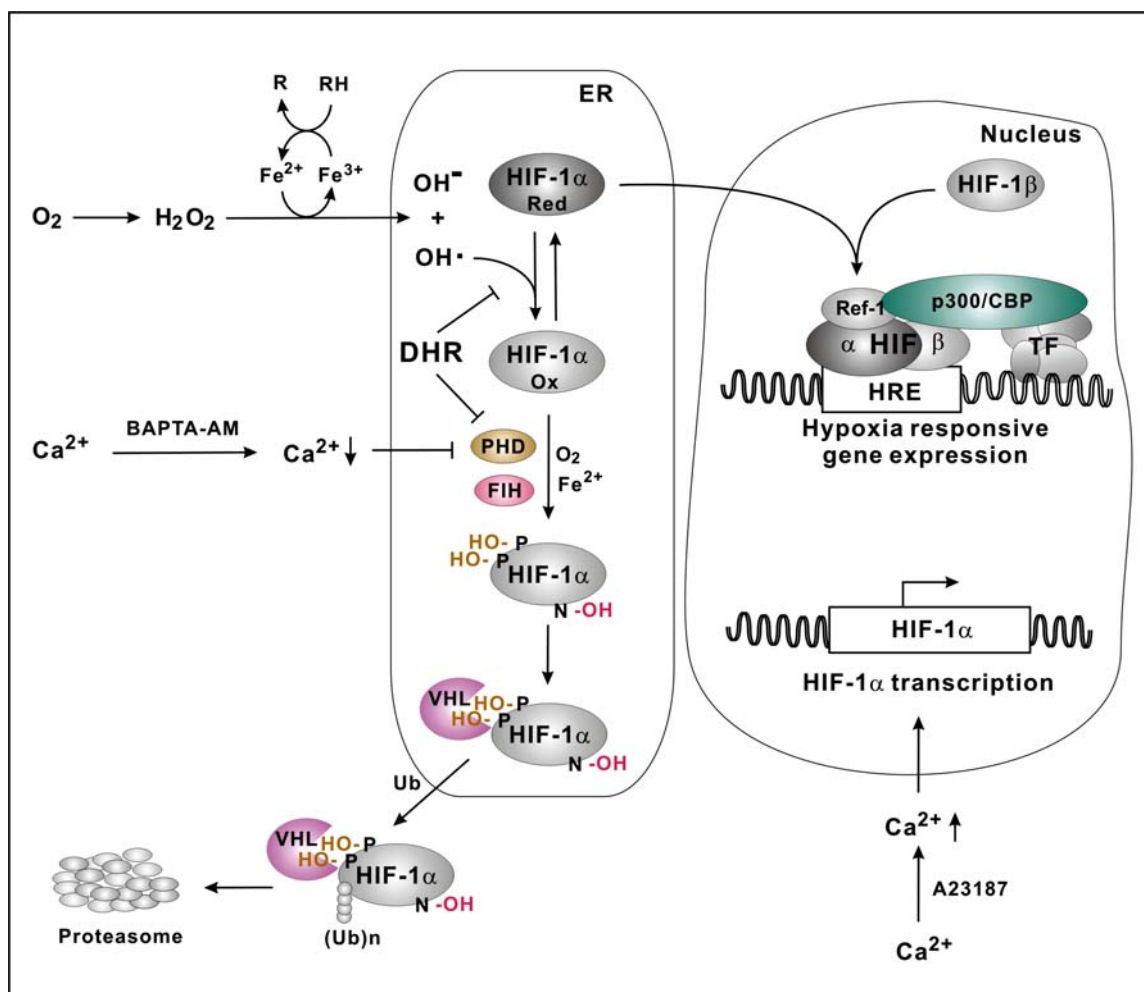


Figure 41. Model of the HIF-1 α regulation. DHR, dihydrorhodamine; ER, endoplasmic reticulum; FIH, factor inhibiting HIF-1; HIF, hypoxia-inducible factor; HRE, hypoxia responsive element; N, asparagine 803 residue; Ox, oxidated; P, proline 402, 564 residues; PHD, prolyl hydroxylase domain; Red, reduced; TF, general transcription factors; VHL, von Hippel-Lindau tumor suppressor protein; Ub, ubiquitin.

Under normoxia HIF-1 α is believed to be oxidized due to oxidative conditions generated by the Fenton reaction. The oxidized HIF-1 α facilitates its hydroxylation by the PHDs and FIH, thereby triggering the binding of VHL its subsequent ubiquitination and proteasomal degradation. DHR, which is a specific OH \bullet scavenger, can block these modifications and mimic hypoxia which induces HIF-1 α accumulation, nuclear translocation, dimerization with HIF-1 β (ARNT), binding of the α/β -dimer to HRE, recruitment of cofactors such as CBP/p300 or Ref-1 which then leads to target gene expression. Furthermore, intracellular Ca²⁺ is also involved into the regulation of HIF-1 α . Elevation of intracellular Ca²⁺ by the calcium ionophore (A23187) can induce expression of HIF-1 α mRNA, thereby leading to the accumulation of HIF-1 α even under normoxia. On the other hand, chelation of intracellular Ca²⁺ by the cell permeable calcium chelator (BAPTA-AM) can cause accumulation of HIF-1 α protein via inhibition of PHD activity.

Further investigations are needed to completely rule out the mechanisms involved in the interdependence of hypoxia and calcium signaling which leads to HIF-1 dependent gene expression.

References

- Archer SL, Reeve HL, Michelakis E, Puttagunta L, Waite R, Nelson DP, Dinauer MC, Weir EK (1999):** O₂ sensing is preserved in mice lacking the gp91 phox subunit of NADPH oxidase. *Proc Natl Acad Sci U.S.A.* 96:7944-7949.
- Arany Z, Huang LE, Eckner R, Bhattacharya S, Jiang C, Goldberg MA, Bunn HF, Livingston DM (1996):** An essential role for p300/CBP in the cellular response to hypoxia. *Proc Natl Acad Sci U.S.A.* 93:12969-12973.
- Arnould T, Michiels C, Alexandre I, Remacle J (1992):** Effect of hypoxia upon intracellular calcium concentration of human endothelial cells. *J Cell Physiol.* 152:215-221.
- Baader E, Tschank G, Baringhaus KH, Burghard H, Gunzler V (1994):** Inhibition of prolyl 4-hydroxylase by oxalyl amino acid derivatives in vitro, in isolated microsomes and in embryonic chicken tissues. *Biochem J.* 300:525-530.
- Berra E, Richard DE, Gothie E, Pouyssegur J (2001):** HIF-1-dependent transcriptional activity is required for oxygen-mediated HIF-1 α degradation. *FEBS Lett.* 49:85-90.
- Bhattacharya S, Michels CL, Leung MK, Arany ZP, Kung AL, Livingston DM (1999):** Functional role of p35srj, a novel p300/CBP binding protein, during transactivation by HIF-1. *Genes Dev.* 13:64-75.
- Bilton RL, Booker GW (2003):** The subtle side to hypoxia-inducible factor (HIF α) regulation. *Eur J Biochem.* 270:791-798.
- Bunn HF, Poyton RO (1996):** Oxygen sensing and molecular adaptation to hypoxia. *Physiol Rev.* 76:839-885.
- Camenisch G, Stroka DM, Gassmann M, Wenger RH (2001):** Attenuation of HIF-1 DNA-binding activity limits hypoxia-inducible endothelin-1 expression. *Pflugers Arch.* 443:240-249.
- Carrero P, Okamoto K, Coumailleau P, O'Brien S, Tanaka H, Poellinger L (2000):** Redox-regulated recruitment of the transcriptional coactivators CREB-binding protein and SRC-1 to hypoxia-inducible factor 1 α . *Mol Cell Biol.* 20:402-415.
- Chance B, Sies H, Boveris A (1979):** Hydroperoxide metabolism in mammalian organs. *Physiol Rev.* 59:527-605.
- Chandel NS, Maltepe E, Goldwasser E, Mathieu CE, Simon MC, Schumacker PT (1998):** Mitochondrial reactive oxygen species trigger hypoxia-induced transcription. *Proc Natl Acad Sci U.S.A.* 95:11715-11720
- Chandel NS, McClintock DS, Feliciano CE, Wood TM, Melendez JA, Rodriguez AM, Schumacker PT (2000):** Reactive oxygen species generated at mitochondrial complex III stabilize hypoxia-inducible factor-1 α during hypoxia: a mechanism of O₂ sensing. *J Biol*

Chem. 275:25130-25138.

Chen C, Okayama H (1987): High-efficiency transformation of mammalian-cells by plasmid DNA. *Mol Cell Biol.* 7: 2745-2752

Chen C, Okayama H (1988): Calcium phosphate-mediated gene-transfer-a highly efficient transfection system for stably transforming cells with plasmid DNA. *Biotech* 6: 632.

Chun YS, Choi E, Yeo EJ, Lee JH, Kim MS, Park JW (2001): A new HIF-1 alpha variant induced by zinc ion suppresses HIF-1-mediated hypoxic responses. *J Cell Sci.* 114:4051-4061.

Chun YS, Choi E, Kim TY, Kim MS, Park JW (2002): A dominant-negative isoform lacking exons 11 and 12 of the human hypoxia-inducible factor-1alpha gene. *Biochem J.* 362:71-79.

Claffey KP, Wilkison WO, Spiegelman BM (1992): Vascular endothelial growth factor. Regulation by cell differentiation and activated second messenger pathways. *J Biol Chem.* 267:16317-16322.

Damert A, Ikeda E, Risau W (1997): Activator-protein-1 binding potentiates the hypoxia-induciblefactor-1-mediated hypoxia-induced transcriptional activation of vascular-endothelial growth factor expression in C6 glioma cells. *Biochem J.* 327:419-423.

Dames SA, Martinez-Yamout M, De Guzman RN, Dyson HJ, Wright PE (2002): Structural basis for Hif-1 alpha /CBP recognition in the cellular hypoxic response. *Proc Natl Acad Sci U.S.A.* 99:5271-5276.

Dorner AJ, Wasley LC, Raney P, Haugejorden S, Green M, Kaufman RJ (1990): The stress response in Chinese hamster ovary cells. Regulation of ERp72 and protein disulfide isomerase expression and secretion. *J Biol Chem.* 265:22029-22034.

Ebert BL, Firth JD, Ratcliffe PJ (1995): Hypoxia and mitochondrial inhibitors regulate expression of glucose transporter-1 via distinct Cis-acting sequences. *J Biol Chem.* 270:29083-29089.

Ebert BL, Gleadle JM, O'Rourke JF, Bartlett SM, Poulton J, Ratcliffe PJ (1996): Isoenzyme-specific regulation of genes involved in energy metabolism by hypoxia: similarities with the regulation of erythropoietin. *Biochem J.* 313:809-814.

Ebert BL, Bunn HF (1998): Regulation of transcription by hypoxia requires a multiprotein complex that includes hypoxia-inducible factor 1, an adjacent transcription factor, and p300/CREB binding protein. *Mol Cell Biol.* 18:4089-4096.

Ehleben W, Porwol T, Fandrey J, Kummer W, Acker H (1997): Cobalt and desferrioxamine reveal crucial members of the oxygen sensing pathway in HepG2 cells. *Kidney Int.* 51:483-491.

Elson DA, Thurston G, Huang LE, Ginzinger DG, McDonald DM, Johnson RS, Arbeit JM

(2001): Induction of hypervascularity without leakage or inflammation in transgenic mice overexpressing hypoxia-inducible factor-1alpha. *Genes Dev.* 15:2520-2532.

Ema M, Taya S, Yokotani N, Sogawa K, Matsuda Y, Fujii-Kuriyama Y (1997): A novel bHLH-PAS factor with close sequence similarity to hypoxia-inducible factor 1alpha regulates the VEGF expression and is potentially involved in lung and vascular development. *Proc Natl Acad Sci U.S.A.* 94:4273-4278.

Ema M, Hirota K, Mimura J, Abe H, Yodoi J, Sogawa K, Poellinger L, Fujii-Kuriyama Y (1999): Molecular mechanisms of transcription activation by HLF and HIF1alpha in response to hypoxia: their stabilization and redox signal-induced interaction with CBP/p300. *EMBO J.* 18:1905-1914.

Estes SD, Stoler DL, Anderson GR (1995): Anoxic induction of a sarcoma virus-related VL30 retrotransposon is mediated by a cis-acting element which binds hypoxia-inducible factor 1 and an anoxia-inducible factor. *J Virol.* 69:6335-6341.

Fandrey J, Frede S, Jelkmann W (1994): Role of hydrogen peroxide in hypoxia-induced erythropoietin production. *Biochem J.* 303:507-510.

Fandrey J, Frede S, Ehleben W, Porwol T, Acker H, Jelkmann W (1997): Cobalt chloride and desferrioxamine antagonize the inhibition of erythropoietin production by reactive oxygen species. *Kidney Int.* 51:492-496.

Fatyol K, Szalay AA (2001): The p14ARF tumor suppressor protein facilitates nucleolar sequestration of hypoxia-inducible factor-1alpha (HIF-1alpha) and inhibits HIF-1-mediated transcription. *J Biol Chem.* 276:28421-28429.

Firth JD, Ebert BL, Pugh CW, Ratcliffe PJ (1994): Oxygen-regulated control elements in the phosphoglycerate kinase 1 and lactate dehydrogenase A genes: similarities with the erythropoietin 3' enhancer. *Proc Natl Acad Sci U.S.A.* 91:6496-6500.

Firth JD, Ebert BL, Ratcliffe PJ (1995): Hypoxic regulation of lactate dehydrogenase A. Interaction between hypoxia-inducible factor 1 and cAMP response elements. *J Biol Chem.* 270:21021-21027.

Flamme I, Frohlich T, von Reutern M, Kappel A, Damert A, Risau W (1997): HRF, a putative basic helix-loop-helix-PAS-domain transcription factor is closely related to hypoxia-inducible factor-1 alpha and developmentally expressed in blood vessels. *Mech Dev.* 63:51-60.

Forsythe JA, Jiang BH, Iyer NV, Agani F, Leung SW, Koos RD, Semenza GL (1996): Activation of vascular endothelial growth factor gene transcription by hypoxia-inducible factor 1. *Mol Cell Biol.* 16:4604-4613.

Freeman BA, Crapo JD (1982). Biology of disease: free radicals and tissue injury (1982).

Lab Invest. 47:412-426.

Fukuda R, Hirota K, Fan F, Jung YD, Ellis LM, Semenza GL (2002): Insulin-like growth factor 1 induces hypoxia-inducible factor 1-mediated vascular endothelial growth factor expression, which is dependent on MAP kinase and phosphatidylinositol 3-kinase signaling in colon cancer cells. *J Biol Chem.* 277:38205-38211.

Galson DL, Tsuchiya T, Tendler DS, Huang LE, Ren Y, Ogura T, Bunn HF (1995): The orphan receptor hepatic nuclear factor 4 functions as a transcriptional activator for tissue-specific and hypoxia-specific erythropoietin gene expression and is antagonized by EAR3/COUP-TF1. *Mol Cell Biol.* 15:2135-2144.

Gerber HP, Condorelli F, Park J, Ferrara N (1997): Differential transcriptional regulation of the two vascular endothelial growth factor receptor genes. Flt-1, but not Flk-1/KDR, is up-regulated by hypoxia. *J Biol Chem.* 272:23659-23667.

Goldberg MA, Dunning SP, Bunn HF (1988): Regulation of the erythropoietin gene: evidence that the oxygen sensor is a heme protein. *Science.* 242:1412-1415.

Goldberg MA, Schneider TJ. Goldberg MA, Schneider TJ (1994): Similarities between the oxygen-sensing mechanisms regulating the expression of vascular endothelial growth factor and erythropoietin. *J Biol Chem.* 269:4355-4359.

Graham FL, Vandereb AJ (1973): New technique for assay of infectivity of human adenovirus 5 DNA. *Virology* 52: 456-467

Graven KK, Yu Q, Pan D, Roncarati JS, Farber HW (1999): Identification of an oxygen responsive enhancer element in the glyceraldehyde-3-phosphate dehydrogenase gene. *Biochim Biophys Acta.* 1447:208-218.

Groulx I, Lee S (2002): Oxygen-dependent ubiquitination and degradation of hypoxia-inducible factor requires nuclear-cytoplasmic trafficking of the von Hippel-Lindau tumor suppressor protein. *Mol Cell Biol.* 22:5319-5336.

Gu Y, Xu YC, Wu RF, Nwariaku FE, Souza RF, Flores SC, Terada LS (2003): p47phox participates in activation of RelA in endothelial cells. *J Biol Chem.* 278:17210-17217.

HAMPL V, Cornfield DN, Cowan NJ, Archer SL (1995): Hypoxia potentiates nitric oxide synthesis and transiently increases cytosolic calcium levels in pulmonary artery endothelial cells. *Eur Respir J.* 8:515-522.

Hewitson KS, McNeill LA, Riordan MV, Tian YM, Bullock AN, Welford RW, Elkins JM, Oldham NJ, Bhattacharya S, Gleadle JM, Ratcliffe PJ, Pugh CW, Schofield CJ (2002): Hypoxia-inducible factor (HIF) asparagine hydroxylase is identical to factor inhibiting HIF (FIH) and is related to the cupin structural family. *J Biol Chem.* 277:26351-26355.

Hildebrandt W, Alexander S, Bartsch P, Droge W (2002): Effect of N-acetyl-cysteine on the

hypoxic ventilatory response and erythropoietin production: linkage between plasma thiol redox state and O₂ chemosensitivity. *Blood*. 99:1552-1555.

Hirose K, Morita M, Ema M, Mimura J, Hamada H, Fujii H, Saijo Y, Gotoh O, Sogawa K, Fujii-Kuriyama Y (1996): cDNA cloning and tissue-specific expression of a novel basic helix-loop-helix/PAS factor (Arnt2) with close sequence similarity to the aryl hydrocarbon receptor nuclear translocator (Arnt). *Mol Cell Biol*. 16:1706-1713.

Ho VT, Bunn HF (1996): Effects of transition metals on the expression of the erythropoietin gene: further evidence that the oxygen sensor is a heme protein. *Biochem Biophys Res Commun*. 223:175-180.

Hockberger PE, Skimina TA, Centonze VE, Lavin C, Chu S, Dadras S, Reddy JK, White JG (1999): Activation of flavin-containing oxidases underlies light-induced production of H₂O₂ in mammalian cells. *Proc Natl Acad Sci U.S.A.* 96:6255-6260.

Hofer T, Desbaillets I, Hopfl G, Gassmann M, Wenger RH (2001): Dissecting hypoxia-dependent and hypoxia-independent steps in the HIF-1 α activation cascade: implications for HIF-1 α gene therapy. *FASEB J*. 15:2715-2717.

Hoffman EC, Reyes H, Chu FF, Sander F, Conley LH, Brooks BA, Hankinson O (1991): Cloning of a factor required for activity of the Ah (dioxin) receptor. *Science*. 252:954-958.

Hogenesch JB, Chan WK, Jackiw VH, Brown RC, Gu YZ, Pray-Grant M, Perdew GH, Bradfield CA (1997): Characterization of a subset of the basic-helix-loop-helix-PAS superfamily that interacts with components of the dioxin signaling pathway. *J Biol Chem*. 272:8581-8593.

Hogenesch JB, Gu YZ, Jain S, Bradfield CA (1998): The basic-helix-loop-helix-PAS orphan MOP3 forms transcriptionally active complexes with circadian and hypoxia factors. *Proc Natl Acad Sci U.S.A.* 95:5474-5479.

Hogenesch JB, Gu YZ, Moran SM, Shimomura K, Radcliffe LA, Takahashi JS, Bradfield CA (2000): The basic helix-loop-helix-PAS protein MOP9 is a brain-specific heterodimeric partner of circadian and hypoxia factors. *J Neurosci*. 20:RC83.

Hon WC, Wilson MI, Harlos K, Claridge TD, Schofield CJ, Pugh CW, Maxwell PH, Ratcliffe PJ, Stuart DI, Jones EY (2002): Structural basis for the recognition of hydroxyproline in HIF-1 α by pVHL. *Nature*. 417:975-978.

Hu J, Discher DJ, Bishopric NH, Webster KA (1998): Hypoxia regulates expression of the endothelin-1 gene through a proximal hypoxia-inducible factor-1 binding site on the antisense strand. *Biochem Biophys Res Commun*. 245:894-899.

Huang LE, Arany Z, Livingston DM, Bunn HF (1996): Activation of hypoxia-inducible transcription factor depends primarily upon redox-sensitive stabilization of its α subunit. *J*

Biol Chem. 271:32253-32259.

Huang LE, Gu J, Schau M, Bunn HF (1998): Regulation of hypoxia-inducible factor 1alpha is mediated by an O₂-dependent degradation domain via the ubiquitin-proteasome pathway. Proc Natl Acad Sci U.S.A. 95:7987-7992.

Hur J, Kim SY, Kim H, Cha S, Lee MS, Suk K (2001): Induction of caspase-11 by inflammatory stimuli in rat astrocytes: lipopolysaccharide induction through p38 mitogen-activated protein kinase pathway. FEBS Lett. 507:157-162.

Ivan M, Kondo K, Yang H, Kim W, Valiando J, Ohh M, Salic A, Asara JM, Lane WS, Kaelin WG Jr (2001): HIFalpha targeted for VHL-mediated destruction by proline hydroxylation: implications for O₂ sensing. Science. 292:464-468.

Iwai K, Drake SK, Wehr NB, Weissman AM, LaVaute T, Minato N, Klausner RD, Levine RL, Rouault TA (1998): Iron-dependent oxidation, ubiquitination, and degradation of iron regulatory protein 2: implications for degradation of oxidized proteins. Proc Natl Acad Sci U.S.A. 95:4924-4928.

Jaakkola P, Mole DR, Tian YM, Wilson MI, Gielbert J, Gaskell SJ, Kriegsheim Av, Hebestreit HF, Mukherji M, Schofield CJ, Maxwell PH, Pugh CW, Ratcliffe PJ (2001): Targeting of HIF-alpha to the von Hippel-Lindau ubiquitylation complex by O₂-regulated prolyl hydroxylation. Science. 292:468-472.

Jeong JW, Bae MK, Ahn MY, Kim SH, Sohn TK, Bae MH, Yoo MA, Song EJ, Lee KJ, Kim KW (2002): Regulation and destabilization of HIF-1alpha by ARD1-mediated acetylation. Cell. 111:709-720.

Jung F, Palmer LA, Zhou N, Johns RA (2000): Hypoxic regulation of inducible nitric oxide synthase via hypoxia inducible factor-1 in cardiac myocytes. Circ Res. 86:319-325.

Kallio PJ, Okamoto K, O'Brien S, Carrero P, Makino Y, Tanaka H, Poellinger L (1998): Signal transduction in hypoxic cells: inducible nuclear translocation and recruitment of the CBP/p300 coactivator by the hypoxia-inducible factor-1alpha. EMBO J. 17:6573-6586.

Kallio PJ, Wilson WJ, O'Brien S, Makino Y, Poellinger L (1999): Regulation of the hypoxia-inducible transcription factor 1alpha by the ubiquitin-proteasome pathway. J Biol Chem. 274:6519-6525.

Karni R, Dor Y, Keshet E, Meyuhas O, Levitzki A (2002): Activated pp60c-Src leads to elevated hypoxia-inducible factor (HIF)-1alpha expression under normoxia. J Biol Chem. 277:42919-42925.

Kasza A, Kiss DL, Gopalan S, Xu W, Rydel RE, Koj A, Kordula T (2002): Mechanism of plasminogen activator inhibitor-1 regulation by oncostatin M and interleukin-1 in human astrocytes. J Neurochem. 83:696-703.

Kaufman RJ (1999): Stress signaling from the lumen of the endoplasmic reticulum: coordination of gene transcriptional and translational controls. *Genes Dev.* 13:1211-1233.

Kietzmann T, Schmidt H, Probst I, Jungermann K (1992): Modulation of the glucagon-dependent activation of the phosphoenolpyruvate carboxykinase gene by oxygen in rat hepatocyte cultures. Evidence for a heme protein as oxygen sensor. *FEBS Lett.* 311:251-255.

Kietzmann T, Schmidt H, Unthan-Fechner K, Probst I, Jungermann K (1993): A ferro-heme protein senses oxygen levels, which modulate the glucagon-dependent activation of the phosphoenolpyruvate carboxykinase gene in rat hepatocyte cultures. *Biochem Biophys Res Commun.* 195:792-798.

Kietzmann T, Freimann S, Bratke J, Jungermann K (1996): Regulation of the gluconeogenic phosphoenolpyruvate carboxykinase and glycolytic aldolase A gene expression by O₂ in rat hepatocyte cultures. Involvement of hydrogen peroxide as mediator in the response to O₂. *FEBS Lett.* 388:228-232.

Kietzmann T, Bratke J, Jungermann K (1997): Diminution of the O₂ responsiveness of the glucagon-dependent activation of the phosphoenolpyruvate carboxykinase gene in rat hepatocytes by long-term culture at venous PO₂. *Kidney Int.* 51:542-547.

Kietzmann T, Porwol T, Zierold K, Jungermann K, Acker H (1998): Involvement of a local fenton reaction in the reciprocal modulation by O₂ of the glucagon-dependent activation of the phosphoenolpyruvate carboxykinase gene and the insulin-dependent activation of the glucokinase gene in rat hepatocytes. *Biochem J.* 335:425-432.

Kietzmann T, Roth U, Jungermann K (1999): Induction of the plasminogen activator inhibitor-1 gene expression by mild hypoxia via a hypoxia response element binding the hypoxia-inducible factor-1 in rat hepatocytes. *Blood.* 94:4177-4185.

Kivirikko KI, Myllyharju J (1998): Prolyl 4-hydroxylases and their protein disulfide isomerase subunit. *Matrix Biol.* 16:357-368.

Kozutsumi Y, Segal M, Normington K, Gething MJ, Sambrook J (1988): The presence of malfolded proteins in the endoplasmic reticulum signals the induction of glucose-regulated proteins. *Nature.* 332:462-464.

Lando D, Pongratz I, Poellinger L, Whitelaw ML (2000): A redox mechanism controls differential DNA binding activities of hypoxia-inducible factor (HIF) 1 α and the HIF-like factor. *J Biol Chem.* 275:4618-4627.

Lando D, Peet DJ, Whelan DA, Gorman JJ, Whitelaw ML (2002a): Asparagine hydroxylation of the HIF transactivation domain a hypoxic switch. *Science.* 295:858-861.

Lando D, Peet DJ, Gorman JJ, Whelan DA, Whitelaw ML, Bruick RK (2002b): FIH-1 is an

asparaginyl hydroxylase enzyme that regulates the transcriptional activity of hypoxia-inducible factor. *Genes Dev.* 16:1466-1471.

Laughner E, Taghavi P, Chiles K, Mahon PC, Semenza GL (2001): HER2 (neu) signaling increases the rate of hypoxia-inducible factor 1alpha (HIF-1alpha) synthesis: novel mechanism for HIF-1-mediated vascular endothelial growth factor expression. *Mol Cell Biol.* 21:3995-4004.

Lee PJ, Jiang BH, Chin BY, Iyer NV, Alam J, Semenza GL, Choi AM (1997): Hypoxia-inducible factor-1 mediates transcriptional activation of the heme oxygenase-1 gene in response to hypoxia. *J Biol Chem.* 272:5375-5381.

Liu Y, Cox SR, Morita T, Kourembanas S (1995): Hypoxia regulates vascular endothelial growth factor gene expression in endothelial cells. Identification of a 5' enhancer. *Circ Res.* 77:638-643.

Lok CN, Ponka P (1999): Identification of a hypoxia response element in the transferrin receptor gene. *J Biol Chem.* 274:24147-24152.

Lopez-Barneo J (1996): Oxygen-sensing by ion channels and the regulation of cellular functions. *Trends Neurosci.* 19:435-440.

Luo JC, Shibuya M (2001): A variant of nuclear localization signal of bipartite-type is required for the nuclear translocation of hypoxia inducible factors (1alpha, 2alpha and 3alpha). *Oncogene.* 20:1435-1444.

Mahon PC, Hirota K, Semenza GL (2001): FIH-1: a novel protein that interacts with HIF-1alpha and VHL to mediate repression of HIF-1 transcriptional activity. *Genes Dev.* 15:2675-2686.

Makino Y, Cao R, Svensson K, Bertilsson G, Asman M, Tanaka H, Cao Y, Berkenstam A, Poellinger L (2001): Inhibitory PAS domain protein is a negative regulator of hypoxia-inducible gene expression. *Nature.* 414:550-554.

Makino Y, Kanopka A, Wilson WJ, Tanaka H, Poellinger L (2002): Inhibitory PAS domain protein (IPAS) is a hypoxia-inducible splicing variant of the hypoxia-inducible factor-3alpha locus. *J Biol Chem.* 277:32405-32408.

Maxwell PH, Wiesener MS, Chang GW, Clifford SC, Vaux EC, Cockman ME, Wykoff CC, Pugh CW, Maher ER, Ratcliffe PJ (1999): The tumour suppressor protein VHL targets hypoxia-inducible factors for oxygen-dependent proteolysis. *Nature.* 399:271-275.

Melillo G, Musso T, Sica A, Taylor LS, Cox GW, Varesio L (1995): A hypoxia-responsive element mediates a novel pathway of activation of the inducible nitric oxide synthase promoter. *J Exp Med.* 182:1683-1693.

Metzen E, Fandrey J, Jelkmann W (1999): Evidence against a major role for Ca²⁺ in

hypoxia-induced gene expression in human hepatoma cells (Hep3B). *J Physiol.* 517:651-657.

Min JH, Yang H, Ivan M, Gertler F, Kaelin WG Jr, Pavletich NP (2002): Structure of an HIF-1 α -pVHL complex: hydroxyproline recognition in signaling. *Science.* 296:1886-1889.

Mottet D, Michel G, Renard P, Ninane N, Raes M, Michiels C (2002): ERK and calcium in activation of HIF-1. *Ann N Y Acad Sci.* 973:448-453.

Mottet D, Dumont V, Deccache Y, Demazy C, Ninane N, Raes M, Michiels C (2003): Regulation of hypoxia-inducible factor-1 α protein level during hypoxic conditions by the phosphatidylinositol 3-kinase/Akt/glycogen synthase kinase 3 β pathway in HepG2 cells. *J Biol Chem.* 278:31277-31285.

Mukhopadhyay CK, Mazumder B, Fox PL (2000): Role of hypoxia-inducible factor-1 in transcriptional activation of ceruloplasmin by iron deficiency. *J Biol Chem.* 275:21048-21054.

Nguyen SV, Claycomb WC (1999): Hypoxia regulates the expression of the adrenomedullin and HIF-1 genes in cultured HL-1 cardiomyocytes. *Biochem Biophys Res Commun.* 265:382-386.

Ohh M, Park CW, Ivan M, Hoffman MA, Kim TY, Huang LE, Pavletich N, Chau V, Kaelin WG (2000): Ubiquitination of hypoxia-inducible factor requires direct binding to the beta-domain of the von Hippel-Lindau protein. *Nat Cell Biol.* 2:423-427.

Oikawa M, Abe M, Kurosawa H, Hida W, Shirato K, Sato Y (2001): Hypoxia induces transcription factor ETS-1 via the activity of hypoxia-inducible factor-1. *Biochem Biophys Res Commun.* 289:39-43.

Okino ST, Chichester CH, Whitlock JP Jr. Okino ST, Chichester CH, Whitlock JP Jr (1998): Hypoxia-inducible mammalian gene expression analyzed in vivo at a TATA-driven promoter and at an initiator-driven promoter. *J Biol Chem.* 273:23837-23843.

Parker BA, Stark GR (1979): Regulation of simian-virus 40 transcription sensitive analysis of the RNA species present early in infections by virus or viral-dna. *J Virol.* 31:360-369.

Pisani A, Bonsi P, Centonze D, Giacomini P, Calabresi P (2000): Involvement of intracellular calcium stores during oxygen/glucose deprivation in striatal large aspiny interneurons. *J Cereb Blood Flow Metab.* 20:839-846.

Porwol T, Ehleben W, Zierold K, Fandrey J, Acker H (1998): The influence of nickel and cobalt on putative members of the oxygen-sensing pathway of erythropoietin-producing HepG2 cells. *Eur J Biochem.* 256:16-23.

Prescott AG, Lloyd MD (2000): The iron(II) and 2-oxoacid-dependent dioxygenases and their role in metabolism. *Nat Prod Rep.* 17:367-383.

Pugh CW, O'Rourke JF, Nagao M, Gleadle JM, Ratcliffe PJ (1997): Activation of hypoxia-inducible factor-1; definition of regulatory domains within the alpha subunit. *J Biol*

Chem. 272:11205-11214.

Richard DE, Berra E, Gothie E, Roux D, Pouyssegur J (1999): p42/p44 mitogen-activated protein kinases phosphorylate hypoxia-inducible factor 1 α (HIF-1 α) and enhance the transcriptional activity of HIF-1. *J Biol Chem.* 274:32631-32637.

Rippe RA, Brenner DA, Leffert HL (1990): DNA-mediated gene transfer into adult rat hepatocytes in primary culture. *Mol Cell Biol.* 10: 689-695.

Rolfs A, Kvietikova I, Gassmann M, Wenger RH (1997): Oxygen-regulated transferrin expression is mediated by hypoxia-inducible factor-1. *J Biol Chem.* 272:20055-20062.

Royall JA, Ischiropoulos H (1993): Evaluation of 2',7'-dichlorofluorescein and dihydrorhodamine 123 as fluorescent probes for intracellular H₂O₂ in cultured endothelial cells. *Arch Biochem Biophys.* 302:348-355.

Salceda S, Beck I, Srinivas V, Caro J (1997): Complex role of protein phosphorylation in gene activation by hypoxia. *Kidney Int.* 51:556-559.

Salnikow K, Kluz T, Costa M, Piquemal D, Demidenko ZN, Xie K, Blagosklonny MV (2002): The regulation of hypoxic genes by calcium involves c-Jun/AP-1, which cooperates with hypoxia-inducible factor 1 in response to hypoxia. *Mol Cell Biol.* 22:1734-1741.

Saltiel AR, Kahn CR (2001): Insulin signalling and the regulation of glucose and lipid metabolism. *Nature.* 414:799-806.

Schoenfeld AR, Davidowitz EJ, Burk RD (2001): Endoplasmic reticulum/cytosolic localization of von Hippel-Lindau gene products is mediated by a 64-amino acid region. *Int J Cancer.* 91:457-467.

Schroedl C, McClintock DS, Budinger GR, Chandel NS (2002): Hypoxic but not anoxic stabilization of HIF-1 α requires mitochondrial reactive oxygen species. *Am J Physiol Lung Cell Mol Physiol.* 283:L922-931.

Semenza GL, Roth PH, Fang HM, Wang GL (1994): Transcriptional regulation of genes encoding glycolytic enzymes by hypoxia-inducible factor 1. *J Biol Chem.* 269:23757-23763.

Semenza GL, Jiang BH, Leung SW, Passantino R, Concordet JP, Maire P, Giallongo A (1996): Hypoxia response elements in the aldolase A, enolase 1, and lactate dehydrogenase A gene promoters contain essential binding sites for hypoxia-inducible factor 1. *J Biol Chem.* 271:32529-32537.

Semenza GL, Agani F, Iyer N, Kotch L, Laughner E, Leung S, Yu A (1999): Regulation of cardiovascular development and physiology by hypoxia-inducible factor 1. *Ann N Y Acad Sci.* 874:262-268.

Sodhi A, Montaner S, Patel V, Zohar M, Bais C, Mesri EA, Gutkind JS (2000): The Kaposi's sarcoma-associated herpes virus G protein-coupled receptor up-regulates vascular

endothelial growth factor expression and secretion through mitogen-activated protein kinase and p38 pathways acting on hypoxia-inducible factor 1 α . *Cancer Res.* 60:4873-4880.

Sorescu D, Weiss D, Lassegue B, Clempus RE, Szocs K, Sorescu GP, Valppu L, Quinn MT, Lambeth JD, Vega JD, Taylor WR, Griendling KK (2002): Superoxide production and expression of nox family proteins in human atherosclerosis. *Circulation.* 105:1429-1435.

Srinivas V, Leshchinsky I, Sang N, King MP, Minchenko A, Caro J (2001): Oxygen sensing and HIF-1 activation does not require an active mitochondrial respiratory chain electron-transfer pathway. *J Biol Chem.* 276:21995-21998.

Tacchini L, Bianchi L, Bernelli-Zazzera A, Cairo G (1999): Transferrin receptor induction by hypoxia. HIF-1-mediated transcriptional activation and cell-specific post-transcriptional regulation. *J Biol Chem.* 274:24142-24146.

Takahashi Y, Takahashi S, Shiga Y, Yoshimi T, Miura T (2000): Hypoxic induction of prolyl 4-hydroxylase α (I) in cultured cells. *J Biol Chem.* 275:14139-14146.

Tanimoto K, Makino Y, Pereira T, Poellinger L (2000): Mechanism of regulation of the hypoxia-inducible factor-1 α by the von Hippel-Lindau tumor suppressor protein. *EMBO J.* 19:4298-4309.

Tan CC, Ratcliffe PJ (1991): Effect of inhibitors of oxidative phosphorylation on erythropoietin mRNA in isolated perfused rat kidneys. *Am J Physiol.* 261:F982-987.

Tanaka K, Nogawa S, Ito D, Suzuki S, Dembo T, Kosakai A, Fukuuchi Y (2000): Activated phosphorylation of cyclic AMP response element binding protein is associated with preservation of striatal neurons after focal cerebral ischemia in the rat. *Neuroscience.* 100:345-354.

Tazuke SI, Mazure NM, Sugawara J, Carland G, Faessen GH, Suen LF, Irwin JC, Powell DR, Giaccia AJ, Giudice LC (1998): Hypoxia stimulates insulin-like growth factor binding protein 1 (IGFBP-1) gene expression in HepG2 cells: a possible model for IGFBP-1 expression in fetal hypoxia. *Proc Natl Acad Sci U.S.A.* 95:10188-10193.

Thannickal VJ, Fanburg BL (2000): Reactive oxygen species in cell signaling. *Am J Physiol Lung Cell Mol Physiol.* 279:L1005-1028.

Treins C, Giorgetti-Peraldi S, Murdaca J, Semenza GL, Van Obberghen E (2002): Insulin stimulates hypoxia-inducible factor 1 through a phosphatidylinositol 3-kinase/target of rapamycin-dependent signaling pathway. *J Biol Chem.* 277:27975-27981.

Vaux EC, Metzen E, Yeates KM, Ratcliffe PJ (2001): Regulation of hypoxia-inducible factor is preserved in the absence of a functioning mitochondrial respiratory chain. *Blood.* 98:296-302.

Wang GL, Semenza GL (1993a): General involvement of hypoxia-inducible factor 1 in

transcriptional response to hypoxia. *Proc Natl Acad Sci U.S.A.* 90:4304-4308.

Wang GL, Semenza GL (1993): Desferrioxamine induces erythropoietin gene expression and hypoxia-inducible factor 1 DNA-binding activity: implications for models of hypoxia signal transduction. *Blood.* 82:3610-3615.

Wang GL, Semenza GL (1995): Purification and characterization of hypoxia-inducible factor 1. *J Biol Chem.* 270:1230-1237.

Wang GL, Jiang BH, Rue EA, Semenza GL (1995): Hypoxia-inducible factor 1 is a basic-helix-loop-helix-PAS heterodimer regulated by cellular O₂ tension. *Proc Natl Acad Sci U.S.A.* 92:5510-5514.

Wenger RH, Marti HH, Schuerer-Maly CC, Kvietikova I, Bauer C, Gassmann M, Maly FE (1996): Hypoxic induction of gene expression in chronic granulomatous disease-derived B-cell lines: oxygen sensing is independent of the cytochrome b558-containing nicotinamide adenine dinucleotide phosphate oxidase. *Blood.* 87:756-761.

Wenger RH, Kvietikova I, Rolfs A, Gassmann M, Marti HH (1997): Hypoxia-inducible factor-1 alpha is regulated at the post-mRNA level. *Kidney Int.* 51:560-563.

Wenger RH (2000): Mammalian oxygen sensing, signalling and gene regulation. *J Exp Biol.* 203:1253-1263.

Yu AY, Frid MG, Shimoda LA, Wiener CM, Stenmark K, Semenza GL (1998): Temporal, spatial, and oxygen-regulated expression of hypoxia-inducible factor-1 in the lung. *Am J Physiol.* 275:L818-826.

Yu F, White SB, Zhao Q, Lee FS (2001): HIF-1alpha binding to VHL is regulated by stimulus-sensitive proline hydroxylation. *Proc Natl Acad Sci U.S.A.* 98:9630-9635.

Acknowledgements

This dissertation was written while I was working at the University of Göttingen in the Institute of Biochemistry and Molecular Cell Biology, Göttingen, Germany.

I am very grateful to Prof. Kurt Jungermann and PD Dr. Thomas Kietzmann, who accepted me as a PhD student in the laboratory and provided me with excellent scientific guidance, instructive ideas and intensive theoretical discussions over the period of my PhD study.

I thank Prof. Dr. D. Doenecke for reviewing my dissertation and Prof. Dr. R. Hardeland for accepting to be the co-referent of this dissertation.

I thank Prof. Dr. Helmut Acker, Utta Berchner-Pfannschmidt and Christoph Wotzlaw for their help with the two photon confocal laser microscopy measurements.

I thank PD Dr. Frank Stümpel and Dr. Bettina Scholtka for their friendly help especially in the first year.

My special thanks to all colleagues in our institute, especially Tolja, Daniela, Elitsa, Ulrike, Katja, Doreen, Jacek for their assistance, discussion, and for providing a pleasant team atmosphere.

Last but not least, I want to thank my husband and my parents, for their patience and encouragement during these years.

Lebenslauf

Name, Vorname: Liu Qing
Geburtsdatum: 27.05.1973
Staatsangehörigkeit: Volksrepublik China

Schule/wissenschaftlicher Werdegang:

1980 – 1985: Grundschule, Shandong
1985 – 1991: Mittelschule, Shandong
1991 – 1996: Medizinstudium an der medizinischen Hochschule (medical college) Taishan, Shandong. Im Rahmen des Studiums wurde ein praktisches Jahr als Arzt in einem Lehrkrankenhaus der Hochschule geleistet.
1996 – 1999: Master-Studium unter der Anleitung von Prof. Dr. Yunqing An am Institut für Mikrobiologie und Immunologie, Universität für medizinische Wissenschaften der Hauptstadt, Beijing. Abschlussarbeit: „Klonierung und Expression des N-terminalen Bactericidal/permeability-increasing (BPI) Gens“.
1999 – 2000: Wellcome Trust Immunology unit, Medical Research Council, Cambridge, UK. Praktikantin mit Beteiligung an dem Projekt „Die Rolle des Notch-Signals in der Entwicklung von B-Zellen“.
2000 – 2003: Promotionsstudium in der Abteilung Biochemie und Molekulare Zellbiologie, Universität Göttingen. Der Titel der in dieser Zeit fertig gestellten Dissertation lautet „The regulation of hypoxia-responsive gene expression by hydroxyl radicals and intracellular calcium“.